

American University in Cairo

## AUC Knowledge Fountain

---

Theses and Dissertations

---

2-1-2017

### Study of Qattara depression and its hydropower potential

Aly El Shafei

Follow this and additional works at: <https://fount.aucegypt.edu/etds>

---

#### Recommended Citation

##### APA Citation

El Shafei, A. (2017). *Study of Qattara depression and its hydropower potential* [Master's thesis, the American University in Cairo]. AUC Knowledge Fountain.

<https://fount.aucegypt.edu/etds/647>

##### MLA Citation

El Shafei, Aly. *Study of Qattara depression and its hydropower potential*. 2017. American University in Cairo, Master's thesis. *AUC Knowledge Fountain*.

<https://fount.aucegypt.edu/etds/647>

This Thesis is brought to you for free and open access by AUC Knowledge Fountain. It has been accepted for inclusion in Theses and Dissertations by an authorized administrator of AUC Knowledge Fountain. For more information, please contact [mark.muehlhaeusler@aucegypt.edu](mailto:mark.muehlhaeusler@aucegypt.edu).

The American University in Cairo  
School of Sciences and Engineering

**Study of Qattara Depression and its Hydropower Potential**

By  
Aly Mamdouh El Shafei

A thesis submitted in partial fulfillment of the requirements for the degree of  
Master of Science in Mechanical Engineering

Under supervision of:  
Dr. Mohamed Amr Serag El Din  
Professor, Department of Mechanical Engineering

January, 2017

## Acknowledgments

The author would also like to show his gratitude to the Dr. Amr Serag El Din for his continuous support during the course of this research. He would also like to express gratitude to Dr. Mohamed Ezz El Din whose work on this area has been of great help and all of the Department faculty members for their help and support. He is deeply indebted to his parents for the unceasing encouragement, support and attention.

# Study of Qattara Depression and its Hydro Power Potential

by

Aly Mamdouh El Shafei

Submitted to the Department of Mechanical Engineering  
on January 12, 2017, in partial fulfillment of the  
requirements for the degree of

## Abstract

The Qattara Depression is a very interesting geomorphic feature that has been suggested to be used for hydropower production. This research will investigate hydrological elements affecting the water balance of the Qattara Depression region. Climatic data obtained from weather stations surrounding the region will be used in the investigation, as climatic factors such as rain and water evaporation would affect the mass balance equation. Then environmental and economic implications of such a project will also be studied. Many schemes have been suggested in the past for the project. All these schemes are compared economically in this work for the first time as far as the author knows. And the model employed investigates elements that had not been previously investigated. The outward seepage calculation and its affect on the plant lifetime is included in the model and the economic study and also its environmental impacts are checked. The effect of the channel flow of water before reaching the lowest point of the depression as it was not previously included in the evaporation calculation, but it is investigated in this model. Also a detailed study of the effect of the salinity increase of the water in the depression is investigated. The way all this enabled is by using data from three weather stations near Qattara Depression (Siwa, Dabaa, Wadi El Natroon) and the data is used on a monthly bases to calculate the evaporation that would occur as it would be used in the mass balance equation that includes the evaporation, that is affected by the progressive salinity increase, the inward and outward seepage, the rainfall, and the inflow from the sea. Using that calculation the progressive increase in the surface level in the depression is always obtained and the best design and economic study is planned accordingly.

# Contents

<b>1</b>	<b>INTRODUCTION</b>	<b>16</b>
1.1	Objectives of Present Research: . . . . .	20
<b>2</b>	<b>LITERATURE SURVEY AND PREVIOUS WORK</b>	<b>21</b>
2.0.1	Hydro power . . . . .	21
2.1	PREVIOUS WORK . . . . .	24
2.1.1	Study of Ball . . . . .	24
2.1.2	Bassler’s Commission . . . . .	28
2.1.3	Gohar’s Study . . . . .	30
2.1.4	Assem Afify . . . . .	31
2.1.5	Mohamed Ezz El Din . . . . .	35
2.2	Geology of Qattara Depression . . . . .	45
2.3	Moghera Aquifer . . . . .	46
2.3.1	Seepage . . . . .	49
2.4	Alternative Resources and Economic Studies . . . . .	52
2.4.1	Solar Energy . . . . .	52
2.4.2	Wind . . . . .	53
2.4.3	Mohamed Ezz el Din’s Cost Analysis . . . . .	56
<b>3</b>	<b>Qattara Depression Evaporation, Salinity, Seepage and Channel Flow Models</b>	<b>58</b>
3.0.1	Solar Radiation Model . . . . .	58
3.0.2	Evaporation Model . . . . .	60

3.0.3	Topography Model . . . . .	63
3.0.4	Salinity Model . . . . .	64
3.0.5	Chanel Flow . . . . .	67
3.0.6	Effect of Salinity on Evaporation Rate . . . . .	70
3.0.7	Seepage . . . . .	78
<b>4</b>	<b>Economic Analysis</b>	<b>84</b>
4.1	Cost estimation . . . . .	88
4.1.1	Economic comparison between conventional power plants and the base load scheme . . . . .	92
4.1.2	Economic comparison between conventional power plants and the pumped hydro storage scheme . . . . .	98
<b>5</b>	<b>Discussion of Results</b>	<b>102</b>
<b>6</b>	<b>Conclusion and Recommendations for Future Work</b>	<b>131</b>
6.0.1	Conclusion . . . . .	131
6.0.2	Recomendations for Future Work . . . . .	132

# List of Figures

1.1	Qattara Depression's location . . . . .	19
2.1	Network Demand . . . . .	22
2.2	Routes D,E and F . . . . .	26
2.3	Qattara Depression's level for different project scenarios . . . . .	27
2.4	Qattara Depression's salinity . . . . .	27
2.5	Qattara Depression's pumped storage alternative route 1 . . . . .	29
2.6	Qattara Depression's pumped storage alternative route 2 . . . . .	29
2.7	Proposal offered by Gohar . . . . .	31
2.8	Qattara Depression's osmotic power plant schematic . . . . .	33
2.9	Qattara Depression's aerial view . . . . .	34
2.10	Qattara Depression's two hydropower plants and a Solar-Pond-Chimney power plant . . . . .	35
2.11	Curve showing relation between temperature and vapor pressure . . .	42
2.12	Monthly Evaporation in Dabaa station . . . . .	43
2.13	Monthly Evaporation in Siwa station . . . . .	44
2.14	Monthly Evaporation in Wadi El Natroon station . . . . .	44
2.15	Qattara Depression's Geology . . . . .	47
2.16	Measured water table variations . . . . .	48
2.17	Transmissivity map for the Moghra aquifer in ( $m^2/day$ ), determined through model calibration . . . . .	49
2.18	Annual Integrated Direct Normal Irradiation $kWh/m^2.yr$ . . . . .	52

2.19	Wind resource map:mean wind speed at 50 m agl(above ground level). Source: Wind Atlas of Egypt . . . . .	54
2.20	Proposed approach with wind turbines and pipes at the Qattara De- pression . . . . .	55
2.21	Previously suggested design for pumped storage . . . . .	55
3.1	Meteorological Data from el Dabaa station . . . . .	62
3.2	Meteorological Data from Wadi El Natroon station . . . . .	63
3.3	Meteorological Data from Siwa station . . . . .	64
3.4	Area change with level . . . . .	65
3.5	Volume change with Level . . . . .	66
3.6	SRTM data . . . . .	68
3.7	Topography . . . . .	69
3.8	Evaporation factor . . . . .	70
3.9	Evaporation rate Wadi El Natron 1999 S.G=1 . . . . .	72
3.10	Evaporation rate Wadi El Natron 1999 S.G=1.1 . . . . .	72
3.11	Evaporation rate Wadi El Natron 1999 S.G=1.15 . . . . .	73
3.12	Evaporation rate Wadi El Natron 1999 S.G=1.2 . . . . .	73
3.13	Evaporation rate Dabaa 1999 S.G=1.25 . . . . .	74
3.14	Evaporation rate Dabaa 1999 S.G=1.3 . . . . .	74
3.15	Evaporation rate Wadi El Natron 1999 S.G=1.25 . . . . .	75
3.16	Evaporation rate Wadi El Natron 1999 S.G=1.3 . . . . .	75
3.17	Evaporation rate Wadi El Natron 1999 S.G=1.35 . . . . .	76
3.18	Evaporation rate Siwa 1999 S.G=1.0 . . . . .	76
3.19	Evaporation rate Siwa 1999 S.G=1.1 . . . . .	77
3.20	Evaporation rate Siwa 1999 S.G=1.15 . . . . .	77
3.21	Evaporation rate Siwa 1999 S.G. = 1.2 . . . . .	78
3.22	Node i . . . . .	81
3.23	TDMA . . . . .	82
3.24	Flow Chart of Matlab Code . . . . .	83



4.1	Data about hydro power plants . . . . .	84
4.2	Cross section . . . . .	86
4.3	Fuel consumption in Egypt . . . . .	87
4.4	HydroHelp 1.6 generating equipment details . . . . .	88
4.5	HydroHelp 1.6 power house details used in cost estimation . . . . .	88
4.6	HydroHelp 1.6 reaction turbine details used in cost estimation . . . . .	89
4.7	HydroHelp 1.6 reaction turbine selection for route D . . . . .	89
4.8	Data used for cost estimation of gas and steam turbine power plants .	91
4.9	Oil prices . . . . .	91
4.10	HydroHelp 1.6 reaction turbine selection for route D . . . . .	96
4.11	HydroHelp 1.6 reaction turbine selection for route E . . . . .	96
4.12	HydroHelp 1.6 reaction turbine selection for route F . . . . .	96
4.13	HydroHelp 1.6 reaction turbine selection for route H1 . . . . .	97
4.14	HydroHelp 1.6 reaction turbine selection for route L1 . . . . .	97
4.15	HydroHelp 1.6 reaction turbine selection for route L2 . . . . .	97
4.16	Power demand and supply with base load scheme . . . . .	98
4.17	Power demand and supply with peak load scheme . . . . .	99
4.18	HydroHelp 1.6 reaction turbine selection for route L2 . . . . .	99
4.19	Egypt's Central Grid . . . . .	101
5.1	Increase in surface level (S.L) in years with a flow of $656m^3/sec$ with no channel flow included was the same as when the channel flow was included . . . . .	103
5.2	Increase in area in years with a flow of $656m^3/s$ salinity included . . .	104
5.3	Increase in the specific gravity with time with a $656m^3/sec$ . . . . .	105
5.4	Surface level increase in years with a $656m^3/sec$ flow and salinity not included . . . . .	106
5.5	Surface level increase in years with seepage and salinity included and a $656m^3/s$ Flow . . . . .	107

5.6	Surface level increase in years with no seepage but new salinity model included in the $656m^3/s$ Flow . . . . .	108
5.7	Salinity increase in years with no seepage included and a $656m^3/s$ flow but the new salinity model included . . . . .	109
5.8	Area increase in years with no seepage included and a $656m^3/s$ flow but the new salinity model included . . . . .	110
5.9	Volume increase in the years . . . . .	111
5.10	Mass of salt increase in the years . . . . .	112
5.11	Rate of change in salinity decreases in years with no seepage included and a $656m^3/s$ Flow but the new salinity model included . . . . .	113
5.12	Surface level increase in years with seepage included and a $656m^3/s$ flow but the new salinity model included . . . . .	114
5.13	Mass of salt increases in years with seepage included and a $656m^3/s$ flow and the new salinity model included . . . . .	115
5.14	Salinity change in years with seepage included and a $656m^3/s$ flow and the new salinity model included . . . . .	116
5.15	Area increase in years with seepage included and a $656m^3/s$ flow and the new salinity model included . . . . .	117
5.16	Volume increase in the years with seepage included . . . . .	118
5.17	Area over Volume ratio decreases in the years . . . . .	119
5.18	Rate of change of salinity decreases in the first years with seepage included and a $656m^3/s$ flow but the new salinity model included . . . . .	120
5.19	Specific gravity increase in the first years with seepage included and a $656m^3/s$ flow and the new salinity model included . . . . .	124
5.20	Difference between rain and evaporation increases generally with the years following the area increase . . . . .	125
5.21	Difference between rain and evaporation decreases with the years when compared to the total volume of the lake . . . . .	126
5.22	Surface level decreases to a lower level when hydraulic conductivity increases . . . . .	127

5.23	mass of salt increases to a higher level when hydraulic conductivity decreases . . . . .	128
5.24	Surface level slightly increases faster when hydraulic conductivity of the soil decreases . . . . .	129
5.25	Surface level increases faster when salinity is included in model by comparison to old models . . . . .	130

# List of Tables

1.1	The biggest depressions . . . . .	19
2.1	routes offered by Ball . . . . .	26
2.2	routes offered by Bassler . . . . .	30
2.3	the different specific gravities tested . . . . .	45
2.4	Economic comparison between the two designs . . . . .	56
2.5	Cost estimates . . . . .	56
3.1	Mean daily maximum hours of sunshine for different months and latitudes	60
3.2	The Latitude and Longitude of each station . . . . .	60
3.3	Variation of the volume and area with the altitude . . . . .	67
3.4	Hydraulic conductivity example 1 including Kharga and Dakhla . . .	79
3.5	Hydraulic conductivity example 2 including Moghera . . . . .	79

# Nomenclature

- $C_{sea}$  Salinity of the sea ( $\text{kg}/\text{m}^3$ )
- $C_{si}$  Salinity of the inward seepage ( $\text{kg}/\text{m}^3$ )
- $E_a$  Evaporation rate using Dalton's equation (2.14) of the boundary layer above the water surface in  $\text{mm}/\text{day}$
- $K$  permeability coefficient ( $\text{m}/\text{s}$ )
- $m_{salt}$  mass of salt ( $\text{kg}$ )
- $Q_s$  monthly mean subsurface inflow ( $\text{m}^3/\text{day}$ )
- $Q_{in}$  monthly mean discharge to be conveyed from the sea ( $\text{m}^3/\text{day}$ )
- $Q_{out}$  monthly mean discharge to be pumped out (when applicable) ( $\text{m}^3/\text{day}$ )
- $R_a$  Mean incident solar radiation at the top of the atmosphere on a horizontal surface  $\text{W}/\text{m}^2$
- SRTM* Shuttle Radar Topographic Mission elevation data product
- $T_a$  Absolute temperature =  $t^\circ\text{C}+273$
- $V_{sea}$  Flow rate of sea water entering the depression ( $\text{m}^3/\text{month}$ )
- $V_{si}$  Flow rate of water entering the depression through seepage ( $\text{m}^3/\text{month}$ )
- $V_{so}$  Flow rate of water leaving the depression through seepage ( $\text{m}^3/\text{month}$ )
- A Qattara Depression surface area at corresponding level ( $\text{m}^2$ )

- C Instantaneous salt concentration in reservoir
- d Maximum possible hours of bright sunshine (mean value), this value is a function of latitude ( $\phi$ )
- E Evaporation in mm/day using Penman equation
- e Actual vapor pressure of air in mm Hg
- H Net radiation flux gained at free water surface in  $W/m^2$
- L Surface level of the Qattara Depression (m)
- n Actual duration of bright sunshine (hours)

# Chapter 1

## INTRODUCTION

Qattara depression as shown in Fig(1.1) is located in the North-West of Egypt. It has a complicated topography and a number of factors that present an opportunity to exploit as the basis for a hydro power plant. Its lowest point reaches 134 meters below sea level. Therefore, it is considered to be the second lowest point in Africa after Lake Assal in Djibouti and it is also the fifth deepest natural depression worldwide as seen in the table (1.1). Moreover, it has by far the largest surface area and is relatively close to the sea. It has a length of around 300 km and a width of 135 km. The surface area at sea level is around 44,000 km<sup>2</sup>, and it covers almost 1/15<sup>th</sup> of Egypt's total land area[1]. The closest point to the Mediterranean Sea is at a distance of 55 km south of El Alamein[2], providing the opportunity to use canals and tunnels, depending on the chosen route, to transfer the water from the Mediterranean sea to the Qattara Depression. Therefore, it has been suggested for decades to use this difference in level to run a hydro power plant by transferring the water from the sea.

There are several challenges that needed to be overcome as the water level in the lake would rise gradually due to the input from the sea, flowing through the chosen path whether a canal, tunnel or both. While the evaporation rate would continuously decrease as the salinity level would gradually increase and that would endanger the lifetime of the project as if the water level reaches the chosen turbine level that would mark the end of the plant life. Other studies had neglected this factor, thus the water level would stabilize as the evaporation rate is not affected. In the thesis salinity will

be examined in detail and it's effect on the plant life taken in to consideration.

The main factors outside our control that would affect the level of water and hence the hydropower production from Qattara Depression are the evaporation rate, inward and outward seepage and the rain. There have been already several studies on the effect of these factors that are used here, but further investigations are added to include the detailed effect of the salinity increase, the outward seepage, and the evaporation of the channel of water formed while the water is moving to the lowest point in the depression.

The proposal is also analyzed economically in relation to the current energy and construction prices using the best possible estimates and conducting a sensitivity analysis when appropriate. The Economic Analysis Chapter also considers the uses of the hydro power plant, for example its potential use as a pumped hydro storage connected to the national electric grid, and whether or not that would be the best set up in this case.

The production of energy in Egypt from hydro-power plants on the river Nile is subordinate to the regulation of water for agriculture; moreover the electrical energy produced is mainly used in the local production zone[1]. Therefore, the energy supply to the northern industries is fluctuating and that is an additional reason and advantage for the Qattara Depression project as it would benefit this region by supplying supplementary energy storage. Coupled with the current situation in the Ethiopian dam, that if built would have disastrous effects on the High dam and effect the total energy in the Egyptian central grid. The Qattara Depression project would present an energy alternative. Salem [3] suggests that water used for the production of energy could be partially put to better use for the cultivation of the area by lowering the target level of the water level in the High dam[3].

Hydro power plant technology includes many factors that are exploited in this study. The turbines that are suggested for use here are of the Francis turbine type because they exhibit the highest efficiencies within their range of operation (40-272.5 m) in the Qattara Depression, as will be shown in the economic analysis chapter. They can be used in generating large amounts of energy and storing it and using it in



peak and medium hours by running the turbines in reverse mode during low energy consumption periods, using surplus grid supplied energy. The amount of energy generated can be obtained almost instantly as it would take from 1-3 minutes for the generator to start producing the needed electricity, which would be very beneficial to Egypt's central grid.

There are several advantages of hydro power which include its ability to produce a clean power source with no contribution to global warming, instantaneous ability of starting and stopping mentioned above, a long useful life, and a very high operational efficiency with an average cost of operation and maintenance lower than any other sources of energy. Also providing other benefits such as drinking water supply, irrigation, flood control as in the High dam. Recreation and the location in remote areas, such as Qattara Depression helps in the development of the surrounding areas which is very important in developing countries, and would be very beneficial to Egypt.

There are also disadvantages to hydro-power that usually include the feasibility that is constrained by the availability of water and head, however this is not the case with Qattara depression where there is an abundance of available water and high head due to the previously mentioned location, area and depth shown in table (1.1). Other disadvantages include, relocation of people in these areas, and possible environmental impacts. This thesis provides a detailed study to the Qattara Depression, that as far as the author knows is not present in any other source. A detailed economic analysis of the project for the different design alternatives that are included in the enhanced model is made. Further the enhanced model includes a seepage model, a channel flow model, and a salinity model that is more accurate than all other models previously proposed.



Figure 1.1: Qattara Depression's location[1]

Table 1.1: The biggest depressions [1]

Location	Elavation [m]	Area [ $km^2$ ]	Distance from sea [km]
Dead sea	-401	3,800	72
Lake Tiberius, sea of Galilee	-212	-	50
Assal	-174	80	15
Turfan	-154	5,000	1,500
Qattara Depression	-133	44,000	56

## 1.1 Objectives of Present Research:

1. Investigating and compiling all previous work conducted on Qattara Depression
2. Collecting relevant data concerning the project, such as meteorological data and the current costs, that would be included in the model and its analysis
3. Building a model computing the change of the level and salinity of the lake with time and comparing the results with the previous work conducted, that has not included the seepage study or the detailed salinity study performed
4. Conducting an economic analysis of the work based on previous and current investigations, and in light of current data collected from the ministry of electricity
5. Recommending a course of action regarding the utilization of the Qattara Depression to generate/store energy

## Chapter 2

# LITERATURE SURVEY AND PREVIOUS WORK

### 2.0.1 Hydro power

The operational terminology concerning hydro power stations is defined as follows: The "construction capacity" is the quantity of power generation capacity that can be achieved in a power plant. That quantity depends on the construction flow rate at the construction drop height. "Maximum capacity" is the capacity achieved from the maximal fall height. The "rated power" is the highest continuous power that can be achieved by the machine [4].

Fig (2.1) shows the power variations that are met by a pumped hydro storage power plant from season to season. That would differ from region to region according to numerous factors such as meteorological data and its variations throughout the day and seasons and characteristics of the turbine propellers in producing energy [4].

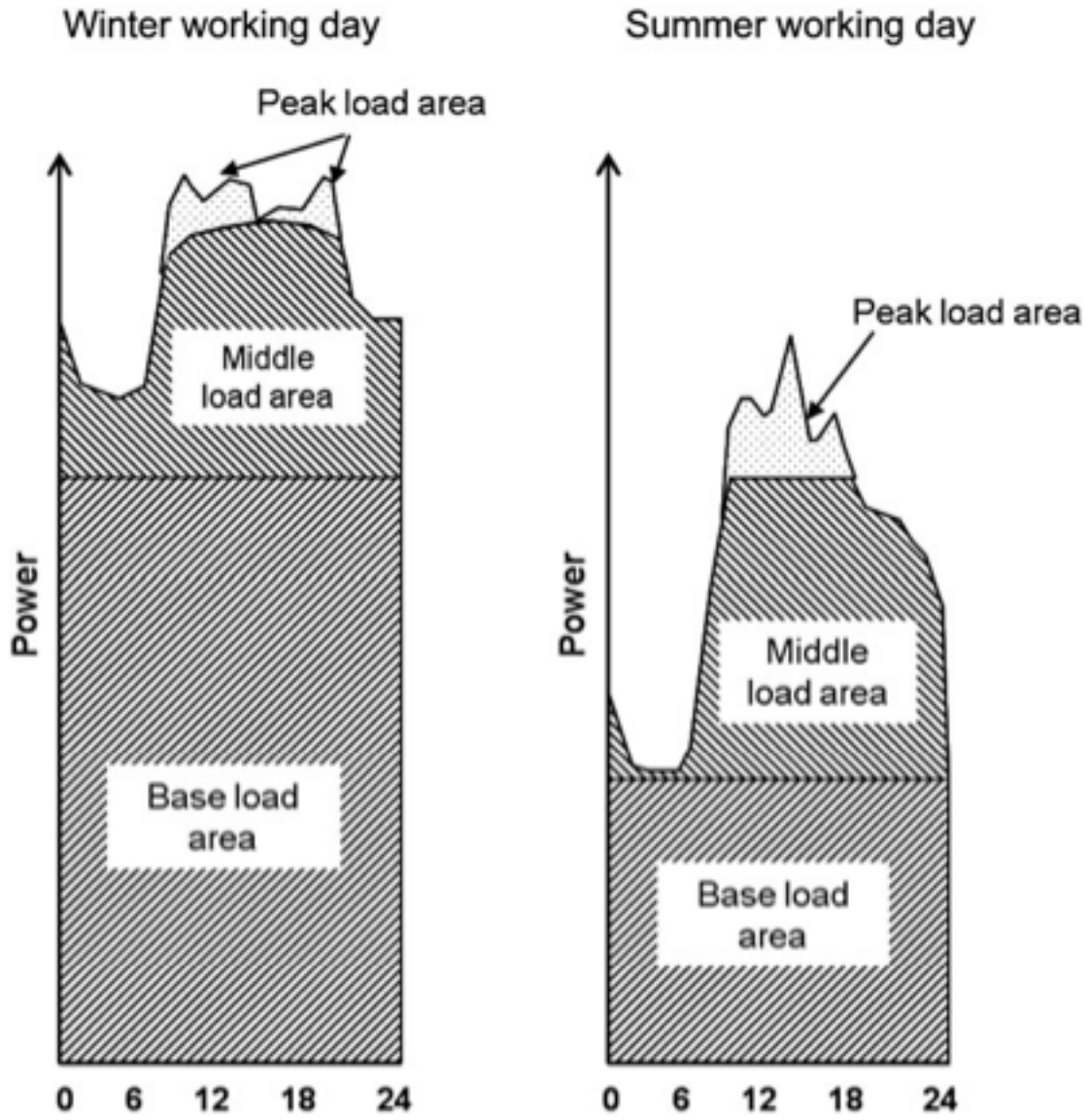


Figure 2.1: Network Demand [4]

There are also legal requirements associated with hydro power plants concerning deviation of water paths and environmental issues. A joint venture is needed especially in developing countries as governments are very unlikely capable of financing the project, therefore private investors are encouraged to become partners with governments to form joint ventures for hydro power plants. This has been suggested as a way to finance the Qattara Depression project [4].

There are many technical aspects that must be investigated when choosing to construct a pumped storage hydro plant. First, the location which is to some extent settled in this study. However, investigations, considering the quantity of the water inflow, need to be made in the Qattara Depression project. The amount of rain flow, also need to be investigated, as it differs throughout the year and varies from year to year so historical data is used. All these changes cause the amount of energy generated throughout the year to differ. Another consideration is the location of the powerhouse that is changed according to the topographic situation at the site where a hydro power plant is planned. And according to the geographic circumstances the location of the turbine is planned. For example, in some cases there is a multiple reservoir system and having a separate reservoir might not be possible because of the lack of a suitable place for installing the turbine. Therefore, a water tunnel can be built that would bring water to one common power plant and would provide the largest head. Also, the fall height affects the planned system. For example, if a huge horizontal distance is present providing a good head of water a common power plant would not be the best choice, as capitalizing on the fall height would need a series of power plants, this is known as cascaded hydro power plants. By these few examples it is shown that several factors have to be investigated while planning for such a project, but the most important aspect is the economic analysis [4].

There are several main parts in a hydro power plant that have to be carefully investigated. First, the turbine that has to be selected, according to the head and flow, to give the optimum output. Electric generator, transformer and power house, upper and lower reservoir, structural parts, dam and spillway, surge chambers that are necessary for temporary storage of water, stilling basins, pen-stock and spiral casing,

tail-race, pressure pipes, caverns and other auxiliary parts. In all the parts used in the hydro power plant that are included in the planning and simulation process for the plant the most crucial and important part is the hydraulic turbine as it must be chosen to provide the highest efficiency possible. All these parts are to be simulated in the study to investigate the operation of a hydro power plant at Qattara Depression and estimate its cost to chose the best design [4].

Qattara Depression is a very interesting prospect that can be actively applied to the Egyptian electricity market. There have been several studies that investigated the capability of the Qattara Depression, that are to be discussed and evaluated in details.

## 2.1 PREVIOUS WORK

### 2.1.1 Study of Ball

Martino [1] shows the investigations done in the subject of the Qattara Depression early on by Ball[1] then later on by Bassler[1] and Gohary[1]. Qattara Depression was first investigated by Ball in 1927 and he published his studies in 1933, as he obtained information from a survey in Egypt, which enabled him to perform a study of the depression in a detailed manner[1]. That was different from the first preliminary investigation that was first conducted when it was first discovered in the beginning of the 20th century were only a simple orientation sketch could have been drawn. The floor of the depression is covered, by Sabakha, a mixture of sand, salt, and water. Formation of that mixture could not have been formed by evaporation of sea water, in fact borings down to 20 m below sea level at a distance of 20 km to the coast were found completely dry. The material was probably formed by continuous seepage of water below the Libyan Desert.

Ball studied the possibility of using this natural phenomenon for hydroelectricity by forming three lakes at levels 50,60 and 70 m below sea level, to which the corresponding surface areas were 13500,12100 and 8600  $km^2$ , respectively[1]. Also, Ball

noted that for these three lakes routes D, E, and F, shown in Fig (2.2), present an appropriate path for water flow. The study also included detailed information about rainfall, evaporation, inward and outward seepage flow, as all these factors would affect the plant life.

First, in regards to rainfall, Ball considered it to be an adverse factor to the lake's level, hence energy generation. Ball assumed that only half the rainfall in Qattara Depression would reach the three lakes, he estimated a daily average rainfall of 0.15, 0.16, and 0.18 mm for the three lakes, respectively. He also believed that the rainfall would double after the salt lake had been formed, due to the evaporation effects. Considering evaporation, which is an important factor in the lake's life, for approximate figures, he referred to the process that occurs in the brackish Birket el Qarun Lake located nearby the depression in Faiyum. But, the lake that would be formed would be saturated with salt that would in turn alter the evaporation environment, so he also studied Karabugas (an enclosed gulf almost saturated with salt, east of the Caspian Sea). In conclusion, the evaporation rates from the three lakes, respectively, were estimated to be 4.6, 4.3 and 4 *mm/day*. The evaporation rate is re-estimated in this study.

Finally, he studied the seepage flow and gave no quantities for the volume of water that might leave the lake due to outward seepage, as it would affect the plant life positively, again this factor will be investigated in detail in this study. While, he estimated that inward seepage volume would result in daily depth changes of 0.21, 0.24, 0.33 mm for lakes of depth -50, -60 and -70 m.

Ball concluded that the daily water discharge into the depression from the turbine outlets should be set at a rate equal to the product of the final lake area and average net depth of water that would be removed by evaporation, after subtracting the average daily inward seepage and rainfall from the figure of evaporated water. He estimated the discharges channeled to the lakes as 656, 546, and 348  $m^3/s$ , respectively, and in his design the lakes would never fill up due to the mass balance of water explained above. Ball estimated the average time for the formation of the lake at the depths of -50, -60 and -70 m and stated that even if the assumption that the inflow to



Table 2.1: routes offered by Ball

route s	D	E	F
Lake level below sea-level (m)	50	60	70
Flow rate ( $m^3/sec$ )	656	546	348
Amounts of power developable (kwh)	200,000	200,000	150,000
Length of conduit from sea to contour (km)	72	76	80
Open channel from sea to tunnels (km)	20	————	————
Diameter of tunnels (m) for 200,000 kwh	12	11	————
Diameter of tunnels (m) for 175,000 kwh	11	10	————
Diameter of tunnels (m) for 150,000 kwh	10.3	9.5	9.2
Diameter of tunnels (m) for 125,000 kwh	9.8	9	8.2

Figure 2.2: routes D,E and F [1]

the depression from the start is maximum after 150, 60 and 30 years respectively the level of the lake would be 1 m below the final level. Followed by that, he studied the progressive increase of salinity stating that it would reach the maximum level after 160, 120 and 100 years[1]. Fig (2.4) shows the salinity changes in the lakes with the progression of time. Fig (2.3) shows Ball's estimation of the time elapsed from the entrance of the water into the depression attaining different levels in the lake. Ball suggested that three circular canals be used for the transmission of water, for the construction to take place in three stages with the first two stages not fulfilling the complete flow of  $656 m^3$ , which is shown in the filling scenario in Fig (2.3), along with all the lake level types. Ball suggested building a single channel for the first 20 km and three tunnels of 11 m diameter picking the sea water from there. Ball preferred the option of the -50 m lake, along route D, due to topographical and geographical reasons, rather than the option of -60 m lake[1].

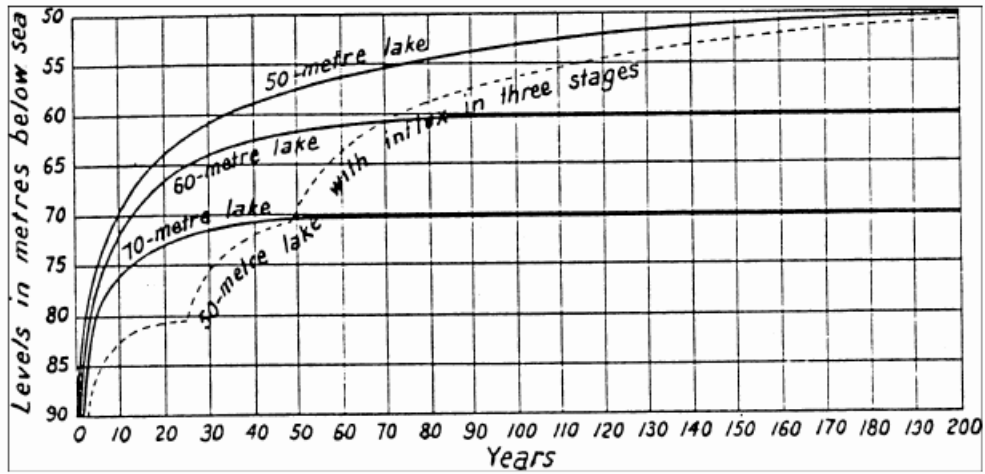


Figure 2.3: Qattara Depression's level [1]

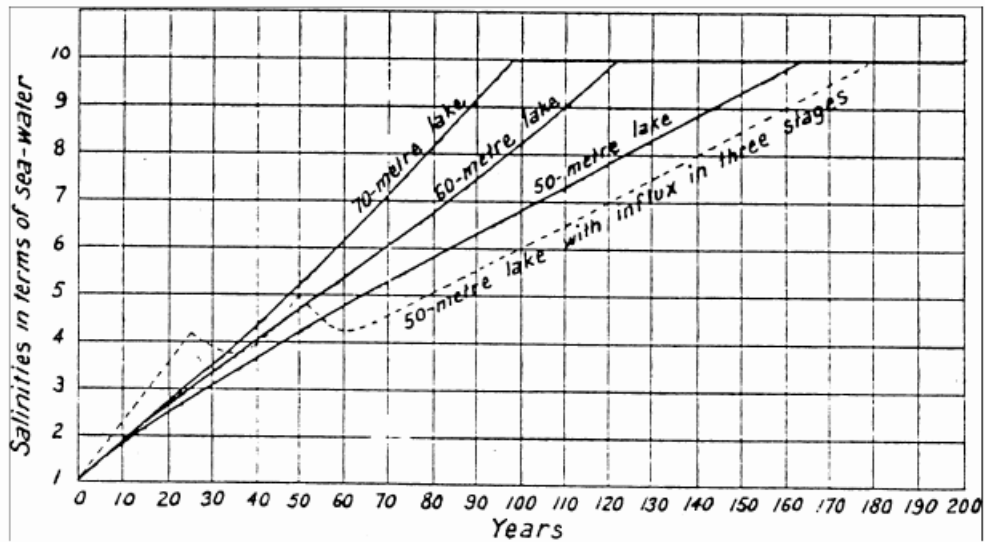


Figure 2.4: Qattara Depression's salinity [1]

### 2.1.2 Bassler's Commission

By the 1950s after Ball's study and proposal the subject was reopened, were Siemens proposed a scheme that would have provided a power potential of 100 MW, with turbines only operating six hours per day[1].

A commission led by Bassler in 1964 with results showing that the Qattara Depression, alternatively to what had previously been said, can be used for pumped-hydro-storage for peak load energy production. As seen in Fig (2.5 and 2.6) and Table (2.2) Bassler offered several configurations some including a canal that would deliver water to the depression as well as being a shipping route towards the Qattara Lake with a harbor and fishing grounds in the depression[5].

The depression was to be filled to a height of 60 m below sea level, which would correspond to an area of 12000  $km^2$ . The volume removed due to evaporation would be 19000 million cubic meters annually, this estimation is different from the 17000 million cubic meters Ball estimated for the lake at this level annually. A flow of 600  $m^3/s$  would be used for the compensation of the evaporation, according to Ball that flow was 546  $m^3/s$ [1]. The tunnels carrying the discharge would be about 80 km long and it would reach an underground power plant at level -54 m[1].

The operation Bassler proposed was that during hours of low network load demand, the energy produced by the project turbines would be used to pump the water into a high-level natural reservoir that has a capacity of 50 million cubic meters as shown in Fig (2.5 and 2.6)[1]. Water located in this zone would offer a valuable head during peak load hours. Therefore, during the peak load periods pumps would not be allowed to work and the extra head obtained would be able to generate a huge amount of power[5]. This system would be able to produce 4000 MW during the peak period and would be adaptable to handle varying demand patterns[5].

In regards to the economic feasibility of the project and its cost, Bassler claimed that no estimate could have been made at the time. Bassler agreed with Ball considering that three tunnels needed to be built that might be undertaken by the means of nuclear excavation or other advanced techniques that might lead to lower construc-

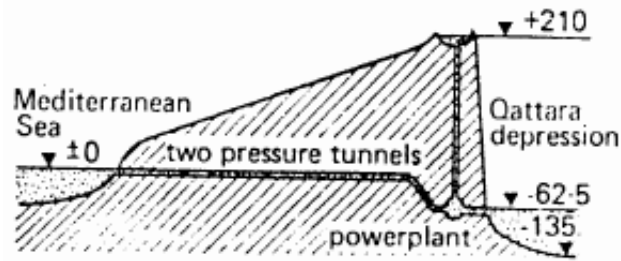


Figure 2.5: Qattara Depression's pumped storage alternative route 1[1]

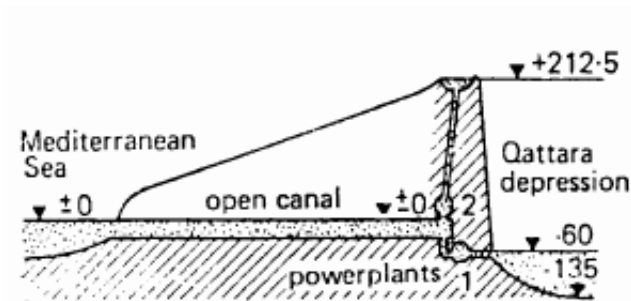


Figure 2.6: Qattara Depression's pumped storage alternative route 2[1]

tion costs by reducing the construction time. But, the topic of using nuclear blasts was part of the reasons that project had never commenced, due to opposition by the Egyptian government.

It would take 35 years to fill the lake to the level of 62.5 m below sea level with the installed capacity of  $656 \text{ m}^3/\text{sec}$ [5]. After that the incoming flow would be set to balance out against the outgoing evaporation and would cause the lake level to stop changing. For his pumped hydro storage scheme an additional  $936 \text{ m}^3$  was said to be required from the upper basin that would be situated 188 m above sea level, providing a 262 m head[5]. Clearly, different designs were produced by Ball and Bassler, partly due to different estimations pointed above, would lead to a misleading economic analysis. Therefore, in this proposal estimations concerning evaporation, rain fall, and seepage will be made to produce reliable results for the life time of the project to avoid a misleading economic analysis.

Table 2.2: routes offered by Bassler

routes	H1	L1	L2
Construction technique	Canal	Canal+ tunnel	Canal+ tunnel
Lake level below sea-level (m)	50	55	62.5
Flow rate ( $m^3/sec$ )	776	740	656
Two tunnels Diameter (m)	15.8	15.5	14.5
Two tunnels Length (km)	16	42	76
Two tunnels volume blasted ( $10^6m^3$ )	7.45	20.6	31.2
Canal length (km)	71	33.3	—
volume excavated ( $10^6m^3$ )	1750	390	—

### 2.1.3 Gohar's Study

A third proposal in 1961 was made by Gohar, using Ball's first proposal but proposing a slight change in route that Gohar believed would provide a greater return on investment. He also believed that the route presented offered great difficulties in construction that his modification eliminated. His modified route is indicated by letter b in Fig(2.2) in which he pointed that the highest point of land between the sea and the depression would be found only 11 km from the Mediterranean coast. Hence, in his scheme water could be pumped to the highest point then water would flow in channel ab as shown in Fig(2.7) and the pump would be driven by the network during low demand hours. In this design the water would be transferred using an overhead reservoir and a pump, unlike the previous tunnel system introduced. If this scheme was used the turbine head would be the head created between point b and point c as shown in Fig(2.7), after subtracting the head used to pump the water to point a. In this design the output generated could be either available the whole time or during the peak hours, at which the pump would be shut off and the turbines supplied by the retained volume of water in channel ab[1].

Gohar decided in his proposal that the lake would best be formed at -75m, channel ab would be at level +80 m, and a  $266 m^3/s$  discharge would be used. Gohar concluded that the net power available would be about 100 MW, while the maximum peaking capacity was about 345 MW and that the cost per KW installed would be

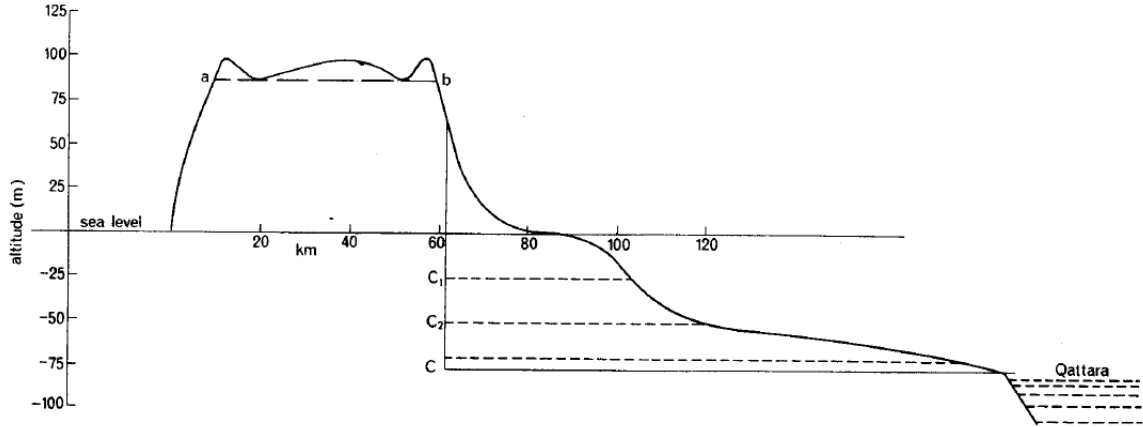


Figure 2.7: Proposal offered by Gohar[1]

less than Ball's scheme[1]. Also, that lakes L1 and L2 shown in Fig(2.2) are very near to channel ab, therefore could be used as a pumped storage reservoir[1]. Finally, Gohar pointed that the open channel would be easier to maintain than the tunnels and a shorter distance would be available from his plant to Alexandria than in Ball's scheme, hence less cost[1]. There are however shortcomings in Gohar's scheme as it was not specified how water would be carried from the underground station (point C) to the depression and the cost of such a process[1]. Also, looking at the Gohar's project outline it is seen that a tunnel of at least 60 km length would be needed to carry the water to the lake, thus that would cancel out the advantage of cost reduction and elimination of Ball's tunnel[1]. Also, the use of artificial lakes L1 and L2 is not made clear as they are far away from his proposal[1].

#### 2.1.4 Assem Afify

First in the MIK technology scheme the concept for power generation relies on the osmosis phenomenon. The concept used is as if a semi permeable layer is placed between water of different salt concentrations, water would tend to flow to the more concentrated solution and this flow can be used drive a power generation turbine. This proposal needed only  $60 \text{ m}^3/\text{s}$  of sea water to generate 360 MW [6]. As shown in Fig (2.8) an area of  $630 \text{ km}^2$  is used as a basin for evaporation where the salinity would increase. This is required as osmotic power requires high salinity brine so this

is the proposal made by Kelada [6]. According to Kelada the osmotic power concept can produce 3 GW at an efficiency of 51 % from the Qattara Depression and 26 MW/ $m^3$  of brine.

This solution would address not only, the energy problem of the country, but also, enhance the country's water and food resources, and also relieve the overpopulated communities [6]. It was suggested that the north section be used to develop high salinity brine needed for osmotic generation while the south section be used as a large lake for farming and marine life, because of its large volume. It would be necessary to maintain the salinity of the water constant for marine life and urban development to thrive. Keeping the salinity constant would also prevent negative ecological effects and help the continuation of evaporation from the lake that would actually help hydro power production continue if it was used along with this proposed scheme [6].

The paper estimated the flow rate necessary to maintain a salinity of 4% according to previously calculated evaporation rates by Ball to be 3400  $m^3/s$ , which is 80% higher than the required rate if 4.5% salinity is maintained[6]. The discharged water as mentioned will be used to fill the brine lake at the north of the depression that would be maintained at 50 m below sea level and present the osmotic potential. In this scheme it was proposed that the excess flow from the process which would be between 1100  $m^3/s$  to 2000  $m^3/s$ , according to the operating concentration would exit the plant through a second canal that it would have to be pumped back through to the sea[6].

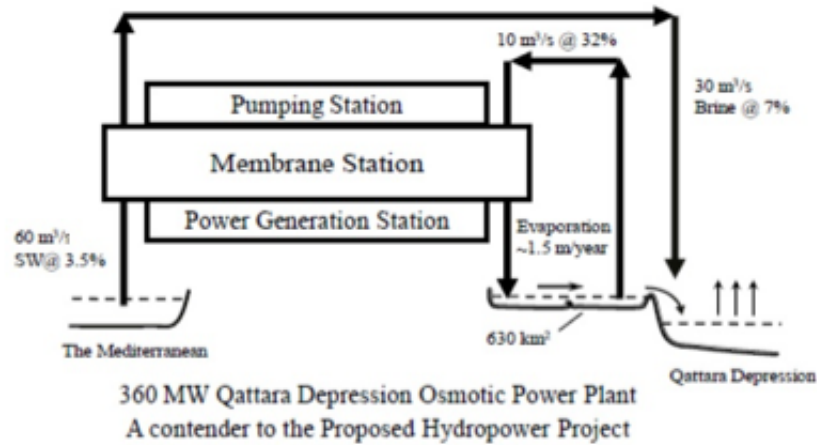


Figure 2.8: Qattara Depression's osmotic power plant schematic[6]

Secondly the Hydro and solar-pond-chimney power scheme is another proposal put forward having a two stage power system the first being the conventional hydro power system fed by sea water and the second was a turbine power system which employs a combination of solar pond and solar chimney technology. It was said that the first stage would produce 190 MW, while the second stage power plants would increase the total production to reach 410 MW [6]. The large salt water body offered by Qattara Depression can be exploited as a solar pond that was suggested to be coupled with a vertical chimney named as a Solar-Pond-Chimney Power Plant (SPP). Fig (2.10) shows a cross section of the combined power system while Fig(2.9) shows an aerial view of the project components. At the left side of the cross section it shows the normal operation of the plant that has been suggested by previous studies. While the right side shows this extra proposal of additional re-used water flow rate of about  $200 \text{ m}^3/\text{s}$  that is said to keep the lake top water level balanced at -50 m. The reused water proposed to be taken from the Delta would have an average salinity of 0.1 % , but the delivery of such water would cost too much and such an action would have to be economically analyzed and politically with the Ethiopian dam at the works.

The design is based on the heating of the air over the surface of the water and in the neighborhood of the chimney base using hydrophobic heat wheels that convey the



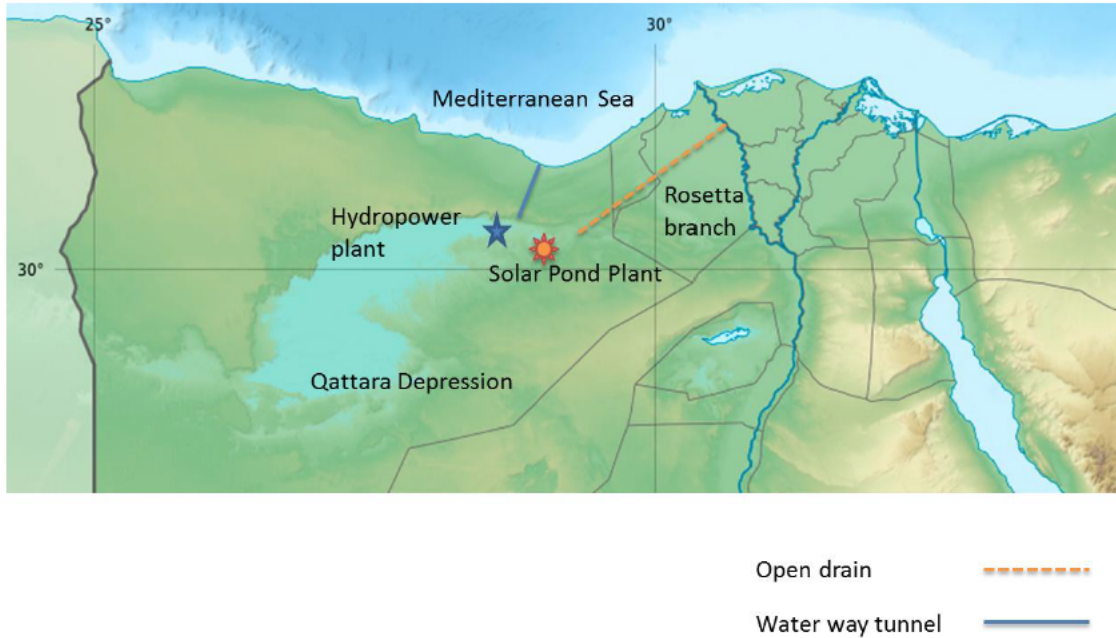


Figure 2.9: Qattara Depression's aerial view[6]

heat from the hot water at the bottom of the lake and then enters the chimney base. Air over the lake surface would have a temperature of  $30^{\circ}\text{C}$  and saturated with water vapor, and after being heated it would reach a temperature of  $80^{\circ}\text{C}$  and a density of  $1\text{ kg/m}^3$ [6]. There would be a pressure differential available as the air would differ in density as air around the chimney would have a density of  $1.2\text{ kg/m}^3$ . This pressure difference would be used to generate electric power estimated to be 200 MW[6].

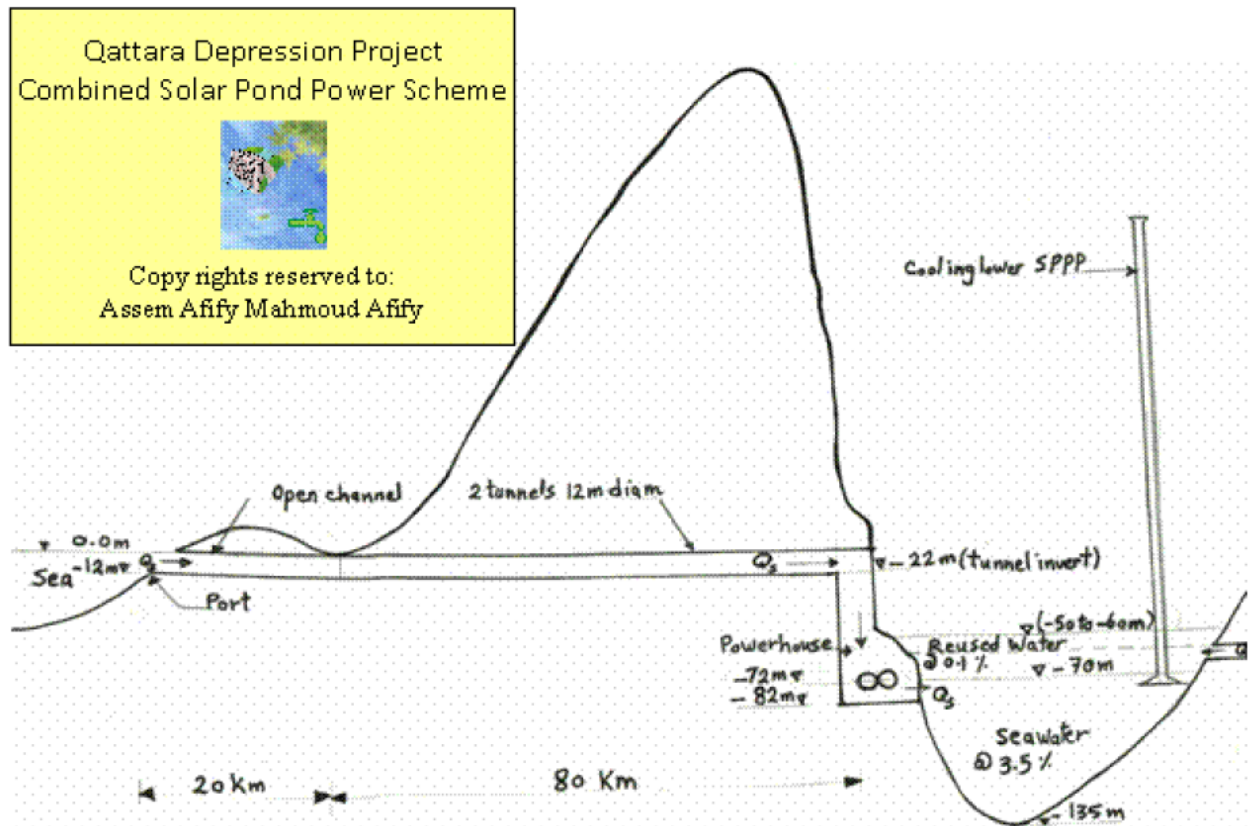


Figure 2.10: Qattara Depression's two hydropower plants and a Solar-Pond-Chimney power plant[6]

The pumped storage alternative proposed by Bassler was mentioned again by Afify[6]. As mentioned in the Bassler section, in the first phase of the project the Qattara station was to generate 670 MW. The second phase was to generate an additional 1200 MW. A pumped-storage hydroelectricity facility would increase the peak production capacity with another 4000 MW, totaling about 6800 MW[6].

### 2.1.5 Mohamed Ezz El Din

An extensive study was done by Ezz El Din[5] who calculated the evaporation rate using Penman's equation, predicted the changes of the Qattara Depression surface level and analyzed the economics of the project at that time.

## Evaporation

There are many formulas available to be used for the estimation of evaporation. Most of them are based on Dalton's fundamental law [7], which states that evaporation will take place if the actual vapor pressure of the air above the water surface is less than the actual vapor pressure at the water surface.

Penman's equation has given very good results especially in humid regions from all the regions that it has been checked around the world[5]. There are also direct measurements that can be used to estimate evaporation using evaporation pans. There are different pan types which include sunken pan, floating pan and surface pan.

When the sunken pan is used direct solar radiation on the side walls becomes negligible as it is placed below the ground surface. But, there are problems that arrive as a result of its placement such as collecting trash, difficulty to install, difficulty to detect leaks and difficulty to quantify the amount of heat that is transferred directly through the walls of the pan to the surrounding soil.

When the floating pan is used it provides the best estimates, but also it has its drawbacks. These drawbacks include its inaccessibility, the problem of wave action causing water into and out of the pan.

Finally, the surface pan which is the most common type used."The standard US-Weather Bureau Class A- pan built of unpainted galvanized iron is currently the most popular."[5]

Ezz El Din[5] modeled the change in the surface level with time using the meteorological data for 360 months (1970-2000). Once using the evaporation rates measured and once using the evaporations rates calculated using Penman's equation, the results showed that the equation is applicable to the monthly average. In Ezz El Din's model, each run had a random year chosen from the 30 years available. The model was designed for different inflows ranging from  $5m^3/sec$  to  $1000m^3/sec$ . for each flow the changes in the surface level and salinity are studied for the different scenarios shown below:

1. Base-load scheme 24 hours production.

2. Peak-load scheme for some hours of production per day for developing hydro power during the peak-load period.
3. Mixed pumped storage scheme which is used to develop the hydro power at peak-load period and pumping at the off-peak period, and the pumping power coming from the grid during off peak period.

Ezz El Din concluded from the results of the three alternatives that salinity would have a severe effect on the lifetime of the project. As increasing the salinity will severely decrease the evaporation rate and lead to the water level increasing much more rapidly and not leveling out, as will be seen in the results, contrary to what Ball and Bassler deduced. Also, he concluded that his third proposal which is the mixed pumped storage scheme developing hydro power at peak-load period and pumping at the off peak period is the best design for the usage of the depression.

The figures of the three stations show the measured results in the three weather stations near Qattara Depression along with the calculated results, that are to be explained below. The comparison shows a close correlation between the measured and calculated results. Therefore, Penman's theory [8], which is based on heat balance equation, was chosen for the evaporation calculation and is represented as follows:

$$R_c * (1 - r) - R_B = H = E + K + S \quad (2.1)$$

Where:

$R_c$  = Incoming short wave solar radiation flux received at the earth surface from the sky on a clear day

$r$  = Reflection coefficient of the water's surface

$R_B$  = Net long wave radiation from the water surface per unit area

$H$  = Net radiation flux gained at free water surface

$E$  = Heat supplied for evaporation per unit area

$K$  = Heat exchange by convection between water surface and air

$S$  = Heat lost by conduction between the evaporation surface and the underlying ground

The heat lost by conduction (S) is considerably smaller in magnitude than the evaporation (E) and heat exchange with the atmosphere (K). Therefore the equation may be approximated to:

$$H = E + K \quad (2.2)$$

The amount of solar radiation coming from the sun is the most effective factor in the net radiation flux. The actual amount of solar radiation  $R_c$  can be expressed as a function of cloud cover (n/d) and extra terrestrial radiation  $R_A$ . Penman[5] represents the cloud cover as the ratio of possible sunshine hours. The following equation is used generally for short wave solar radiation flux:

$$R_c = R_A * (a + b \frac{n}{d}) \quad (2.3)$$

where:

$R_A$  = Mean incident solar radiation at the top of the atmosphere on a horizontal surface

a = A constant depending upon the latitude ( $\phi$ ) and equals to  $(0.29 * \cos \phi)$

b = A constant having an average value of 0.54

n = Actual duration of bright sunshine (hours)

d = Number of daylight hours; this value is a function of latitude ( $\phi$ )

For example, Penman represents southern England with the following equation:

$$R_c = R_A * (0.18 + 0.54 \frac{n}{d}) \quad (2.4)$$

Whereas Proscott represents ( $R_c$ ) for Canberra Australia with the following equation which is more appropriate for the Qattara Depression it is closer to climate to Australia than Southern England:

$$R_c = R_A * (0.25 + 0.54 \frac{n}{d}) \quad (2.5)$$

But, for this proposal the latitude used is directly from Qattara Depression, tak-

ing an average latitude of  $30^\circ$ , leading to a more accurate result than Ezz El Din's work that would prevent this proposal from misleading conclusions. The reflection coefficient differs for the incoming short wave radiation ( $R_c$ ) for different water surfaces, and depends on depth, as well as surface reflectivity which depends on algal population and color. Penman takes an average value of the reflection coefficient ( $r$ ) as 0.06[5] for water surfaces which can be used in the Qattara Depression, while it is taken in the range of 0.15-0.25 in close ground crops, for example, which is not the case here.

Ezz El Din [5] expresses the net long wave radiation ( $R_B$ ) for Qattara Depression by the expression shown below as a function of the vapor pressure, air temperature, and cloud cover[5].

$$R_B = \alpha * T_a(0.47 - 0.077\sqrt{e}) * (0.2 + 0.8\frac{n}{d}) \quad (2.6)$$

Where:

$\alpha$  = Lummer and Pringsheim constant =  $117.79 * 10^{-9}$  g.cal /  $cm^2$  / day

$T_a$  = Absolute temperature =  $t^\circ C + 273$

$e$  = Actual vapor pressure of air in mm Hg

Since, the net amount of radiation energy remaining at a free water surface is given by:

$$H = R_c * (1 - r) - R_B \quad (2.7)$$

Therefore, incorporating equations 2.5 and 2.6 in equation 2.7 yields the below equation for obtaining the net radiation flux

$$H = R_a * (0.25 + 0.54\frac{n}{d}) * (1 - 0.06) - 117.79 * 10^{-9} * T_a^4 * (0.47 - 0.077\sqrt{e}) * (0.2 + 0.8\frac{n}{d}) \quad (2.8)$$

The ratio between the latent heat of evaporation (E) and rate of heat exchange by convection (K) is determined by Penman with the assumption that the transport of vapor and heat are controlled by the same mechanism. Vapor transportation

is governed by vapor pressure gradient ( $e'_s - e$ ), and heat exchange is governed by temperature difference ( $t'_s - t$ ) thus  $\frac{K}{E}$  ratio can be approximated as:

$$\frac{K}{E} = B = \frac{\gamma(t'_s - t)}{e'_s - e} \quad (2.9)$$

Where:

$\gamma$  = Psychomotor constant = 0.66 if temp in  $^{\circ}C$  and e in millibar or 0.485 if e is in mm Hg

$e'_s$  = Saturation vapor pressure at temperature  $t'_s$

$t'_s$  = Temperature of surface ( $^{\circ}C$ )

$e$  = Saturation vapor pressure at temperature  $t$

$t$  = Temperature of the air ( $^{\circ}C$ )

Now as:

$$H = E + K = E + E * B = E * (1 + B) \quad (2.10)$$

Then

$$E = \frac{H}{1 + B} \quad (2.11)$$

Penman made use of saturation vapor pressure curve Fig (2.11) in order to eliminate the terms  $(t'_s - t)$  by substitution, as the temperature of the boundary layer isn't practically measured. This approximation is reasonable because small intervals can be considered as a straight line segment and  $(t_s)$  is not far from  $(t)$ . So it can be presented as below:

$$t'_s - t = \frac{(e'_s - e_a)}{\Delta} \quad (2.12)$$

Where:

$\Delta$  = The slope of vapor pressure curve at  $(t)$  as shown in Fig (2.12)

$e_a$ =Actual vapor pressure mm Hg

Hence,

$$B = \frac{\gamma(e'_s - e_a)}{\Delta(e'_s - e)} \quad (2.13)$$



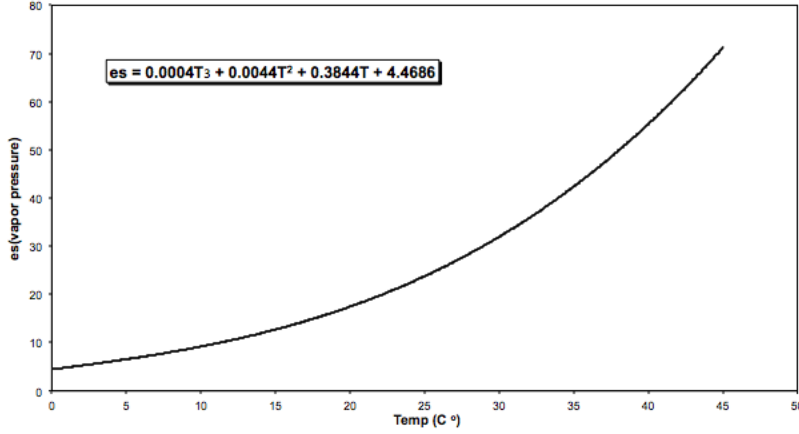


Figure 2.11: Curve showing relation between temperature and vapor pressure[5]

Penman's approach related the previous mentioned hypothetical case, air and water surface have the same temperature, in which the Evaporation rate can be represented as follows :

$$E_a = (e_s - e) * f(u) \quad (2.14)$$

Where:

$f(u)$  is a function of the horizontal wind speed velocity

$E_a$ =Open water evaporation per unit time mm/day

$e_s$ =Saturation vapor pressure of the air at  $t^\circ\text{C}$  (mm mercury)

In general:

$$E = (e'_s - e) * f(u) \quad (2.15)$$

The naturally occurring case is that the water surface and air temperature are of different temperatures. So  $e'_s$  is the saturation vapor pressure of the boundary layer between air and water with a different  $t'_s$  that is virtually impossible to measure.

Then:

$$\frac{E_a}{E} = \frac{e_s - e}{e'_s - e} \quad (2.16)$$

Then can  $(e'_s - e)$  be written in the form:

$$(e'_s - e) = (e'_s - e) - (e_s - e) \quad (2.17)$$

By substituting the value of these relations into equation (2.11) the following form of Penman formula is obtained to represent the evaporation in mm/day by using the Psychomotor constant  $\gamma$ :

$$E = \frac{\Delta * H + \gamma * E_a}{\Delta + \gamma} \quad (2.18)$$

Fig (2.12), Fig(2.13), and Fig(2.14) show that a close correlation between the measured values of evaporation in mm/day from the Siwa, Wadi El Natroon, and Dabaa stations and the calculated values. Therefore, Penman's equation is used in the Ezz El Din's model and also in this proposal for the calculation of evaporation in mm/day obtaining more reliable results than Ball and Bassler.

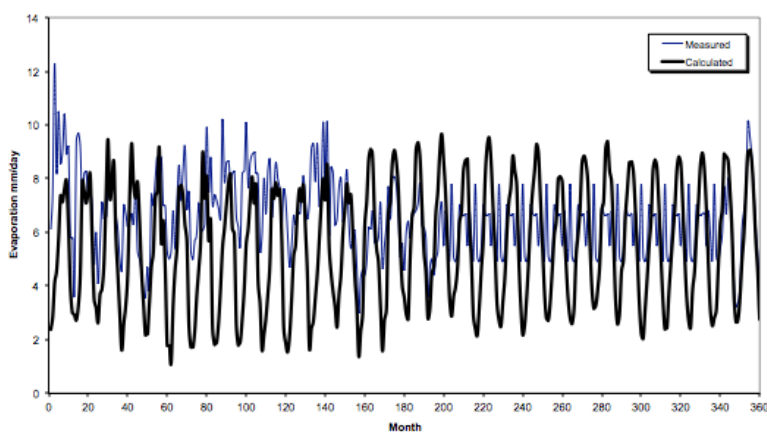


Figure 2.12: Monthly Evaporation in Dabaa station [5]

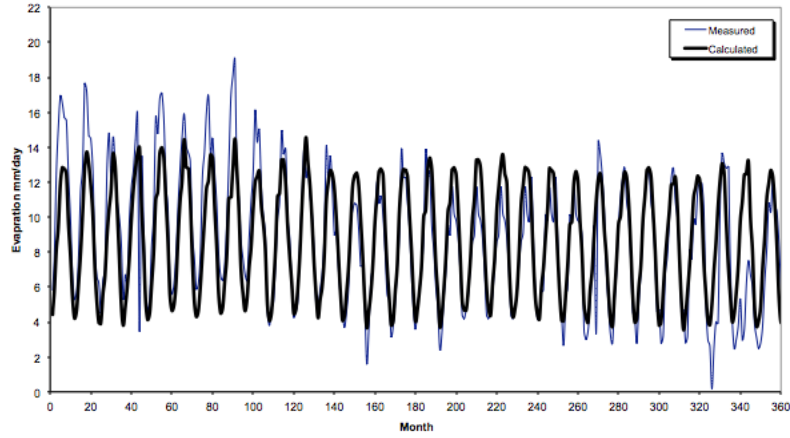


Figure 2.13: Monthly Evaporation in Siwa station [5]

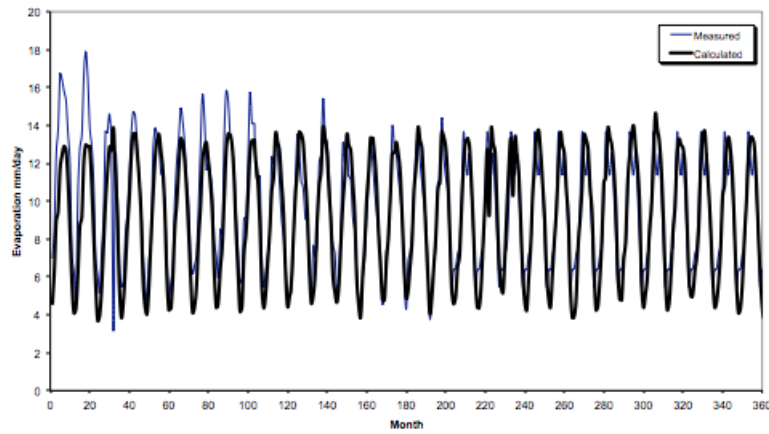


Figure 2.14: Monthly Evaporation in Wadi El Natroon station[5]

### Salinity

A major factor in the study that needs to be understood is the effect of salinity on the evaporation rate. The vapor pressure of a liquid is determined by its temperature and the difference in vapor pressure between water and the atmosphere affects the evaporation rate. Lowering the vapor pressure of water would lower the evaporation rate and the presence of solutes would do just that. According to Raoult's law[9] the pressure of a solution behaves as shown:

$$(P_o - P)/P_o = n_2/(n_1 + n_2)$$

Where:

$P_o$  : vapor pressure of the pure solvent at a given temperature

P : is the vapor pressure of the solution at the same temperature

$n_1$  : Moles of solvent

$n_2$ : Moles of solute

But solutions that obey Raoult's law exactly are called ideal solutions, which are very rare. Hence, it is obvious that the evaporation rate from Qattara is difficult to be calculated theoretically. This is due to many factors affecting the evaporation rate and salts with different percentages and nature that are present in the Qattara Depression[5]. The problem necessitated experimental investigation by Jayy-oussi khalil (1990)[5] to understand the pattern that the evaporation rate in Qattara Depression will adhere to during the plant's life. Seven standard A-pans were used to study the evaporation rate changes with different salt concentrations, the specific gravity (S.G) is used to indicate water salinity level.

Table 2.3: the different specific gravities tested

Pan Number	1	2	3	4	5	6	7
Specific Gravity (S.G)	1.00	1.10	1.15	1.20	1.25	1.30	1.35

Solutions of different salinities were prepared in stainless steel pans painted black to make it similar to the water body in absorption of temperature and radiation. Then the pans were monitored by hydrometers to record the changes in specific gravity of each pan. Also thermometers were used to measure the temperature changes and correlate it to calculate the relative humidity. Wind speed was measured by anemometer and a radiometer was used to measure incoming short wave radiation[5], the detailed effect of salinity will be introduced in the chapter presenting our model.

## 2.2 Geology of Qattara Depression

The area of Qattara Depression has been studied geologically. It is divided into horizontal layers of Miocene to Eocene sediments[2]. As shown in Fig(2.15) the bedrock for large areas is covered with sabkha deposits. The north-eastern part of the depression is formed of sand and clay layers of lower Miocene age. While the south

and west boundaries are formed of white limestone of the Middle Miocene Marmarica Formation. Understanding the different geological features is necessary for such a huge project to define the hydraulic conductivity of each layer that would affect the seepage flow rates. Also, geological features of the land surrounding the depression is necessary to determine the construction costs and time in accordance to the soil and rocks mechanical characteristics. For that reason in 1981 a macro-engineering geological study was published by the Ministry of Electricity and Energy, Arab Republic of Egypt. The geological data gathered for the land area between the Mediterranean Sea to Qattara Depression was necessary to assess the civil infrastructures and the slope stability conditions at the northern depression rim. At the time three main alternatives had been put forward. The first alternative known as the Nuclear Head-race Solution proposed having a canal with a maximum capacity of  $1200 \text{ m}^3/\text{s}$ [2]. The second alternative known as the Head-race Tunnel solution was to use two tunnels of diameter 15.3 m. The third alternative known as the One Way Pumped Storage Solution was based on Bassler's scheme[1] where water is pumped during off peak hours, using electricity from the grid, to a higher reservoir that provides an extra head during peak hours.

Topographic data about Qattara Depression is desperately needed for such a project. Data produced from the Shuttle Radar Topographic Mission elevation data product (SRTM) was used in mapping Qattara Depression[2]. The following procedure was followed to produce the volume and area of Qattara Depression at different altitudes which is necessary for our model. Using the SRTM data a digital elevation model (DEM) file is produced which is imported to Golden Software Surfer that produces the volume and surface area data at different levels[2].

## 2.3 Moghera Aquifer

It is necessary to understand the effect of aquifers, close to the Qattara Depression, would have on the project and what effect the project would have on them.

The Moghera aquifer system is close to Qattara Depression, therefore it is studied

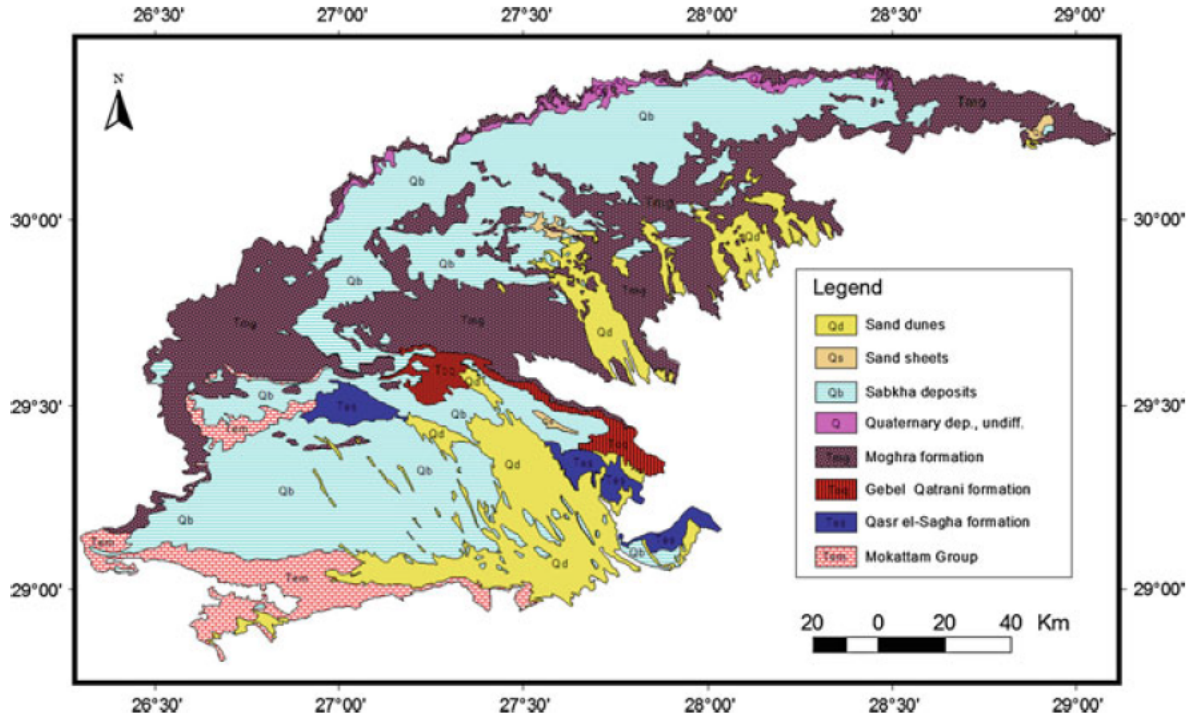


Figure 2.15: Qattara Depression's Geology [2]

to determine what effect of such a project would have[10]. The Moghera aquifer has a porosity of 20% and salinity of 1000 ppm in the east, near the Nile Delta, and 12000 ppm in the west[10], near Qattara Depression. The hydraulic gradients are less than 0.2 m/km and the aquifer has an average thickness of 300 m and is considered a non-renewable aquifer system[10]. Water discharged from the aquifer is evaporated in Qattara and Wadi El Natron depressions and lateral seepage occurs into carbonate rocks in the western part of the Qattara Depression.”The base of the aquifer slopes from ground level near Cairo to 1000 m below mean sea level west of Alexandria. The saturated thickness is between 70 and 700 m.” Transmissivity ranges between 500 and 5000  $m^2/day$ [10].

As shown in Fig(2.16) the water table elevation map shows that the Moghra aquifer flows into the Qattara Depression from the north, east, and south. Pumping tests conducted by Joint-Venture Qattara (1981) showed that the aquifer's horizontal hydraulic conductivity varies from 0.2 m/day to 12 m/day[10]. Due to the anisotropic nature of the Moghra aquifer, the vertical hydraulic conductivity was assumed by Ezzat (1984)

to range from 0.01 to 0.001 m/day of the horizontal hydraulic conductivity[10].

A program was built to model the water level after the proposed Qattara Depression reservoir; in that study the reservoir was at level -60 m below sea level[11]. It was assumed that, the simulations included steady state and transient models. Transmissivity values and boundary conditions were calibrated until the difference between computed and field measured head was less than 2 m[10]. The model predicted that when the Qattara Depression reservoir is steady at -60 m below sea level there will be a direct hydraulic connection with the aquifer. A leakance coefficient of  $9.3 \times 10^{-8}/s$ [11] was obtained by dividing the vertical hydraulic conductivity of the Moghra aquifer ( $4 \times 10^{-3} m/day$ ) by the thickness of sediments between the reservoir's base and the underlying water table (average of 0.5 m)[11]. The evaporation rate from the reservoir was calculated in the model and put into consideration. A rise in the Moghra aquifer's water table was seen in the results of the model due to seepage from Qattara Depression. that has also been anticipated by previous authors among them Ezzat (1982) and Diab(1983). In this study the results show a close agreement with field results from Joint Venture Qattara shown in Fig(2.16)[11]. Also, transmissivity values determined by the model show agreement with field results[11].

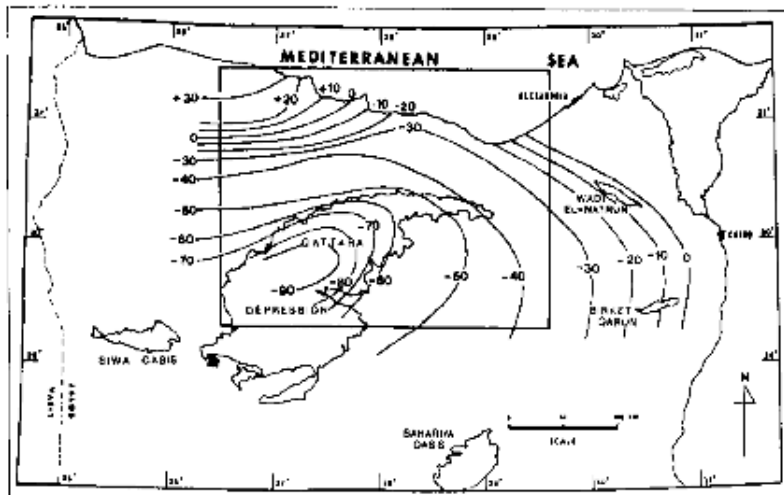


Figure 2.16: Measured water table variations [11]

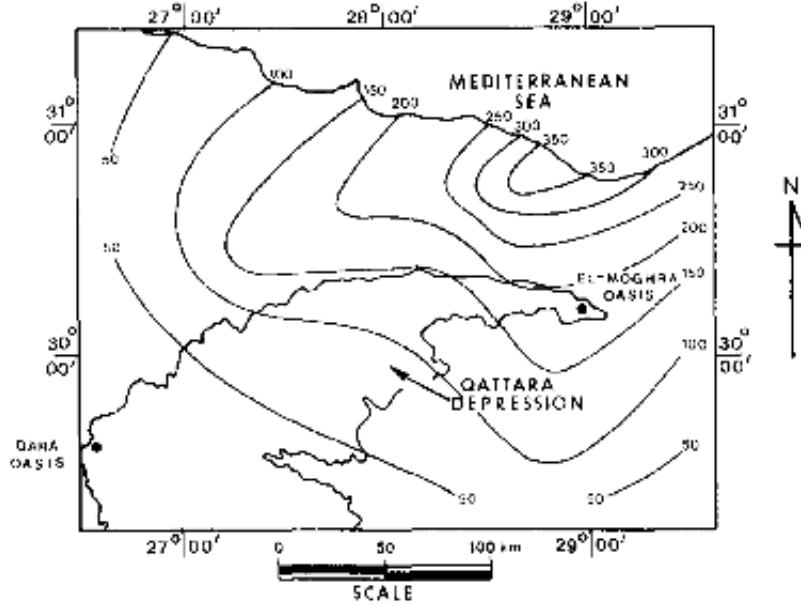


Figure 2.17: Transmissivity map for the Moghra aquifer in ( $m^2/day$ ), determined through model calibration [11]

### 2.3.1 Seepage

The outward seepage flow will be considered in this research and incorporated in the model, to show whether it has a negligible effect or not on the hydro-power plant life. All the other studies neglected the outward seepage calculation, on the ground that, it would affect the lifetime of the plant positively, and not worth calculating. Therefore, an appropriate method had to be chosen for the seepage calculation just as it was done for the evaporation calculation. Hence, different types of seepage estimations were considered and the most appropriate was chosen.

Burcharth and Andersen [12] discuss the history of seepage calculation methods for different scenarios. The flow through porous media is discussed for steady flow, where the Navier-Stokes equations are the basis used from which derivations are obtained. Also turbulent flow equations are suggested with their derivations based on a pipe analogy and dimensional analysis. While for non-steady state flow which is the case in this research the derivations are based on a cylinder/sphere analogy leading to a virtual mass coefficient. The virtual mass coefficient is chosen according



to experimental data available however it is not conclusive because the data available is scarce[12].

Various classifications of the flow are available, i.e. "creeping flow, laminar flow with non-linear convective inertia forces and fully turbulent flow. These flow regimes are referred to as the Darcy, the Forchheimer and the fully turbulent flow regimes, respectively"[12], each regime will explained.

### **Stationary flow**

First Darcy defined empirically the relation between the hydraulic gradient (I) and the discharge velocity (V) through porous sands and sandstones by the following equation:

$$V = KI \tag{2.19}$$

Where:

K= permeability coefficient (m/s)

This is known as Darcy's law and it applies to laminar flow without the convective inertia forces, i.e. creeping flow.

Results of physical models were presented by Dybbs and Edwards (1984). Porous objects such as Plexiglas spheres in a hexagonal packing and glass and Plexiglas rods arranged in a complex, fixed three-dimensional geometry were used and both water and oil were used for testing. Based on the results four flow regimes were identified.

1. The Darcy or creeping flow regime occurs at  $Re \leq 1$ . It is mainly dominated by viscous forces and the exact nature of the velocity distribution is determined by local geometry
2.  $Re$  between 1 and 10 initiates the inertial flow regime that persists to  $Re$  150
3. Between  $Re$  150 and 300 an unsteady laminar flow regime persists
4.  $Re$  above 300 leads to a turbulent flow

In [12] these regimes were denoted as the Darcy flow regime, the Forchheimer flow regime, while the third regime was considered a transitional phase between the Forchheimer flow regime and the fully turbulent flow regime. The below equation was presented to express flow by Forchheimer.

$$I = aV + b|V|V \quad (2.20)$$

Where a and b are coefficients presented differently by many authors.

### Non-stationary flow

The Forchheimer expression is extended with an inertia term as shown below in the case of unsteady flow in coarse granular media[12]

$$I = aV + b|V|V + C\frac{dV}{dt} \quad (2.21)$$

The inertia terms vary with porosity just as in the stationary flow. But, macroscopic convective accelerations appear next to the local acceleration  $\frac{dV}{dt}$ . While considering porous flow, local and macroscopic convective accelerations must be treated separately.

### Turbulent flow equation

Where coefficients depends on Re, the gradation and the grain size, and also depends on the relative surface roughness.

$$-\frac{1}{\rho g} \frac{dp}{dx} = \frac{1 + C_m^* \frac{1-n}{n}}{g} \frac{dV}{dt} \quad (2.22)$$

$$\frac{d^2h}{dz^2} = (\alpha + n\beta) \frac{\gamma}{k} \frac{dh}{dt} \quad (2.23)$$

The virtual mass coefficients ( $C_m^*$ ) selected from various tests are presented in [12] and (n) is the porosity defined as the fluid volume divided by the total volume. However, it was concluded that the results are too scarce to form definite conclusions about the values of the virtual mass coefficient, thus, it is not used in this proposal.

## 2.4 Alternative Resources and Economic Studies

The economic analysis of the project is a very important aspect as according to the results it would be decided whether this project would be economically feasible, and what it would add to Egypt's central grid. Ragheb [13] and Ezz El Din [5] discussed some economic issues concerning the project that have to be considered. By examining the use of different energy sources in the project and the impact these energy sources would have on the project design and cost.

### 2.4.1 Solar Energy

From the Fig (2.18) it is observed that the Sahara desert provides optimal conditions for solar power usage. This solar energy could be used for a solar pond and for water desalination. Water desalination could be performed either directly or indirectly. In the direct method a solar collector is used along with a distilling mechanism; this method is expensive because of the high cost of property and material used in construction. While the indirect method consists of a solar collection array and a separate desalination plant, for example a reverse osmosis plant. And this could be an economic aspect and it can also be used to power the pump if a pumped hydro storage scheme is to be used [13].

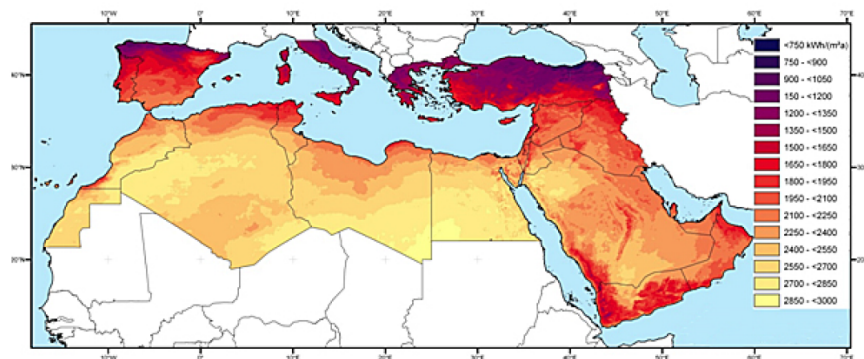


Figure 2.18: Annual Integrated Direct Normal Irradiation  $\text{kWh}/\text{m}^2.\text{yr}$  [13]

## 2.4.2 Wind

The power content of a wind stream is  $P = \frac{1}{2}\rho SV^3 = \frac{1}{2}\rho\frac{\pi D^2}{4}V^3$

Where:

P = rated turbine power in watts (W)

$\rho$  = air density in ( $kg/m^3$ )

S = swept area of the turbine in ( $m^2$ )

D = turbine diameter in (m)

V = wind speed in (m/s)

The high capital that would be used in the installation of wind turbines is compensated by a zero cost for the fuel and low maintenance costs. That would lead to many jobs that would be provided in their manufacture, construction, operation and maintenance. From the figure below the wind energy that could be obtained from this area is shown, producing up to 200 TW/yr[13]. But, wind has the problem of being too intermittent making it paramount to use solar energy next to it.

As shown in the schematic below in Fig (2.20) the size of the Deir Kourayim Reservoir would have to be enlarged but compared to the excavation of the tunnels the reservoirs can be much easily achieved by small chemical explosions that are much more economical[13]. As it is seen in Fig(2.20) wind turbines can be used to pump the water to the reservoir. It was suggested that if the below pipe excavation project is compared to previous projects it would be more economical. The price had been estimated to be about 24,750 \$/m for the tunnel cost, which is \$1.98 billion for the 80 km tunnel in the Qattara Depression[13]. Although, nuclear excavation would be cheaper, but that wouldn't be an option for political concerns[13]. That estimation has been done by Fermilab, Illinois, funded by the USA department of energy[13].

In this design the cost of the wind farm has to be considered. The cost would be \$1.2 million per installed rated MW of power[13]. With an installed rated power of 3,800 MW, therefore the wind farms would cost approximately about \$4.56 billion by adding the cost of the five pipes of the wind turbines the total cost reaches \$5.52 billion[13]. In order to compare the economic side of each design the cost per



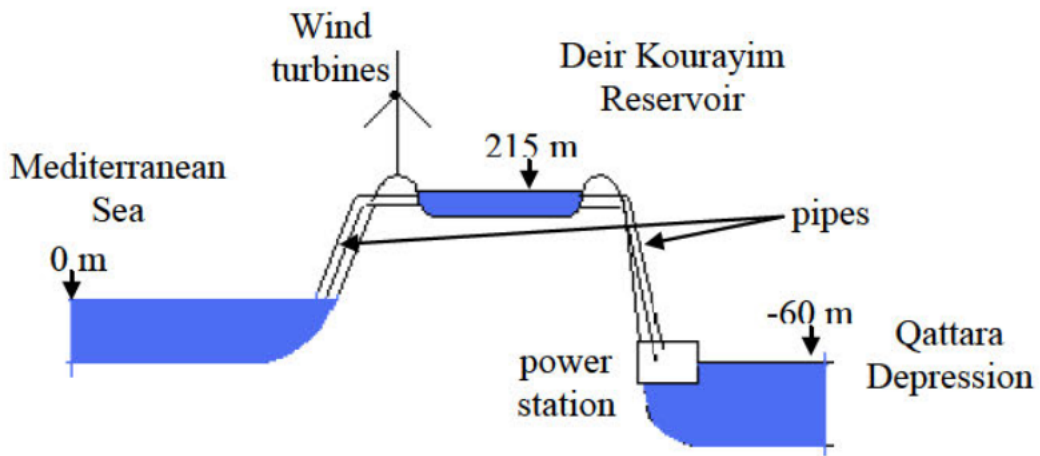


Figure 2.20: Proposed approach with wind turbines and pipes at the Qattara Depression [13]

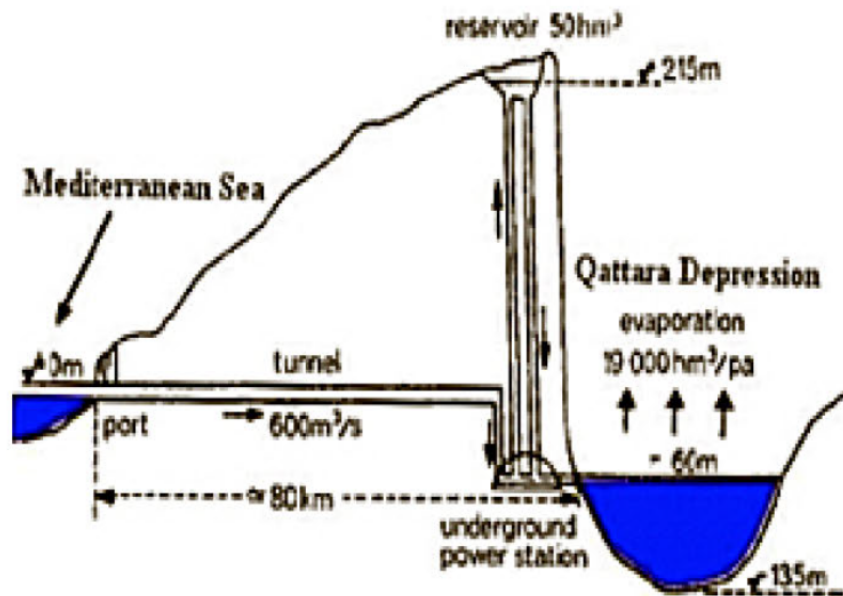


Figure 2.21: Previously suggested design for pumped storage [13]

unit power generated also has to be calculated and the proposed design with wind farms is more economical because it has a much greater power output and much less cost per unit installed capacity[13]. The hydro power unit would have a theoretical hydroelectric potential of 160 MW to generate 1.2 billion kW.hr per year of electrical energy with an installed capacity of 480 MW and operating at peak power for 8 hours per day[13]. The economical reasoning used by this Ragheb[13] is very close the economical reasoning that will be shown in the chapter Economic analysis in this proposal.

Table 2.4: Economic comparison between the two designs

	Tunnelling Approach	Proposed Pipes+Wind farms
Capital cost (excluding the power block and the pipes between reservoir and depression)	\$1.98 billion	\$5.52 billion
Average power output	338 MWe	1,550 MWe
Initial cost per unit of installed capacity	5,860 \$/MWe	3,560 \$/MWe

### 2.4.3 Mohamed Ezz el Din's Cost Analysis

As has been previously shown there are several paths proposed for the project some consist of tunnels some of canals and some of both. As previously mentioned, all components of the of the hydropower station have to be considered, these components were included in Ezz el Din's study. Intake structures, Trash racks, Gates and valves, Tunnels and penstocks, Water hammer and surge tanks, Powerhouse, Turbines, and pumps.

The data presented below shows the prices at the time of Ezz El Din's study that were used in his economic study, these prices have increased nowadays and the updated prices will be used in this proposal, as will be seen in the economic analysis chapter.

Table 2.5: Cost estimates

Earth Excavation	50 LE/ $m^3$
Concrete works	500 LE/ $m^3$
Penstock steel	3000 LE/ton
Machines	500 LE/hp

Using these values the total cost of the project was calculated by Ezz El Din[5] for all the alternatives including base load scheme, peak load scheme and mixed pumped hydro storage using the benefit cost ratio internal rate of return.



# Chapter 3

## Qattara Depression Evaporation, Salinity, Seepage and Channel Flow Models

The model is used to track the meteorological data and calculate the solar radiation at different time steps and use that to calculate the evaporation. But, other sub-models are used, for example, a topography model is used to track the change in area and elevation with time and a salinity model is used to track the salinity changes with time and its effect on the evaporation. A channel flow model is used to model the flow of water as a channel until it reaches the depression as according to the breadth and height of the channel it would be investigated what changes it would have on the evaporation. Lastly a seepage model is used to model the outward seepage that occurs during with time in the lifetime of the plant.

### 3.0.1 Solar Radiation Model

Meteorological data from Siwa, Dabaa, and Wadi El Natroon weather stations were obtained for a 30 year span, from 1970 to 2000[5]. Among the different radiation models, it was found by Ezz El Din that Penman's theory [5] provided the best estimate for our model, as previously explained. The theory is based on two assumptions, firstly

that there has to be a supply of heat for latent heat of vaporization, and secondly, a mechanism for the removal of the vapor. Penman's mathematical representation used for obtaining the net amount of radiation energy on the surface of the depression is as follows:

$$H = R_a * (0.18 + 0.55 \frac{n}{d}) * (1 - 0.06) - 117.79 * 10^{-9} * T_a^4 * (0.47 - 0.077 \sqrt{e}) * (0.2 + 0.8 \frac{n}{d}) \quad (3.1)$$

Where:

$R_a$  = Mean incident solar radiation at the top of the atmosphere on a horizontal surface  $W/m^2$

H = Net radiation flux gained at free water surface in  $W/m^2$

$T_a$  = Absolute temperature =  $t^{\circ}C + 273$

e = Actual vapor pressure of air in mm Hg

n = Actual duration of bright sunshine (hours)

d = Maximum possible hours of bright sunshine (mean value), this value is a function of latitude ( $\phi$ )

a = A constant depending upon the latitude ( $\phi$ ) and equals to  $(0.29 * \cos \phi)$  which equals 0.18 in the above equation

The constant 0.06 represents the reflection coefficient and the constant  $117.9 * 10^{-9}$  is the Lummer and Pringsheim constant ( $g.cal/cm^2/day$ ) which multiplied by the following terms represent the  $R_B$  which is the radiation from the earth surface. The values of d along the year are obtained from the Table 3.1 and the latitudes and longitudes of each station are also shown in Table 3.2 which are necessary in the calculation of radiation, and the number between the brackets for each location indicates the station number. In our model instead of using Canberra Australia, as Ezz El Din[5] did for the close correlation, the constant (a) is calculated in this model for the location of Qattara Depression, but it shows a very close correlation with average Ezz El Din[5] used.

Or the number of sunshine hours can be obtained by the equation below which

Table 3.1: Mean daily maximum hours of sunshine for different months and latitudes [5]

Latitude	North	Jan.	Feb.	March	April	May	June	July	Aug.	Sept.	Oct.	Nov.	Dec.
	South	July	Aug.	Sept.	Oct.	Nov.	Dec.	Jan.	Feb.	March	April	May	June
50°		8.5	10.1	11.8	13.8	15.4	16.3	15.9	14.5	12.7	10.8	9.1	8.1
48°		8.8	10.2	11.8	13.6	15.2	16.0	15.6	14.3	12.6	10.9	9.3	8.3
48°		9.1	10.4	11.9	13.5	14.9	15.7	15.4	14.2	12.6	10.9	9.5	8.7
44°		9.3	10.5	11.9	13.4	14.7	15.4	15.2	14.0	12.6	11.0	9.7	8.9
42°		9.4	10.6	11.9	13.4	14.6	15.2	14.9	13.9	12.5	11.1	9.8	9.1
40°		9.6	10.7	11.9	13.3	14.4	15.0	14.7	13.7	12.5	11.2	10.0	9.3
35°		10.1	11.0	11.9	13.1	14.0	14.5	14.3	13.5	12.4	11.3	10.3	9.8
30°		10.4	11.1	12.0	12.9	13.6	14.0	13.9	13.2	12.4	11.5	10.6	10.2
25°		10.7	11.3	12.0	12.7	13.3	13.7	13.5	13.0	12.3	11.6	10.9	10.6
20°		11.0	11.5	12.0	12.6	13.1	13.3	13.2	12.8	12.3	11.7	11.2	10.9
15°		11.3	11.6	12.0	12.5	12.8	13.0	12.9	12.6	12.2	11.8	11.4	11.2
10°		11.6	11.8	12.0	12.3	12.6	12.7	12.6	12.4	12.1	11.8	11.6	11.5
5°		11.8	11.9	12.0	12.2	12.3	12.4	12.3	12.3	12.1	12.0	11.9	11.8
0°		12.1	12.1	12.1	12.1	12.1	12.1	12.1	12.1	12.1	12.1	12.1	12.1

represents the time between sunrise and sunset.

Table 3.2: The Latitude and Longitude of each station

Station	Dabaa (309)	Wadielnatron (357)	Siwa (417)
Latitude	30.56	30.24	29.12
Longitude	28.28	32.22	25.29

### 3.0.2 Evaporation Model

As shown equation (3.1) can be used to calculate the net radiation flux (H) at Qattara Depression, with the value of (d) obtained from table 3.1. The value of ( $R_a$ ) is easily derived as it is the extra terrestrial solar radiation; the values of (e),(n) and ( $T_a$ ) can be obtained from each weather station used around Qattara Depression. The data used from each weather station is shown in Fig(3.1-3.3). The following form of Penman formula is used in the model to obtain the evaporation rate in mm/day:

$$E = \frac{\Delta * H + \gamma * E_a}{\Delta + \gamma} \quad (3.2)$$

Where:

E= Evaporation in mm/day

$\Delta$  = The slope of vapor pressure vs temperature curve as shown in Fig (2.11)

$E_a$ =Evaporation rate using Dalton's equation (2.14) of the boundary layer above the water surface in mm/day

$\gamma$ = psychomotor constant = 0.66 if temp in  $^{\circ}C$  and e in millibar or 0.485 if e is in mm Hg

Hence using equation (3.2) for the evaporation, for the variations in the monthly water storage were obtained by Ezz El Din [5] using the below equation:

$$\Delta S = P * A + Q_s + Q_{in} - Q_{out} - E * A * \Delta t \quad (3.3)$$

Where:

$\Delta S$ =monthly change in Qattara Depression accumulated water ( $m^3$ )

P=monthly mean precipitation ( $m/day$ )

$Q_s$ =monthly mean subsurface inflow ( $m^3/day$ )

$Q_{in}$ =monthly mean discharge to be conveyed from the sea ( $m^3/day$ )

$Q_{out}$ =monthly mean discharge to be pumped out (when applicable) ( $m^3/day$ )

E=monthly mean evaporation rate from sea surface ( $m/day$ )

A=Qattara Depression surface area at corresponding level ( $m^2$ )

$\Delta t$  =Time interval (month)

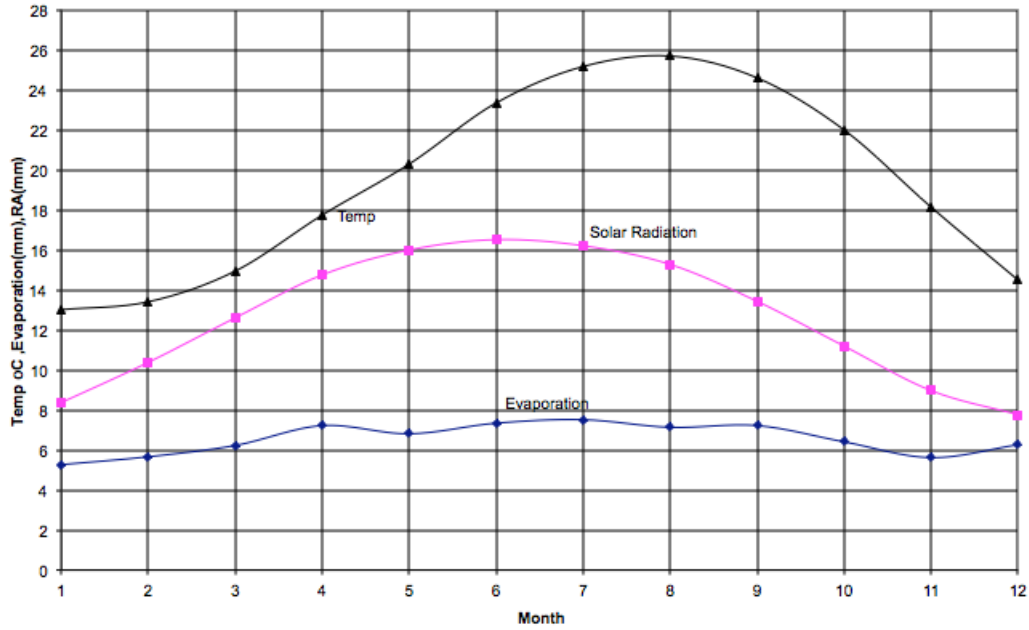


Figure 3.1: Meteorological Data from el Dabaa station [5]

The subsurface inflow was estimated to be  $(Q_s)$  57.5 million  $m^3/year$ [5]. While  $(Q_{out})$  represents the discharge to be pumped back to the sea. The latter term is based on a proposal by Ezz El Din [5] to pump water from the depression back to the Mediterranean Sea since his calculations showed that the evaporation rate at some point is negligible due to the increase in salinity. This is in direct contrast to what Ball and Bassler deduced which is that the evaporation would continue and would balance with the inflow.  $(Q_{out})$  is not considered by the author in his model due to its high cost, therefore the term is taken as zero.

Figures (3.1-3.3) show monthly meteorological data from each of the stations that was used in the model. According to the proximity of each station to the Qattara Depression the values that is set up on monthly time steps in accordance with the values of the rain and evaporation of the Wadielnatroon, Dabaa and Siwa stations are assigned weighting factors of 0.15,0.2,and 0.65, respectively.

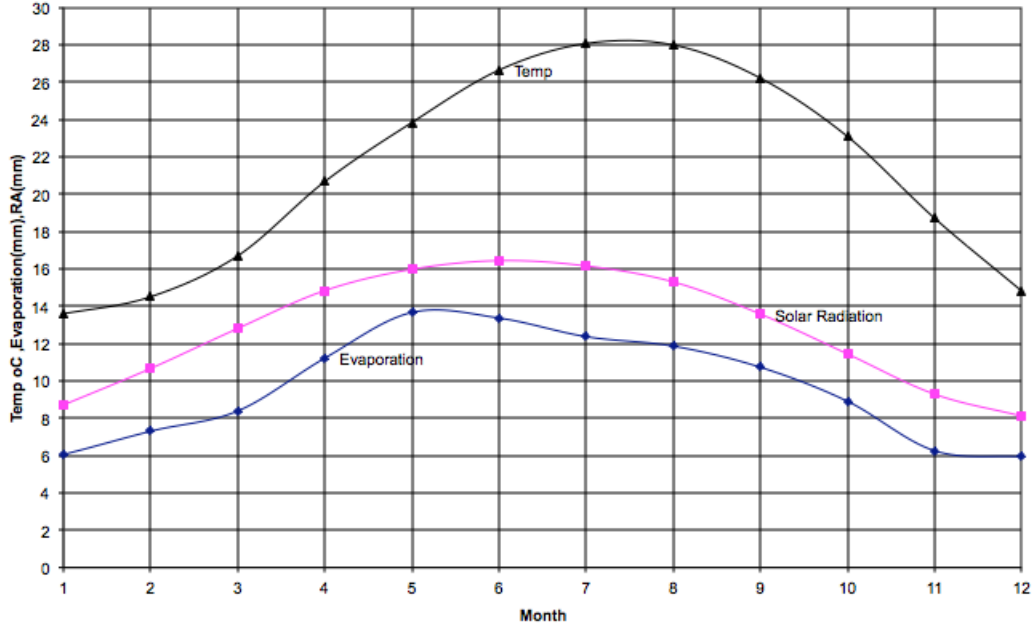


Figure 3.2: Meteorological Data from Wadi El Natroon station [5]

### 3.0.3 Topography Model

It was previously mentioned that using the Shuttle Radar Topographic Mission (SRTM) and its digital elevation model (DEM) file produced by the golden software [2] a relation between the area and the elevation was obtained. As shown in Fig (3.4) the surface area (A) has a relation with the surface elevation (L) from which the following functions are deduced and used in the model progression to track the increase in the surface level elevation as time progresses[2]:

$$A = 117.5 * L + 19500 \text{ for } (-40 \leq L \leq 0)$$

$$A = 0.0085 * L^4 + 2.1211 * L^2 + 7286.7 * L + 118522 \text{ for } (-90 \leq L \leq -40)$$

$$A = 463073 * e^{0.0682 * L} \text{ for } (-120 \leq L \leq -90)$$

Where:

A = Total area of the Qattara Depression surface ( $m^2$ )

L= Surface level of the Qattara Depression (m)

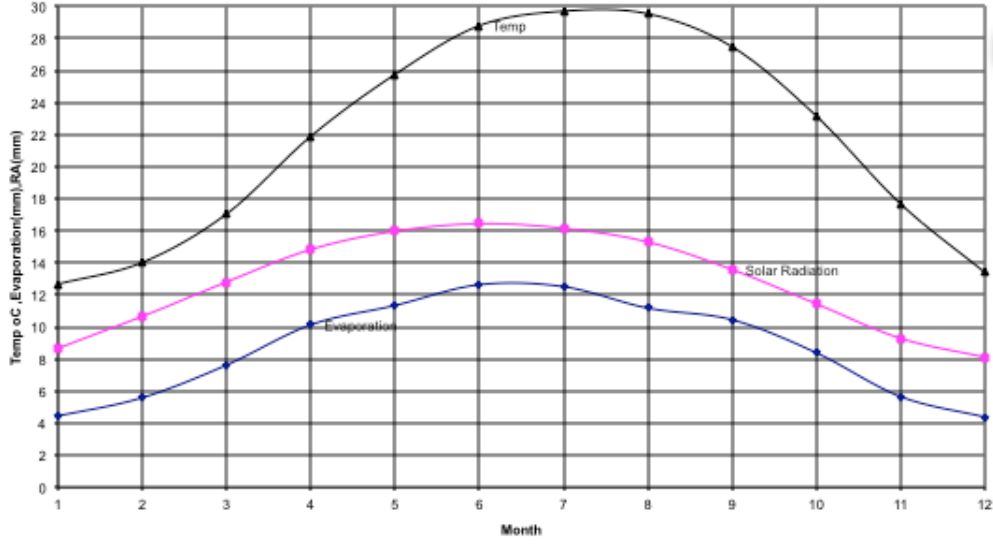


Figure 3.3: Meteorological Data from Siwa station[5]

Hence, our model can track the progressive increase in elevation in the Qattara Depression, while keeping track of the surface area ( $A$ ) that is needed to determine the evaporation, and also keeping track of the volume ( $V$ ) in Fig (3.5) needed in calculations to determine the progressive increase in salinity.

### 3.0.4 Salinity Model

However, a factor, that had previously been neglected in earlier studies, is the salinity that would progressively increase leading to a decrease of the evaporation rate, which in turn would lead to a rise in water level and consequent decrease in head available and therefore power output. Specific gravity of the sea water entering Qattara depression ( $S.G$ ) is taken as 1.025 as this represents the ( $S.G$ ) of the Mediterranean Sea. Variations in the specific gravity of the Qattara Depression lake ( $g_s$ ), were considered in calculations using the general equation shown below:

$$S.G = \frac{\Delta S * g_s + V_o * S.G_o}{V_o + \Delta S} \quad (3.4)$$

Where:

$S.G_o$  = Initial value of specific gravity in the lake in the time step

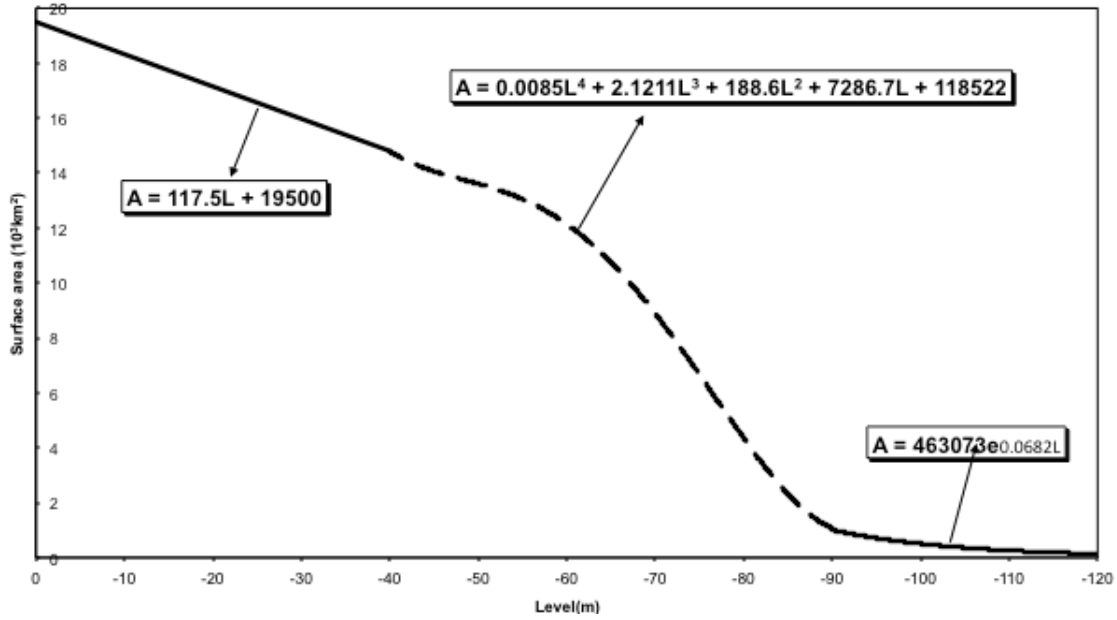


Figure 3.4: Area change with level [5]

$V_o$  = Initial volume of sea water in the lake in the time step ( $m^3$ )

$g_s$  = The specific gravity for the differential volume added each time step to the lake

$\Delta S$  = Change in volume of water i.e the differential volume ( $m^3$ )

Equation was used in Ezz El Din's model was found to be very approximate so for more accuracy in our model the following equations are used.

$$C = \frac{\text{mass of salt}}{\text{volume of water}} \quad (3.5)$$

Where:

C: Instantaneous salt concentration in reservoir

$$\delta C = \frac{dC}{dm_{salt}} * \delta m_{salt} + \frac{dC}{dV} * \delta V \quad (3.6)$$

$$\delta m_{salt} = [V_{sea} * C_{sea} + \sum V_{si} C_{si} - (V_{so} + V_{pumped})C] \quad (3.7)$$



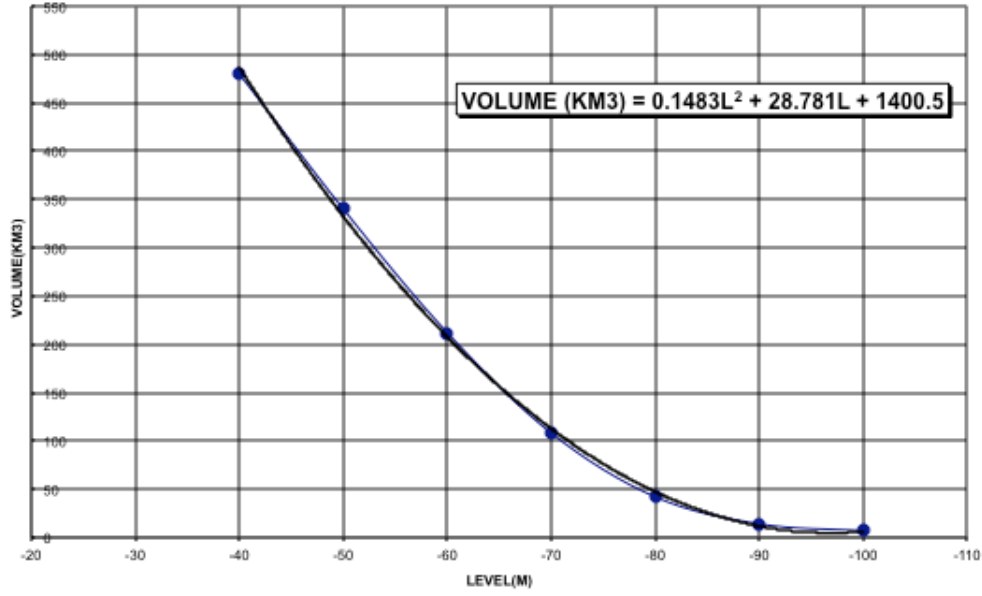


Figure 3.5: Volume change with Level [5]

$$\frac{dc}{dt} = \frac{1}{V} [V_{sea} * C_{sea} + \sum V_{si} C_{si} - (V_{so} + V_{pumped}) C] - \frac{m_{salt}}{V^2} [V_{sea} + V_{rain} + \sum V_{si} - V_{so} - V_{evap} - V_{pump}] \quad (3.8)$$

Where:

$\frac{dc}{dt}$  = Rate of change of salinity

V = Volume of water ( $m^3$ )

$V_{sea}$  = Flow rate of sea water entering the depression ( $m^3/month$ )

$C_{sea}$  = Salinity of the sea in  $kg/m^3$

$V_{si}$  = Flow rate of water entering the depression through seepage ( $m^3/month$ )

$C_{si}$  = Salinity of the inward seepage in  $kg/m^3$

$V_{so}$  = Flow rate of water leaving the depression through seepage ( $m^3/month$ )

$V_{pumped}$  = Flow rate of sea water pumped out of the depression ( $m^3/month$ )

C = Salinity  $kg/m^3$

$m_{salt}$  = Mass of salt in kg

$V_{rain}$  = Flow rate of water entering the depression through rain ( $m^3/month$ )

$V_{evap}$  = Flow rate of water leaving the depression through evaporation ( $m^3/month$ )

The predictor corrector method is then used in matlab for equation to obtain

accurate values for the C in every time step which is then converted to specific gravity to find the effect of salinity on the evaporation rate.

The table below shows a representation for the change of the depression filled water versus height. The calculated area and volume from the surfer software are plotted against the altitude, and for each range of altitudes equations are generated from the plot that are used in the model, to track volume and area changes with time and surface level progression. It is observed from the results that 80% of the depression volume is contained between contours 0 and -60 m, and that below contour line -70 m the volume becomes negligible.

Table 3.3: Variation of the volume and area with the altitude [2]

Altitude (m)	Volume (km <sup>3</sup> )	Percent of volume (%)	Surface area (km <sup>2</sup> )
0	1,213	100	19,605
-10	1,021	84	18,692
-20	839	69	17,646
-30	668	55	16,573
-40	508	42	15,405
-50	360	30	14,065
-60	227	19	12,510
-70	113	9.3	9,740
-80	39	3.2	4,652
-90	15	1.3	1,314
-100	6.3	0.5	526
-110	2.8	0.2	236
-120	0.8	0.07	153

### 3.0.5 Chanel Flow

Fig (3.6) shows the set of contour lines for Qattara Depression generated from SRTM elevation data. The topographic data shows that the depression is relatively flat, but the western side is rough and irregular. And the slope at the borders of the depression is aggressive which would provide inertia for the seawater at the entrance.

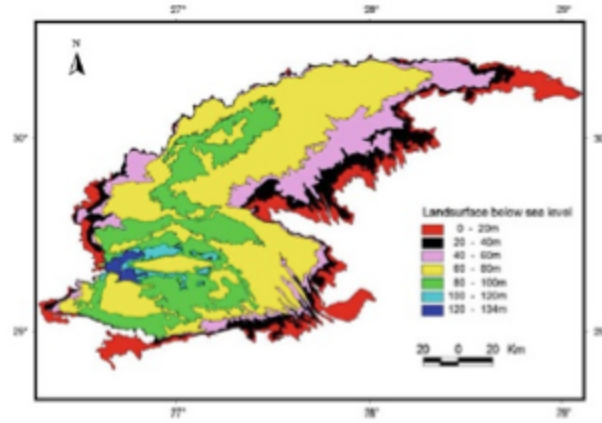


Figure 3.6: SRTM data [2]

The study shows that the maximum width from north to south is 145 km at longitude 27°30'E[2] . While the maximum length from east to west is 300 km at approximately latitude 29°45'N. The deepest point is at 134 b.m.s.l.[2], and is located at the depression's western corner (29°23'33"N. latitude by 26°43'57"E. longitude)[2] . In our model the sea water flowing out of the turbines is assumed to follow a channel like flow towards the lowest point in the depression. Analysis of the topography of the depression indicates a slope of approximately 0.4 m/km. Moreover the terrain is assumed to have a manning coefficient  $n=0.035$  based on comparison with similar terrains. The effect caused by this channel on the filling scenario has never been studied before. Manning's formula for channel flow was used as shown below.

$$Q = \frac{1}{n} * A * R^{\left(\frac{2}{3}\right)} * \sqrt{S} \quad (3.9)$$

Where:

Q = Flow Rate ( $m^3/s$ )

V = Velocity (m/s)

A = Flow Area ( $m^2$ )

n = Manning's Roughness Coefficient

R = Hydraulic Radius (m)

S = Channel Slope (m/km) taken as 0.4 m/km

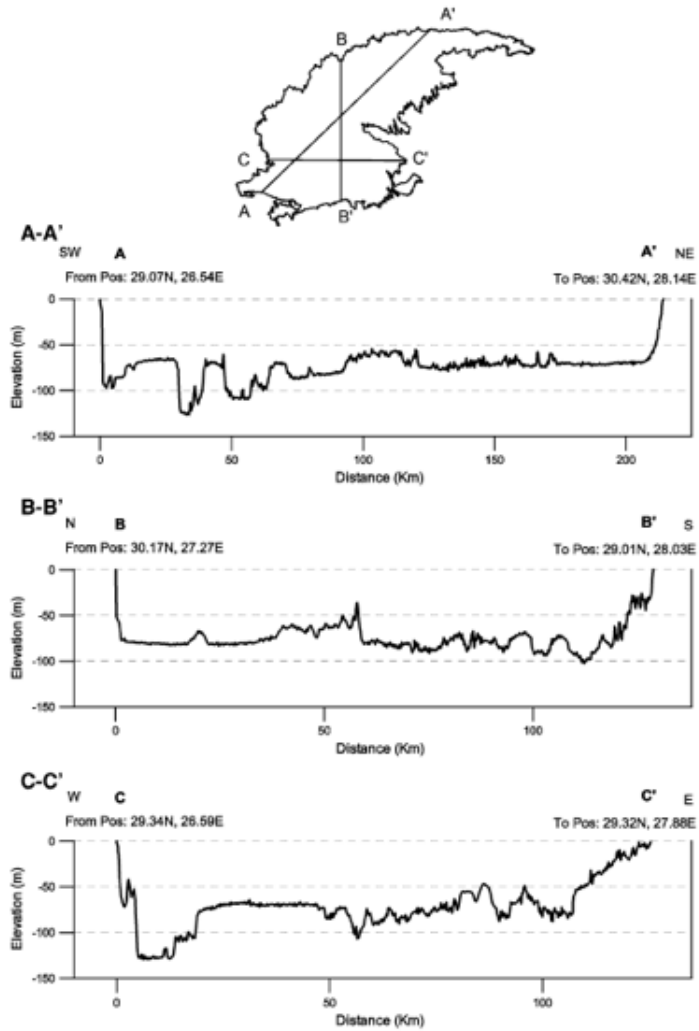


Figure 3.7: Topography [2]

$$R = \frac{A}{P} = \frac{b * h}{2h + b} \quad (3.10)$$

Where:

P=Perimeter (m)

b=breadth(m)

h=height(m)

Since:

$$Q = V * A \quad (3.11)$$

Therefore:

$$V = \frac{1}{n} * R^{\left(\frac{2}{3}\right)} * \sqrt{S} \quad (3.12)$$

From the given topography (h) can be considered in the range of 0.5 to 2 m, with (b) ranging from 378 to 3810 m. These values are used in the model to see if the channel would have an effect on the filling scenario and the evaporation rate and also to estimate the time the journey would take to reach the lowest point in the Qattara Depression, the latter was found to be of the order of 2 days.

### 3.0.6 Effect of Salinity on Evaporation Rate

The value of the salinity obtained from each run is used to calculate the specific gravity of the downstream reservoir water, from which the evaporation factor is derived according to Fig (3.8)[5] . This factor is multiplied in the model to the value of evaporation calculated and it can reach zero if the salinity of the water reaches a certain threshold.  $E_s$  represents the value of evaporation at the salinity reached in Fig (3.8) and  $E_o$  represents evaporation at normal conditions.

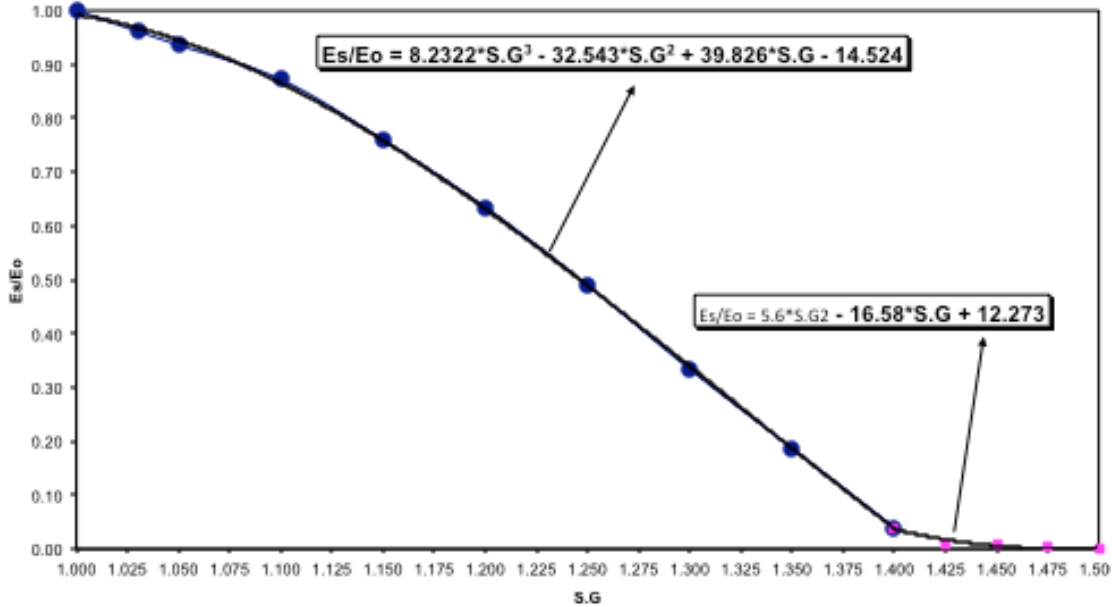


Figure 3.8: Evaporation factor [5]

Jayyoussi-khalil (1990)[5] observed that when the specific gravity (S.G) increases the evaporation rate decreases. Such a relation could have a tremendous effect on the Qattara Depression plant life as it depends greatly on evaporation for the balance of the water level. Therefore, the curve prepared shows the relation between the relative evaporations  $E_s/E_o$  versus the specific gravity S.G as shown in Fig (3.8). It can be seen from Fig (3.8) that  $E_s/E_o$  diminishes to zero as S.G approaches 1.5 and the equations shown on the curve are used in our model and are shown below.

For  $S.G < 1.4$

$$\frac{E_s}{E_o} = 8.2322 * S.G^3 - 32.543 * S.G^2 + 39.826 * S.G - 14.524 \quad (3.13)$$

For  $1.4 < S.G < 1.5$

$$\frac{E_s}{E_o} = 5.6 * S.G^2 - 16.58 * S.G + 12.273 \quad (3.14)$$

Ezz El Din[5] proposed the use of those equations in the Qattara Depression model. As shown in Fig (3.9) to Fig (3.21) for the year 1999 evaporation in (mm/day) for different specific gravity values is plotted for Dabaa, Wadielnatron and Siwa stations. The figures showed consistency with changes in the climatic factors such as average daily temperature, the wind velocity, and the relative humidity. Therefore, these equations have been used by Ezz El Din [5] and in this proposal with some confidence.

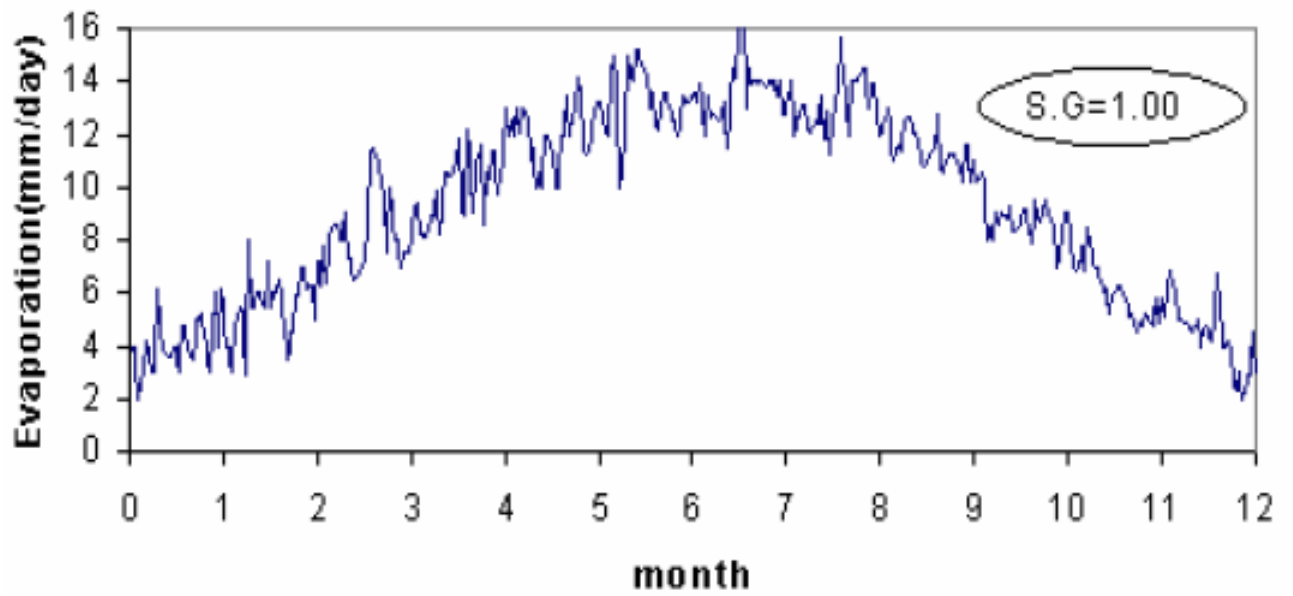


Figure 3.9: Evaporaion rate Wadi El Natron 1999 S.G= 1[5]

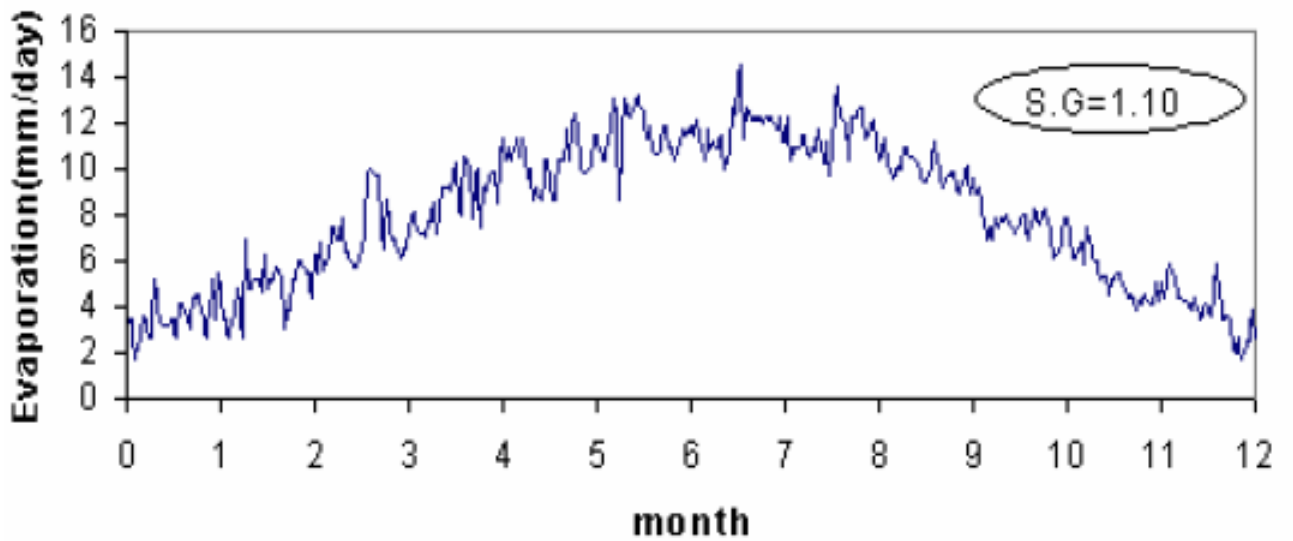


Figure 3.10: Evaporaion rate Wadi El Natron 1999 S.G= 1.1[5]

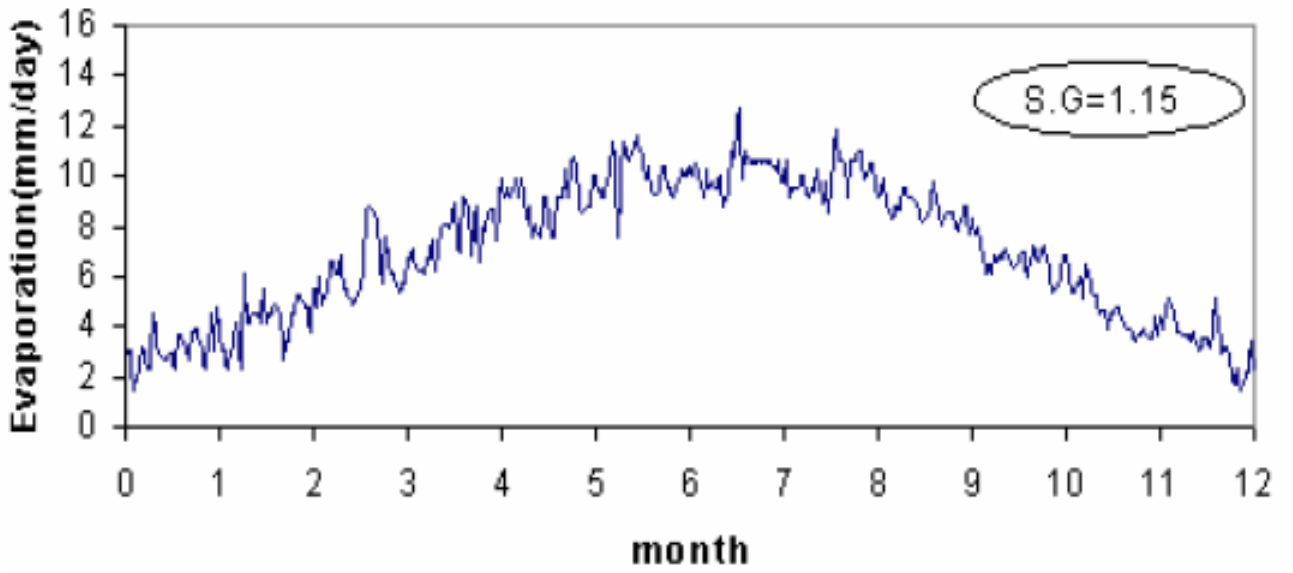


Figure 3.11: Evaporaion rate Wadi El Natron 1999 S.G= 1.15[5]

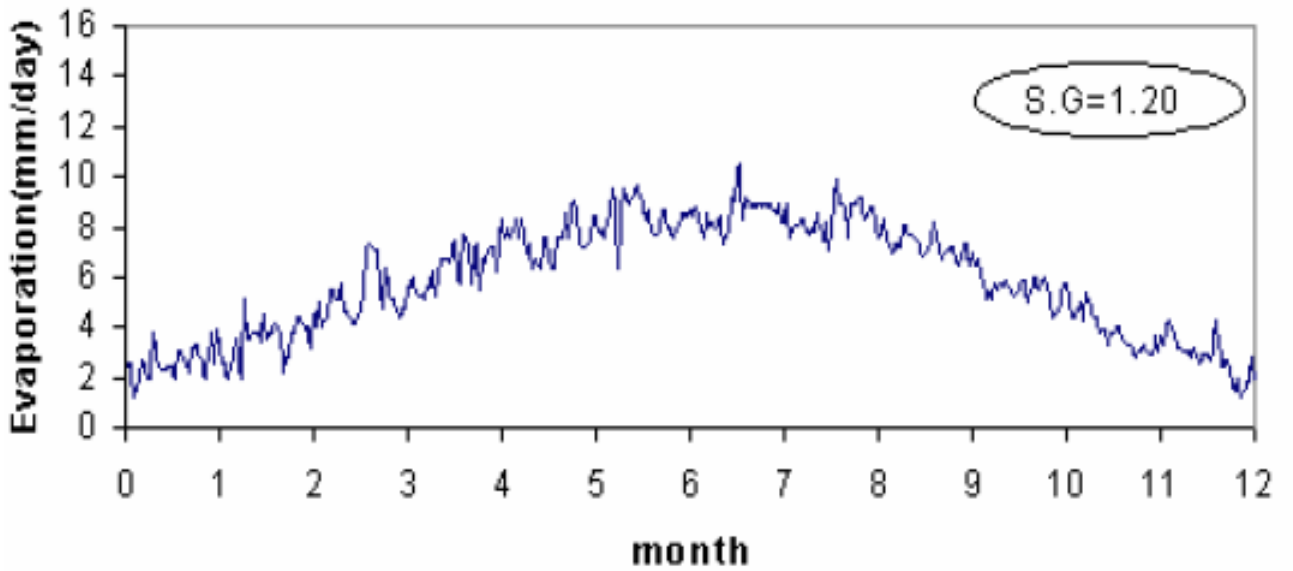


Figure 3.12: Evaporaion rate Wadi El Natron 1999 S.G= 1.2[5]



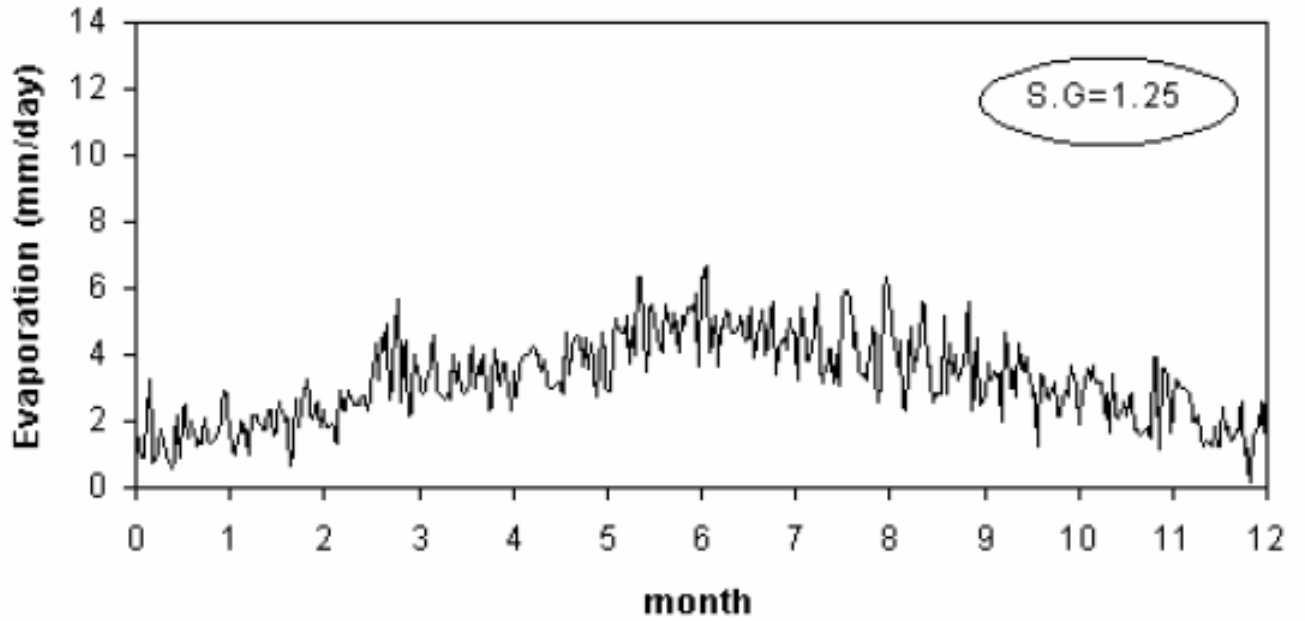


Figure 3.13: Evaporation rate Dabaa 1999 S.G= 1.22[5]

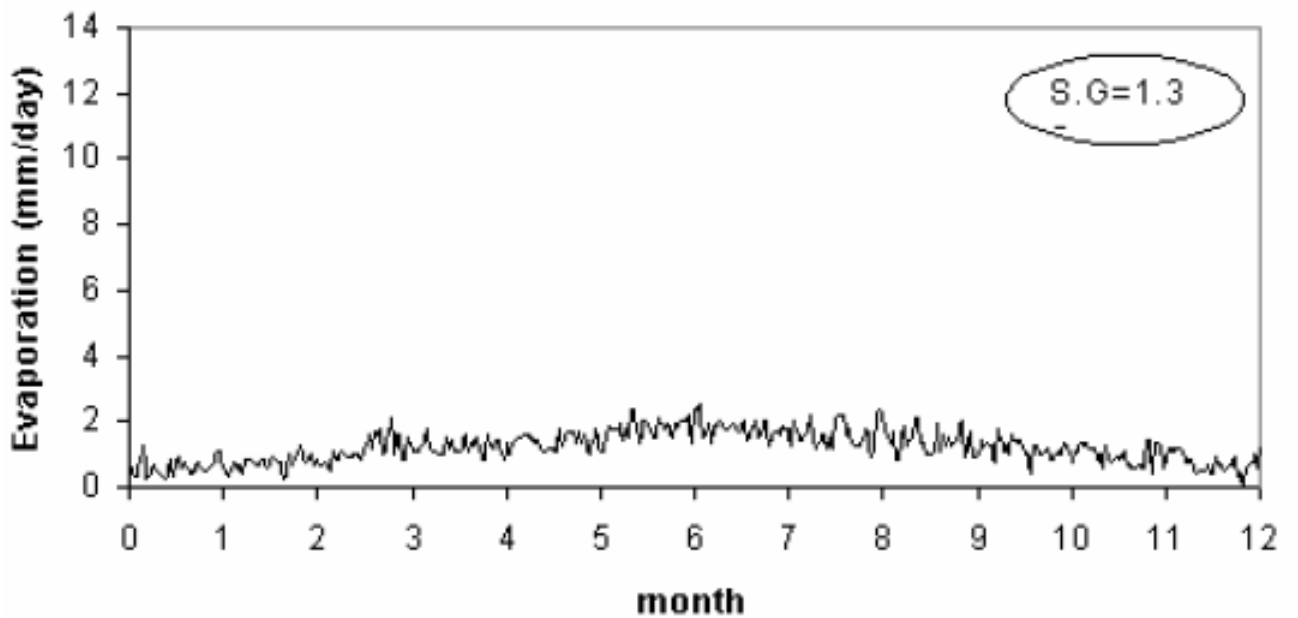


Figure 3.14: Evaporation rate Dabaa 1999 S.G= 1.3[5]

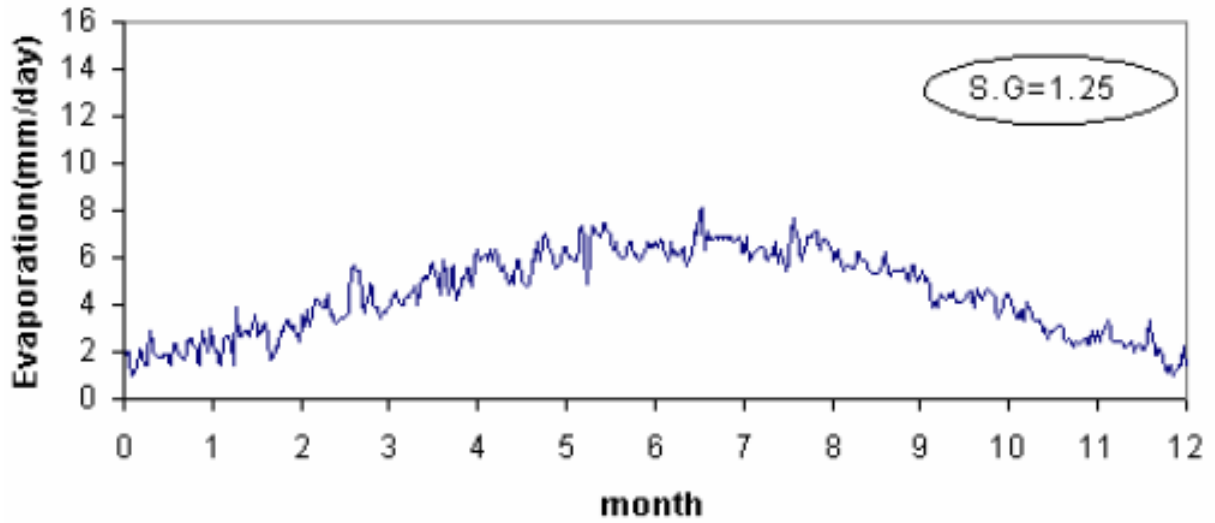


Figure 3.15: Evaporaion rate Wadi El Natron 1999 S.G= 1.25[5]

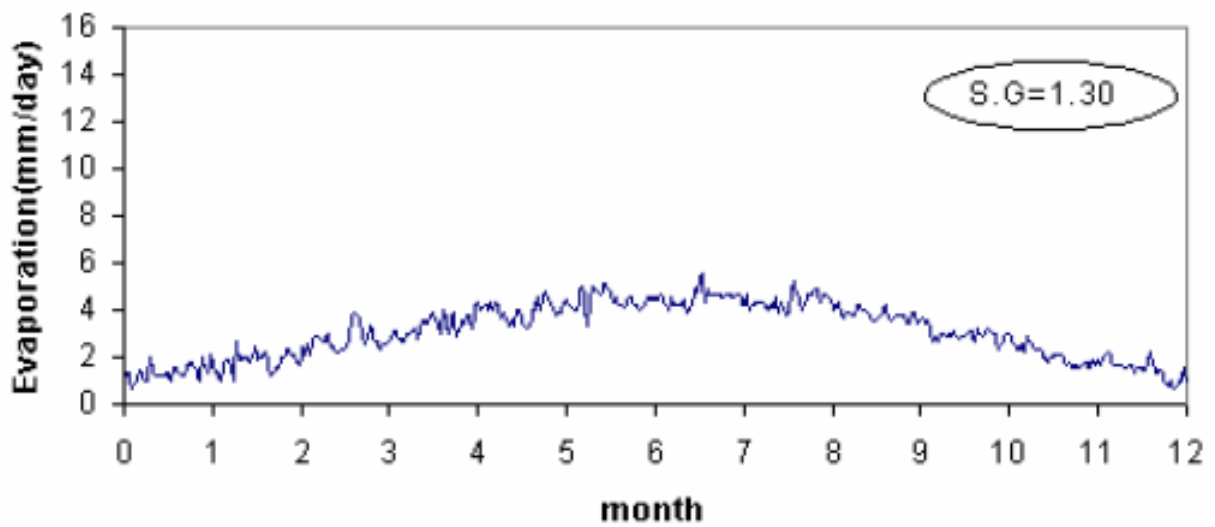


Figure 3.16: Evaporaion rate Wadi El Natron 1999 S.G= 1.3[5]

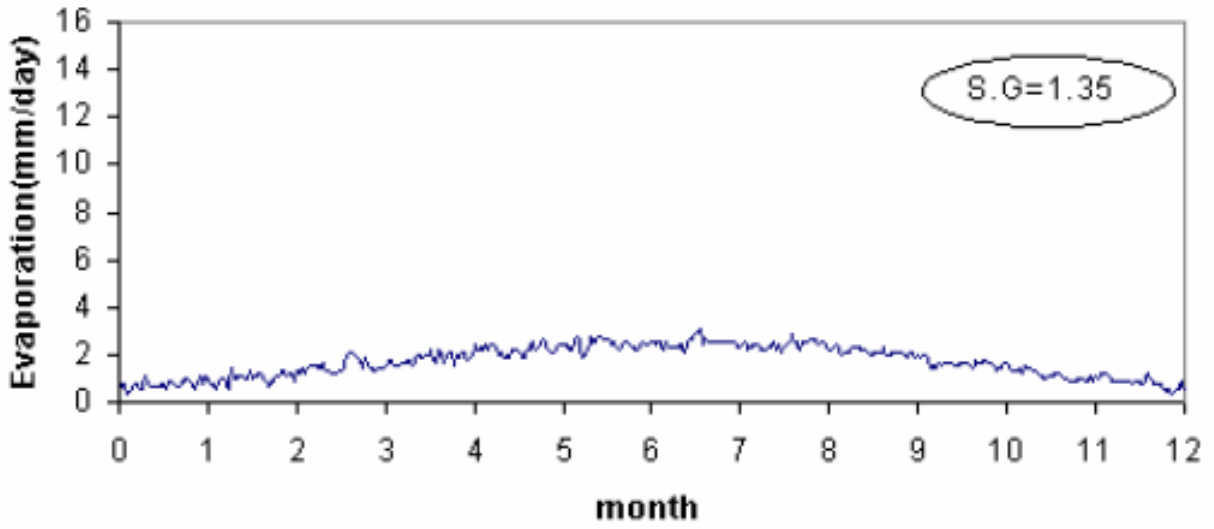


Figure 3.17: Evaporaion rate Wadi El Natron 1999 S.G= 1.35[5]

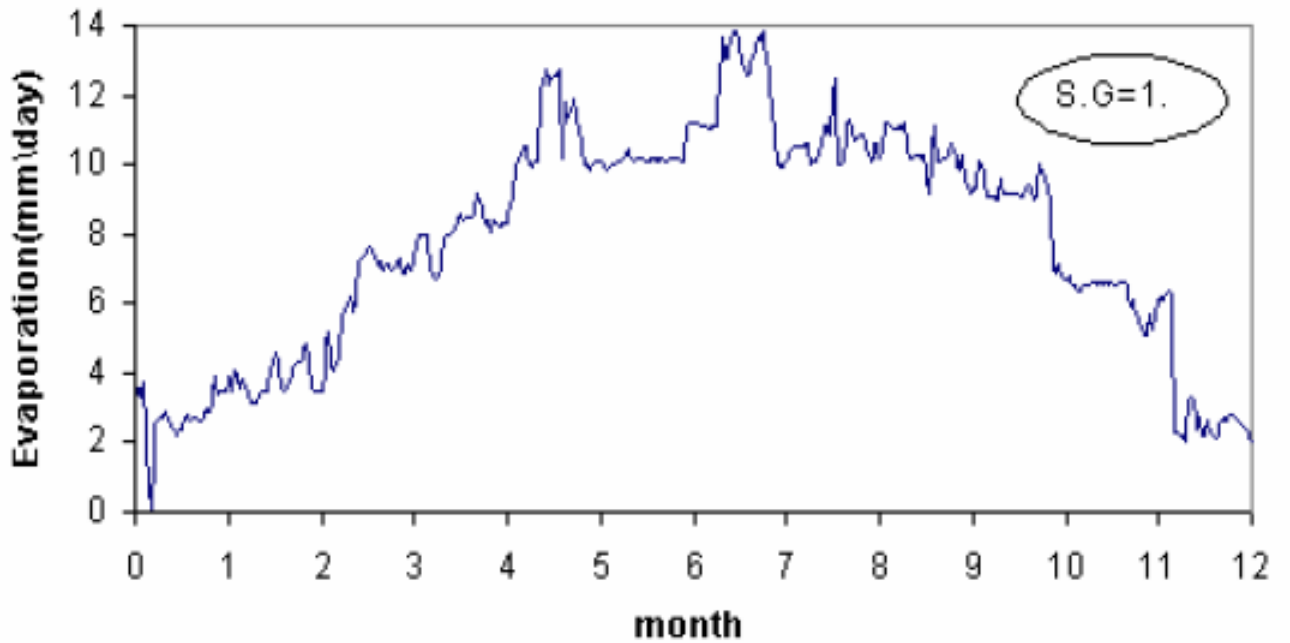


Figure 3.18: Evaporaion rate Siwa 1999 S.G= 1[5]

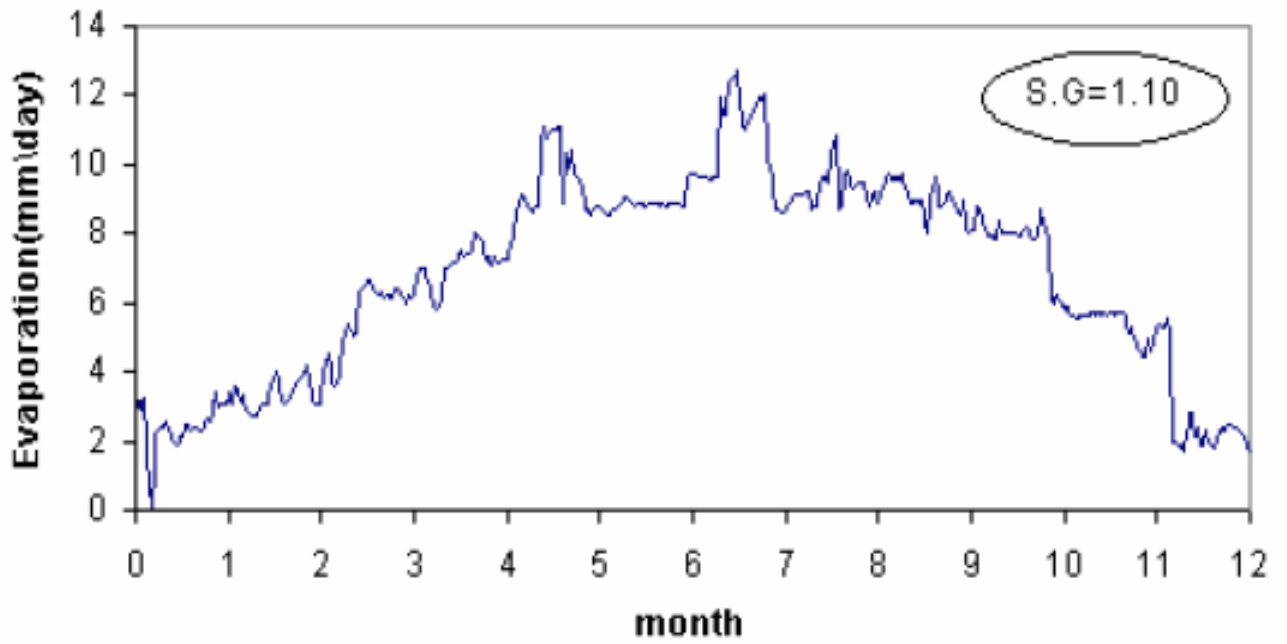


Figure 3.19: Evaporaion rate Siwa 1999 S.G= 1.1[5]

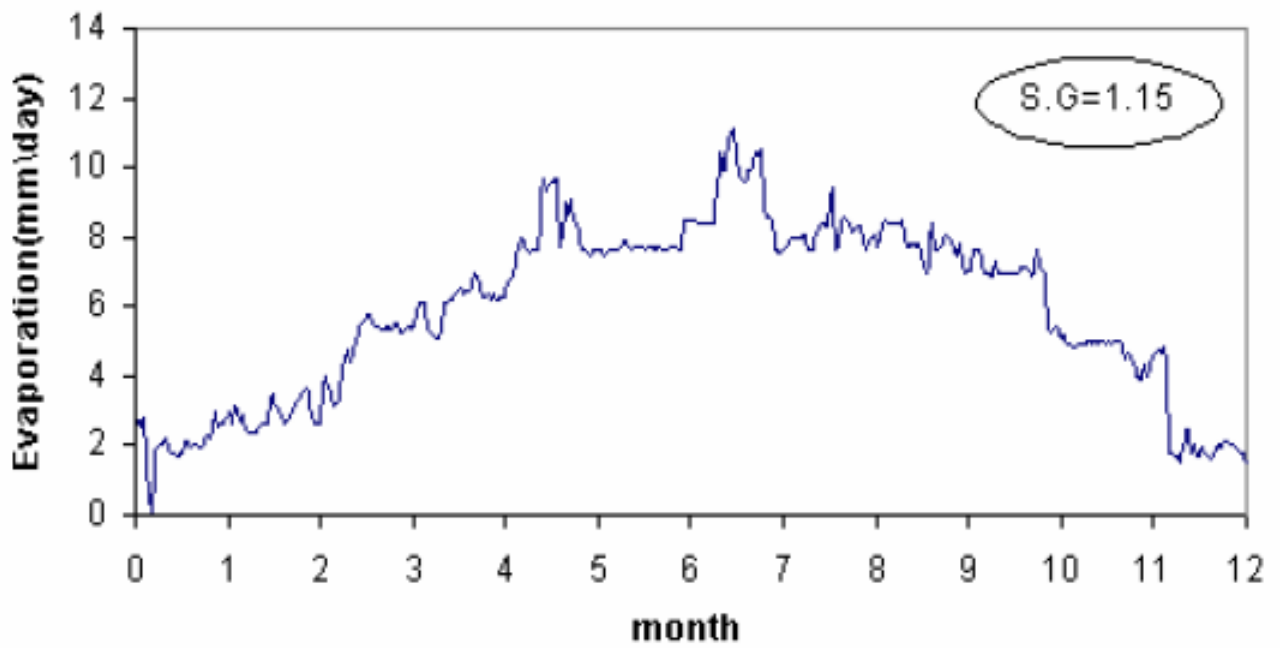


Figure 3.20: Evaporaion rate Siwa 1999 S.G= 1.15[5]

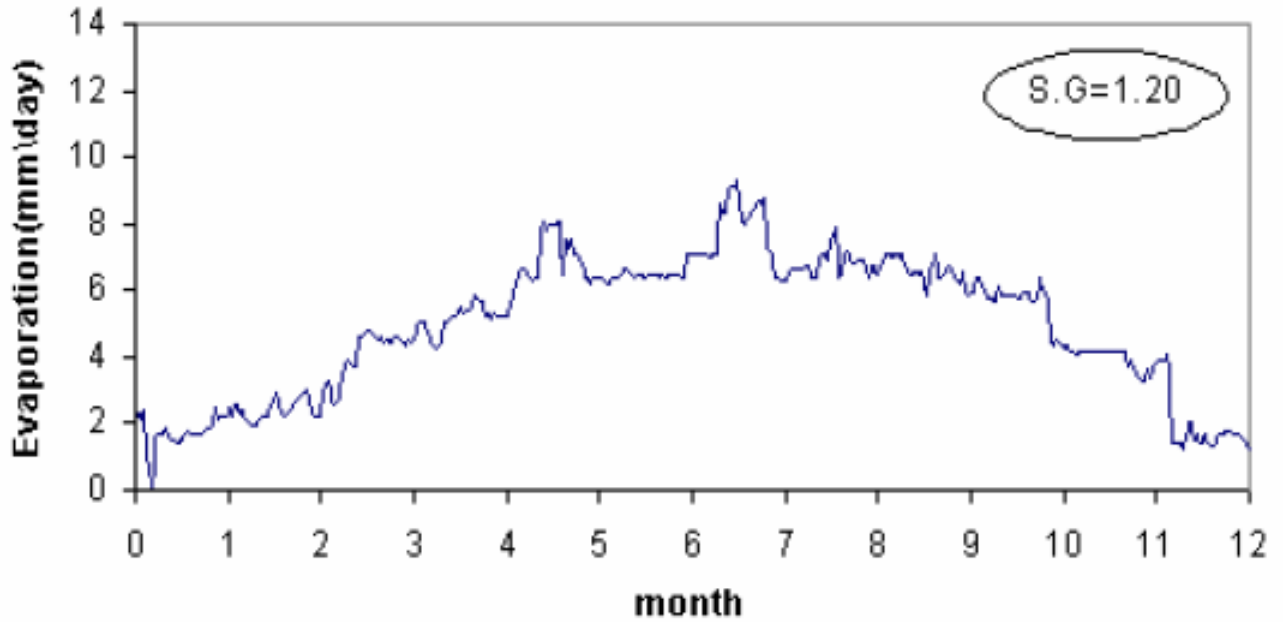


Figure 3.21: Evaporation rate Siwa 1999 S.G= 1.2[5]

### 3.0.7 Seepage

D Fredlund [14] presents a three dimensional partial differential equation for seepage through a heterogenous, anisotropic, saturated-unsaturated soil and satisfies conservation of mass for a representative elemental volume. The equation shown below assumes that the total stress remains constant during a transient process [14]. This same equation was used by several other investigations[12-13].

$$\frac{d}{dx}(k_x \frac{dh}{dx}) + \frac{d}{dy}(k_y \frac{dh}{dy}) + \frac{d}{dz}(k_z \frac{dh}{dz}) = m\gamma \frac{dh}{dt} \quad (3.15)$$

Where:

$\gamma$ =Unit weight of water

$k$ =Coefficient of permeability of the soil in the x,y and z direction

$m$ =The slope of the soil water characteristic curve (water storage)

The one dimensional form of the above equation is used in our matlab code to model Qattara Depression; the justification being that the lateral extent of the seepage

flow is much larger than its depth, leading to vertical gradients being much larger than lateral ones. The value of the coefficient of permeability for this region is obtained from S.Rizk [11] as 0.00025 m/sec as an average value for the Qattara Depression. The hydraulic conductivity varies from one region to another in the depression for that a sensitivity analysis will be performed to determine the effect of the hydraulic conductivity changes on the model. The tables below show values for the hydraulic conductivity and storage coefficient for many locations including Kharga, Dakhla, and Moghera which are close to the Qattara Depression.

Table 3.4: Hydraulic conductivity example 1 including Kharga and Dakhla[11]

Region	Country	Number of Pumping Tests	Saturated Thickness (m)	Average Screen length (m)	Transmissivity (m <sup>2</sup> /sec)	Hydraulic Cond. (m/sec)	Storage Coefficient (s)
Wadi-Qena	Egypt	6	650	250	9.905E-04	3.96x10 <sup>-6</sup>	
Wadi EILaquita	Egypt	2	500	200	3.975E-03	1.98x10 <sup>-5</sup>	
Bahareya	Egypt	10	1880	196	8.700E-03	4.3x10 <sup>-5</sup>	8.0x10 <sup>-4</sup>
Farafra	Egypt	8	2600	221	1.200E-02	5.4x10 <sup>-5</sup>	
Abu Munqar	Egypt	3	2500	250	5.469E-02	2.18x10 <sup>-4</sup>	
Dakhla	Egypt	21	1850	181	1.100E-02	6.100E-05	6.35x10 <sup>-4</sup>
Kharga	Egypt	59	1280	205	5.900E-03	2.900E-05	2.84x10 <sup>-4</sup>
East Oweinat	Egypt	6	410	185	2.400E-02	1.300E-04	
Siwa	Egypt		500	200	6.944E-02	3.42x10 <sup>-4</sup>	
Aswan	Egypt	1	200	100	2.778E-03	2.778x10 <sup>-5</sup>	
Tazerbo	Libya	5	2500	200	1.878E-02	9.4x10 <sup>-5</sup>	
Kufra	Libya	60	3000	134	8.749E-03	5.03x10 <sup>-5</sup>	2.34x10 <sup>-3</sup>
West Selima	Sudan		339	181	2.600E-02	1.436x10 <sup>-4</sup>	1.43x10 <sup>-4</sup>
El Atrun	Sudan		210	80	1.200E-02	1.500E-04	
Wadi Howar	Sudan		374	39	1.700E-03	4.400E-05	
Um Hilal	Sudan		139	80	2.600E-02	3.300E-04	
El Hashi	Sudan				1.360E-02	2.390E-04	
Dongola Area	Sudan	29	161	9	1.064E-02	1.18x10 <sup>-3</sup>	

Table 3.5: Hydraulic conductivity example 2 including Moghera[11]

Region	Country	Number of Pumping Tests	Saturated Thickness (m)	Average Screen length (m)	Transmissivity (m <sup>2</sup> /sec)	Hydraulic Cond. (m/sec)	Storage Coefficient
West Sarir	Libya	3	615	260			
Pr1	Libya		720	9	7.5x10 <sup>-2</sup>	2.88x10 <sup>-4</sup>	2x10 <sup>-2</sup>
Pr2	Libya		706	206	1.25x10 <sup>-2</sup>	1.38x10 <sup>-3</sup>	5x10 <sup>-4</sup>
Pr3	Libya			130	1.27x10 <sup>-2</sup>	6.16x10 <sup>-5</sup>	3x10 <sup>-2</sup>
North Sarir	Libya	6		130	5.8x10 <sup>-2</sup>	4.4x10 <sup>-4</sup>	5x10 <sup>-4</sup>
South Sarir	Libya	39			(1.435x10 <sup>-2</sup> )	1.1x10 <sup>-4</sup>	5x10 <sup>-4</sup>
Marada	Libya						
Shallow					2.3x10 <sup>-3</sup>	2.3x10 <sup>-3</sup>	0.1-0.44
Deep					1.3x10 <sup>-4</sup>	1.3x10 <sup>-4</sup>	5x10 <sup>-4</sup>
Jalo/ Ojla	Libya				1.731x10 <sup>-2</sup>	1.73x10 <sup>-2</sup>	2x10 <sup>-2</sup> -2x10 <sup>-2</sup>
Moghra	Egypt	11		31	2.75x10 <sup>-4</sup>	2.75x10 <sup>-4</sup>	
Moghra	Egypt	3		26	2.1x10 <sup>-3</sup>	2.1x10 <sup>-3</sup>	
Marmarica	Egypt	3		35	8.0x10 <sup>-4</sup>	8.0x10 <sup>-4</sup>	
Western Plateau	Egypt	1		46	6.4x10 <sup>-5</sup>	6.4x10 <sup>-5</sup>	

While the value for the water storage is obtained from Johnson[15]. This paper presented hydrologic properties of earth materials and that was used to determine the amount of water storage that would occur in the Qattara Depression soil during the seepage process in the model.

Definitely a site survey preformed on the exact nature of soil in the Qattara Depression would present more accurate results. But, using this study the model is run using different specific yields and for sand classified in the paper as fine or coarse and the results are compared. The value of the storage coefficient will be taken as an average of  $2.84 * 10^{-4}$  and a sensitivity analysis performed.

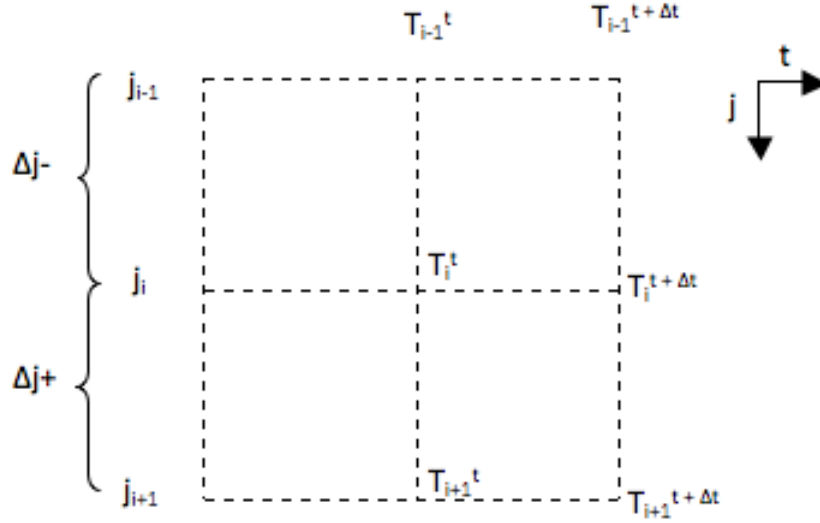


Figure 3.22: Node i

### Model

$$\frac{d}{dz} \left( k \frac{dh}{dz} \right) = m\gamma \frac{dh}{dt} \quad (3.16)$$

Equation (3.13) is going to be solved by employing the finite volume method as shown in Fig(3.22).

Initial conditions:

$$\text{at } t=0 \left( \frac{dh}{dz} \right)_t=0$$

Boundary conditions:

$$h = \rho g H$$

$$\frac{dh}{dz} = 0$$

Where:

H=Instantaneous height of water above the ground which can reach up to 80 m

z=Depth of integration domain which is taken variably to see its effect as we can not know exactly what the exact depth is so we started with a depth of 100 m and increased

$$\int_t^{t+\Delta t} \int_z^{z+\Delta z} \frac{d}{dz} \left( k * \frac{dh}{dz} \right) dz \cdot dt = m\gamma \int_z^{z+\Delta z} \int_t^{t+\Delta t} \frac{dh}{dt} dt \cdot dz \quad (3.17)$$



taking  $x = \frac{k}{m\gamma}$  integrating the DE over a finite volume extending between  $z$  and  $z+\delta z$ , and time  $t$  to  $t+\delta t$  yields:

$$(1 + 2x)h_j^{t+\Delta t} - xh_{j+1}^{t+\Delta t} - xh_{j-1}^{t+\Delta t} = xh_{j+1}^t + (1 - 2x)h_j^t + xh_{j-1}^t \quad (3.18)$$

Equations(3.15) expressed at all nodes across the domain constitute a set of linear algebraic equations displaying a tri-diagonal matrix of coefficients, as displayed in Fig(3.23). Here the constant vector  $d$  represents the RHS of equation(3.15), whereas the coefficients  $a_i, b_i, c_i$  represent the local values of the tridiagonal matrix algorithm, used to solve this set of equations. The time steps are taken as daily steps and the space steps are taken as 1 m. In equation (3.15) the values on the R.H.S are summed at each node represent  $d_1, d_2, \dots$  shown in Fig (3.24). While  $a, b$  and  $c$  shown in Fig(3.24) express  $1+2x, x$  and  $x$ , respectively. The values  $x_1, x_2, x_3, \dots$  shown in Fig (3.24) present the seepage that occurs at different depths from the surface and are shown in Fig (3.24). An assumption is made that there are no rocks underneath the surface and that the seepage will continue. So for each time step the head is calculated for all the nodes from  $x_1$  to  $x_n$ . The head is then used to obtain the velocity at each node as it is the difference between the head between two nodes multiplied by the hydraulic conductivity. The velocity at the first node is then multiplied by the instantaneous area being solved for and that presents the outward seepage  $m^3/\text{month}$ .

$$\begin{bmatrix} b_1 & c_1 & 0 & \dots & \dots & \dots & \dots & 0 \\ a_2 & b_2 & c_2 & 0 & \dots & \dots & \dots & 0 \\ 0 & a_3 & b_3 & c_3 & \dots & \dots & \dots & 0 \\ 0 & 0 & a_4 & b_4 & c_4 & \dots & \dots & \dots \\ \dots & \dots & \dots & \dots & \dots & \dots & \dots & \dots \\ \dots & \dots & \dots & \dots & \dots & \dots & c_{n-2} & 0 \\ \dots & \dots & \dots & \dots & \dots & a_{n-1} & b_{n-1} & c_{n-1} \\ 0 & 0 & 0 & 0 & \dots & 0 & a_n & b_n \end{bmatrix} \begin{bmatrix} x_1 \\ x_2 \\ x_3 \\ \dots \\ \dots \\ \dots \\ \dots \\ x_n \end{bmatrix} = \begin{bmatrix} d_1 \\ d_2 \\ \dots \\ \dots \\ \dots \\ \dots \\ \dots \\ d_n \end{bmatrix}$$

Figure 3.23: TDMA

The flow chart below presents the TDMA model

Where:

$$\text{seep} = \frac{k}{m\gamma}$$

A=instantaneous lateral area covered by the seepage flow

a,b,c,x,d as represented in Fig (3.23)

While flow chart Fig (3.24) presents the entire model

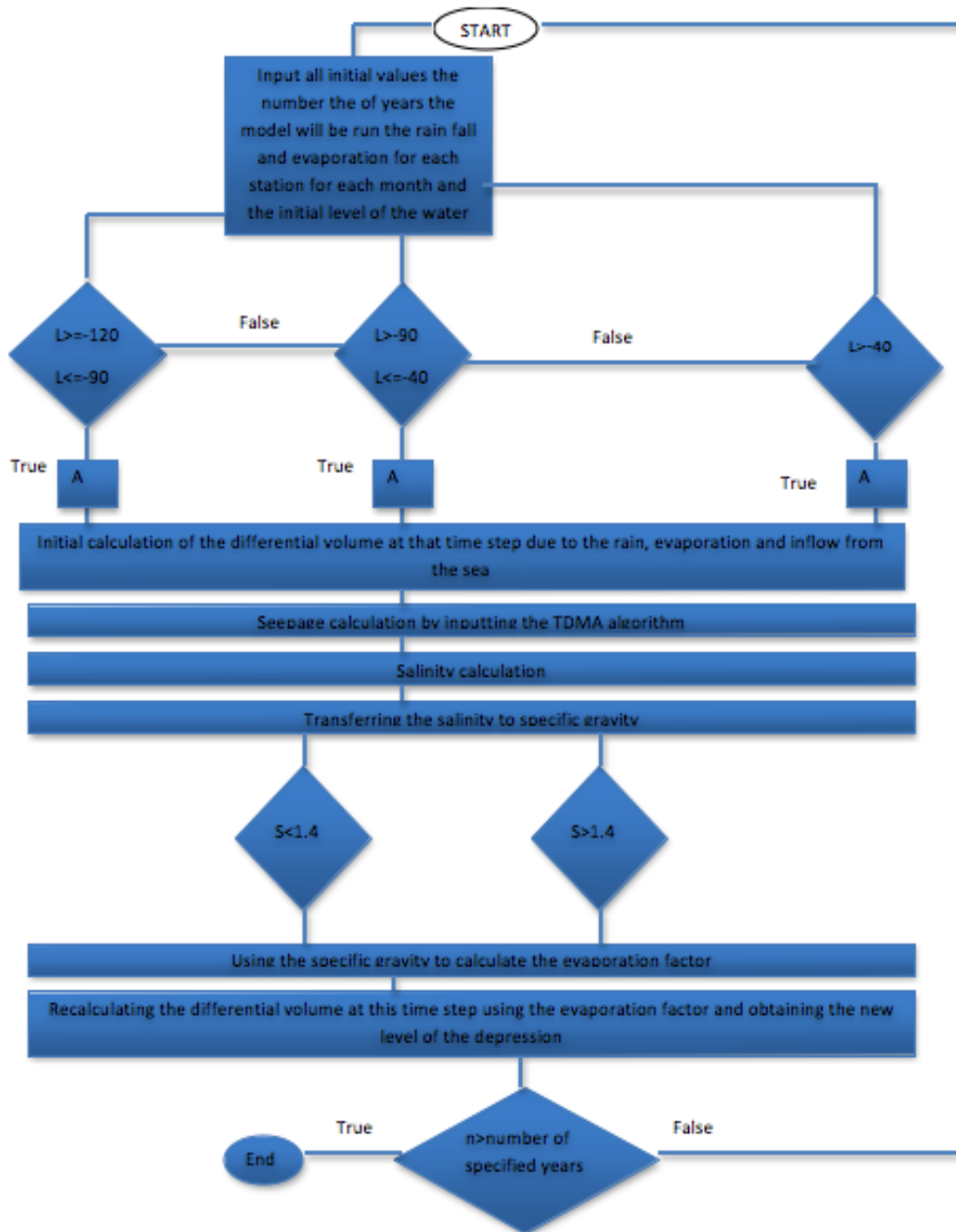


Figure 3.24: Flow Chart of Matlab Code

# Chapter 4

## Economic Analysis

To understand the economic effect of having such a huge hydropower project would have on Egypt's central grid it is necessary to understand the cost calculation methods which are available in different sources. The International Renewable Energy Agency produced a report on hydropower that was useful for this research [16]. The below table shows a good indication of the costs for installing hydropower plants of different scales. The operational and maintenance cost would be 2.5% annually of the initial investment per KW. The costs per KW for hydropower is generally low. The levelised cost of electricity (LCOE) for large hydropower projects typically ranges from \$ 0.02 to \$ 0.19/kWh assuming a 10% cost of capital, making the best hydropower power projects the most cost competitive generating option available today[16]. Hydropower associated with storage would provide the needed stability to Egypt's central grid as spinning turbines can be ramped up more rapidly than any other generation source.

	Installed costs (USD/kW)	Operations and maintenance costs (%/year of installed costs)	Capacity factor (%)	Levelised cost of electricity (2010 USD/kWh)
Large hydro	1 050 - 7 650	2 - 2.5	25 to 90	0.02 - 0.19
Small hydro	1 300 - 8 000	1 - 4	20 to 95	0.02 - 0.27
Refurbishment/upgrade	500 - 1 000	1 - 6		0.01 - 0.05

Figure 4.1: Data about hydro power plants [16]

There are different measurements for cost including equipment costs, replacement costs, financing costs, total installed cost, fixed and variable operating and maintenance costs, fuel costs and the levelised cost of energy. The following factors are to be considered in the economic analysis according to the operation of the plant.

#### Load factor

Calculated as a ratio over a period of time that can be taken as a day, a week, a month or a year by taking the average load over the time period chosen in relation to the maximum load over the same period of time. The daily load factor can be calculated for example by taking the ratio of the average load in 24 hours with maximum load in the 24 hours inspected[17].

#### Capacity factor

Again calculated over the chosen period of time, by taking the ratio of the average output of the power plant to its installed capacity. For a hydroelectric plant, the capacity factor normally varies between 0.25 and 0.75[17]

#### Utilization factor

Over the chosen period of time of a hydroelectric plant the power varies depending on the demand in the power grid. This factor is precisely relevant to our studies specially for the mixed hydro storage scheme. The utilization factor is obtained by dividing the maximum production by the installed capacity over the chosen period of time. For hydroelectric plants the utilization factor varies from 0.4 to 0.9 depending upon the installed capacity, load factor and storage[17].

#### Routs

Based on data collected from projects constructed in Egypt nowadays the price of earth excavation can be taken as  $200 \text{ LE}/\text{m}^3$  and as seen in the cross section the excavation will be greatly through lime stone and the depth of the excavation will be over 10 m .

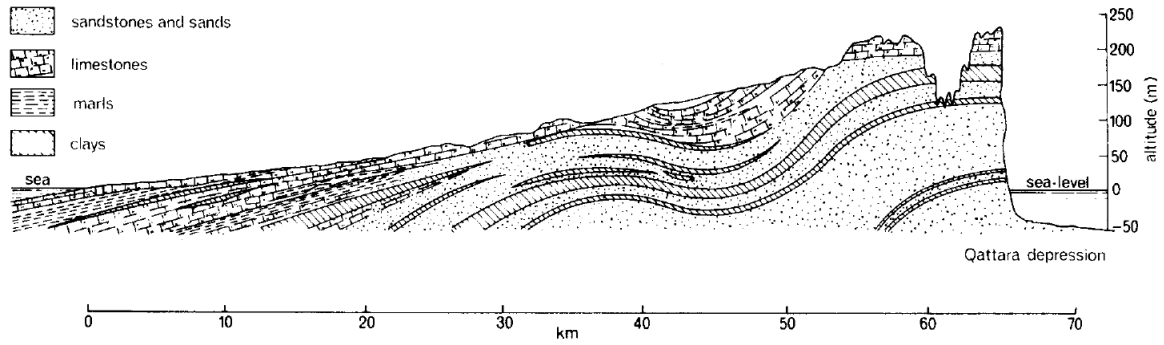


Figure 4.2: Cross section [1]

Fig (4.3) shows different power plants in Egypt categorized according to their location and the last category are not connected to the central grid. These power plants are shown with their fuel consumption with the progression of time. The data provided is obtained from the Egyptian Ministry of electricity for the fuel consumption by steam turbine power plants, gas turbine power plants, and combined cycle power plants from 2009 to 2014.

### Development of Fuel Consumption by Power Plants (ktoe)\*

Comp.	Station		09/10	10/11	11/12	12/13	13/14
Cairo	Shoubra El-Kheima	(St)	1776	1853	1331	1445	1406
	Cairo West	(St)	516	429	228	157	-
	Cairo West Ext.	(St)	931	1176	1541	1624	1776
	Tebbin	(St)	-	838	848	614	603
	Cairo South I	(CC)	727	668	619	409	402
	Cairo South II	(CC)	204	224	188	166	108
	Cairo North	(CC)	1577	1614	1677	1482	1257
	Wadi Hof	(G)	62	51	49	61	49
	6 October	(G)	-	-	148	699	423
	Giza North	(CC)	-	-	-	-	37
East Delta	Ataka	(St)	937	854	1089	819	478
	Abu Sultan	(St)	728	840	955	954	806
	Shabab	(G)	65	79	39	76	85
	Port Said	(G)	30	25	23	37	41
	Arish	(St)	132	132	94	124	134
	Oyoun Mousa	(St)	991	1056	1112	991	1072
	Damietta	(CC)	1521	1478	1453	1575	1594
	Sharm El-Sheikh	(G)	42	31	17	23	19
	Huraghda	(G)	63	40	19	44	52
	New Gas Damietta	(G)	-	-	766	773	860
	New Gas Shabab	(G)	-	-	1655	1373	540
	Damietta West	(G)	-	-	-	688	813
	Middle Delta	Talkha	(CC)	473	463	402	413
Talkha steam 210		(St)	633	317	535	468	581
Talkha 750		(CC)	784	870	575	790	842
Nubaria 1,2		(CC)	1679				
Nubaria 3		(CC)	438	1944	1831	1723	2522
Mahmoudia		(CC)	479	466	483	490	484
El-Atf		(CC)	646	811	909	921	955
Banha		(CC)	-	-	-	-	130
West Delta	Kafr El-Dawar	(St)	721	600	585	831	861
	Damanhour Ext.	(st)	445	409	136	16	169
	Damanhour	(St)	306	261	308	303	300
	Damanhour	(CC)	247	233	226	220	231
	Abu Kir	(St)	1098	1037	1279	1296	1245
	New Abu Kir	(St)	-	-	-	1095	1586
	El-Seiuf	(G)	82	70	83	106	115
	Karmouz	(G)	4	3	3	4	3
	Sidi Krir	(St)	952	879	848	869	828
	Sidi Krir	(CC)	750	782	868	764	845
	Matrouh	(St)	109	124	106	102	100
	Walidia	(St)	639	431	743	845	850
Upper Egypt	Assiut	(St)	138	132	124	142	113
	Kuriemat	(St)	1611	1912	1625	1888	1830
	Kuriemat 1	(CC)	760	780	791	641	726
	Kuriemat 2	(CC)	755	787	771	751	811
	<b>Total</b>		<b>24052</b>	<b>24698</b>	<b>27083</b>	<b>28811</b>	<b>29158</b>
Private Sector (BOOT)	Sidi krir 3 , 4	(St)	940	897	915	938	908
	Suez Gulf North	(St)	891	925	847	972	1001
	Port Said East	(St)	889	910	883	1029	1012
	<b>Total BOOT</b>		<b>2720</b>	<b>2732</b>	<b>2645</b>	<b>2939</b>	<b>2921</b>
<b>Grand Total</b>		<b>26772</b>	<b>27430</b>	<b>29728</b>	<b>31750</b>	<b>32079</b>	

\* Including commissioning tests.

Figure 4.3: Fuel consumption in Egypt

## 4.1 Cost estimation

To provide an estimation for the cost of the hydro power plant HydroHelp 1.6 software was used for each route. The optimum conduit head loss from the intake to the power house was taken to be 2% at full load as an assumption, the system frequency was taken to be 50 Hz. The generator power factor was taken to be 0.9, maximum allowable gear box power taken as 2 MW, 8 in-line reaction turbines would be used because that was the most economic according to the calculations performed by the software depending on the set up of the plant head and the flow. The figures below show the data used to calculate the reaction turbine selection to include the power house costs, ancillary equipment. The inflation ratio used for calculation in later years in the project for the replacement of the turbine is 1.8. The calculation of the water to wire cost includes the supply and installation of the electromechanical equipment from the turbine inlet to the low voltage side of the transformer. Also, all the low voltage switch gears and controls are included with the manufacturers Supervisory control and data acquisition (SCADA) system, which is not usually compatible with the utility SCADA. And the turbine chosen is the one with the least cost.

Generating equipment details.	Reaction unit.	Impulse unit.
Turbine runner speed, rpm.	136.4	0.0
Reaction turbine runner throat diameter, m.	4.31	-----
Required powerhouse crane capacity, tonnes. <b>Comment.</b>	250.4	0.0
Crane span, m.	23.7	0.00
Reaction unit vertical axis, casing centerline elevation.	-3.28	-----
Generating unit capacity, MW.	67.84	0.00
<b>Powerplant capacity, MW.</b>	<b>271.38</b>	<b>0.00</b>

Figure 4.4: HydroHelp 1.6 generating equipment details

Powerhouse statistics.	Reaction unit.	Impulse unit.
Overburden excavation volume, m3.	5,195	0
Rock excavation volume, m3.	118,831	0
Concrete volume, m3.	21,049	0
Additional concrete required to counter floatation, m3.	0	Not applicable
Steel superstructure weight, metric tonnes.	505	0
Powerhouse length, m.	85.7	0.0
Powerhouse footprint area, m2.	2,033	0
Distance between unit centerlines, m.	17.13	0.00
Approximate turbine floor level, Elevation, m.	1.04	0.00
Draft tube sill level, elevation, m.	-14.7	0.00
Powerhouse and ancilliary equipment cost, \$millions.	Reaction unit.	Impulse unit.
Powerhouse excavation, concrete and superstructure.	62.07	0.01
Total cost of draft tube gate guide and hoist equipment.	2.92	0.00
Total cost of powerhouse crane, HVAC and water systems.	6.84	0.00
<b>Cost of powerhouse and miscellaneous equip. - no units</b>	<b>71.34</b>	<b>0.01</b>

Figure 4.5: HydroHelp 1.6 power house details used in cost estimation

Reaction turbine selection to include powerhouse costs, ancilliary equipment and effect of tailwater level.		
<b>Additional input data.</b>		
Unit cost of overburden excavation, \$/m3.	50	
Unit cost of rock excavation, \$/m3.	200	
Unit cost of concrete, including forms and reinforcing, \$/m3.	1500	
Unit cost of walls and roof, \$/m2.	200	
Unit cost of steel in superstructure, \$/ton.	11,000	
Average rock level at powerhouse, elevation, m.	50.0	Comment
Average depth of overburden at powerhouse, m.	2.0	

Figure 4.6: HydroHelp 1.6 reaction turbine details used in cost estimation

Ball had proposed three routes that will be examined the volume excavated is calculated by multiplying the area of the tunnel or canal by the length.

$$\text{Volume excavated in route D} = 72 * 10^3 * 452.4 = 3 * 10^7 m^3$$

Excavation cost in route D=\$706 million

Power plant capacity=270.38 MW

Water to wire cost of generating units (3% are added as transportation cost)=\$166.8 million

Type of reaction turbine to be used is a vertical axis Francis turbine with steel casing.

Cost of civil work on powerhouse, crane, draft tube gates/hoist and generating equipment=\$206.82 million

Turbine cost=\$145.05 million

Transformer cost=\$1.182 million

Station service transformer cost=\$0.193 million

Total cost of route D Qattara Depression=\$1019.2 million

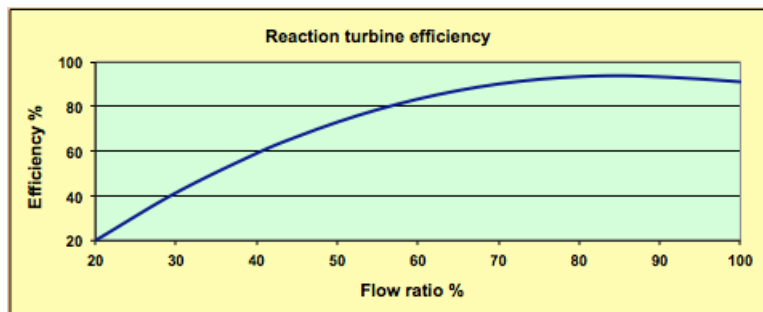


Figure 4.7: HydroHelp 1.6 reaction turbine selection for route D

Most of the power plants in Egypt are either steam turbine or gas turbine power plants, mostly combined cycle. In this economic analysis these types of power plants



are compared with the Qattara Depression project. Putting many aspects into consideration the plant life, the carbon footprint that will be reduced, and the fixed and variable costs. The utilization factor will vary from year to year according to the demand in the central grid, therefore an estimate will be given of 0.5 to normal power plants and also to the hydro power station for a fair economic comparison. A very important factor in the study is the strategic operation of the Qattara Depression project it would be best and most strategic to the central grid if the water is stored and it is operated during the peak load, which is the main problem in Egypt. The scheme that provides this possibility is the pumped hydro storage scheme and as previously presented the wind can be used in this area to operate the pump, making the project more economic. Taking the fixed cost for a power plant substituting the energy that would be produced by route D as \$162 million as 600 \$/KW is used for pricing as seen in the figures below the variable costs would include the operation and maintenance cost and the fuel cost. The operation and maintenance cost include the expenses for staff salaries and insurance fees and any cost that remains constant, unrelated to the plants power output [18] this value can be assumed as 2.5% of the capital cost which in this case amounts to \$4.05 million. While the fuel cost, which also belongs to the variables costs category, can be calculated as follows On a dollars per megajoule basis, the cost of oil at \$100 per standard 42-gal barrel (\$0.63/L) with a heating value of 43.733 MJ/kg (18,800 Btu/lb) and a specific gravity of 0.91 is  $(\$0.63/L)/[(43.733 \text{ MJ/kg})(0.91 \text{ kg/L})] = \$0.016/\text{MJ}$ , keeping in mind that the price of oil is variable and is naturally inflating as shown in the fig (4.9) [17]. Therefore, the cost of oil would be \$134.6 million.

Year	Capital Cost (\$/kW)	Variable O&M (\$/MWh)	Fixed O&M (\$/kW-yr)	Heat Rate (Btu/kWh)	Construction Schedule (Months)	POR (%)	FOR (%)	Min. Load (%)	Spin Ramp Rate (%/min)	Quick Start Ramp Rate (%/min)
2008	671	-	-	-	-	-	-	-	-	-
2010	651	29.9	5.26	10,390	30	5.00	3.00	50	8.33	22.20
2015	651	29.9	5.26	10,390	30	5.00	3.00	50	8.33	22.20
2020	651	29.9	5.26	10,390	30	5.00	3.00	50	8.33	22.20
2025	651	29.9	5.26	10,390	30	5.00	3.00	50	8.33	22.20
2030	651	29.9	5.26	10,390	30	5.00	3.00	50	8.33	22.20
2035	651	29.9	5.26	10,390	30	5.00	3.00	50	8.33	22.20
2040	651	29.9	5.26	10,390	30	5.00	3.00	50	8.33	22.20
2045	651	29.9	5.26	10,390	30	5.00	3.00	50	8.33	22.20
2050	651	29.9	5.26	10,390	30	5.00	3.00	50	8.33	22.20

Table 3. Emission Rates for a Gas Turbine Power Plant

SO <sub>2</sub> (Lb/mmbtu)	NO <sub>x</sub> (Lb/mmbtu)	PM10 (Lb/mmbtu)	CO <sub>2</sub> (Lb/mmbtu)
0.0002	0.033	0.006	117

Figure 4.8: Data used for cost estimation of gas and steam turbine power plants [17]

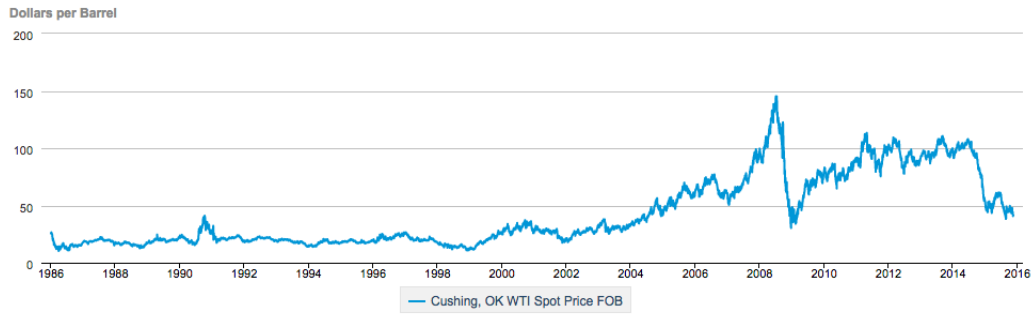


Figure 4.9: Oil prices [17]

The equation below can be used in the calculation of the specific Power Plant Costs:

$$C_{pp} = C_{fix} + C_{var} * T_A$$

$C_{fix}$ =annual fixed costs in  $\$/MW_{el}/a$

$C_{var}$ =variable operating costs in  $\$/MWh_{el}$

$T_A$ =utilization factor in h/a

For a conventional power plan in Egypt connected to the central grid the specific annual power plant costs:

$$C_{pp}=162+138.65*0.5=231.3 \text{ million } \$/MW_{el}/a$$

For Qattara Depression route D

$$C_{pp}=1019.2+25.48*0.5=1031.9 \text{ } \$/MW_{el}/a$$

While the equation below can be used in the calculation of electricity generation costs  $C_{el}$  in  $\$/MWh_{el}$

$$C_{el} = C_{pp}/T_A$$

$C_{pp}$ =specific annual power plant costs in  $\$/MW_{el}/a$

$T_A$ =utilization factor in h/a

#### 4.1.1 Economic comparison between conventional power plants and the base load scheme

For a conventional power plan in Egypt connected to the central grid  $C_{el}=231.3/0.5=462.5$  million  $\$/MW_{el}$

For Qattara Depression route D

$$C_{el} = 1031.9/0.5 = 2063.8 \text{ } \$/MW_{el}$$

As seen from this analysis it might appear that the conventional power plant might be more economic but these are the costs for the first year only in later years the initial capital investment is removed and by doing that the project will break-even in the 9th year. That is other than that the power station would be operable for about 30 years while Qattara depression would last much longer according to the operation as will be seen in the results. But, using the schemes in the economic study it would

last for a minimum of 200 years but along its operation the Francis turbine units will have to be replaced every 50 years. The carbon foot print also will be reduced which is a huge problem in Cairo the  $CO_2$  emissions can be taken as 0.2 t/MWh . Therefore  $467 * 10^3$  tones of carbon dioxide would be eliminated annually by route D.

Volume excavated in route E= $76 * 10^3 * 380 = 2.9 * 10^7 m^3$

Excavation cost in route E=\$682 million

Power plant capacity=273.14 MW

Water to wire cost of generating units (3% are added as transportation cost)=\$160.3 million

Type of reaction turbine to be used is a vertical axis Francis turbine with steel casing. Cost of civil work on powerhouse, crane, draft tube gates/hoist and generating equipment=\$187.08 million

Turbine cost=\$135.3 million

Transformer cost=\$1.182 million

Station service transformer cost=\$0.193 million

Total cost=\$1166.1 million

Volume excavated in route F= $80 * 10^3 * 266 = 2 * 10^7 m^3$

Excavation cost in route F=\$470 million

Power plant capacity=204.25 MW

Water to wire cost of generating units (3% are added as transportation cost)=\$113.3 million

Type of reaction turbine to be used is a vertical axis Francis turbine with steel casing.

Cost of civil work on powerhouse, crane, draft tube gates/hoist and generating equipment=\$126.47 million

Turbine cost=\$95.65 million

Transformer cost=\$1.182 million

Station service transformer cost=\$0.193 million

Total cost=\$806.7 million

Volume excavated in route H1= $1757.45 * 10^6 m^3$

Excavation cost in route H1=\$413.6\*10<sup>2</sup> million

Power plant capacity=321.07 MW

Water to wire cost of generating units (3% are added as transportation cost)=\$203.5 million

Type of reaction turbine to be used is a vertical axis Francis turbine with steel casing.

Cost of civil work on powerhouse, crane, draft tube gates/hoist and generating equipment=\$254.14 million

Turbine cost=\$171.79 million

Transformer cost=\$1.182 million

Station service transformer cost=\$0.193 million

Total cost=\$41990.8 million

Volume excavated in route L1=410\*10<sup>6</sup>m<sup>3</sup>

Excavation cost in route L1=\$96\*10<sup>2</sup> million

Power plant capacity=338.79 MW

Water to wire cost of generating units (3% are added as transportation cost)=\$205.1 million

Type of reaction turbine to be used is a vertical axis Francis turbine with steel casing.

Cost of civil work on powerhouse, crane, draft tube gates/hoist and generating equipment=\$243.41 million

Turbine cost=\$173.18 million

Transformer cost=\$1.182 million

Station service transformer cost=\$0.193 million

Total cost=\$10223 million

Volume excavated in route L2=31.2\*10<sup>6</sup>m<sup>3</sup>

Excavation cost in route L2=\$7.4\*10<sup>2</sup> million

Power plant capacity=333.21 MW

Water to wire cost of generating units (3% are added as transportation cost)=\$191.7 million

Type of reaction turbine to be used is a vertical axis Francis turbine with steel casing.

Cost of civil work on powerhouse, crane, draft tube gates/hoist and generating equipment=\$224.27 million

Turbine cost=\$161.87 million

Transformer cost=\$1.182 million

Station service transformer cost=\$0.193 million

Total cost=\$1319.2 million

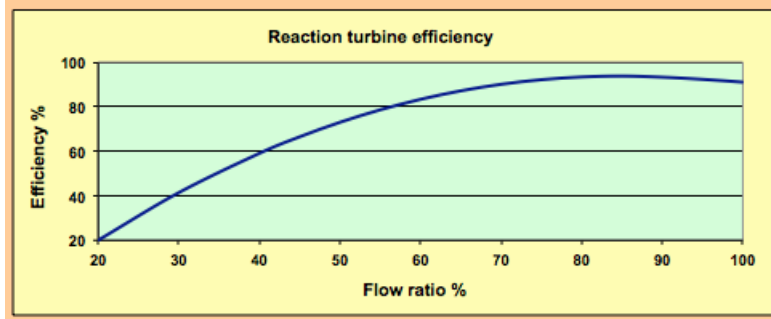


Figure 4.10: HydroHelp 1.6 reaction turbine selection for route D

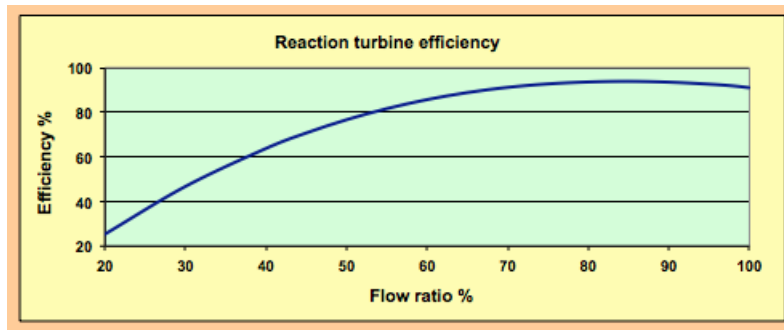


Figure 4.11: HydroHelp 1.6 reaction turbine selection for route E

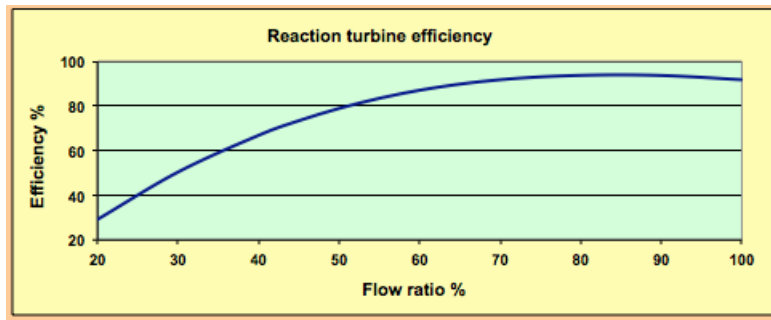


Figure 4.12: HydroHelp 1.6 reaction turbine selection for route F

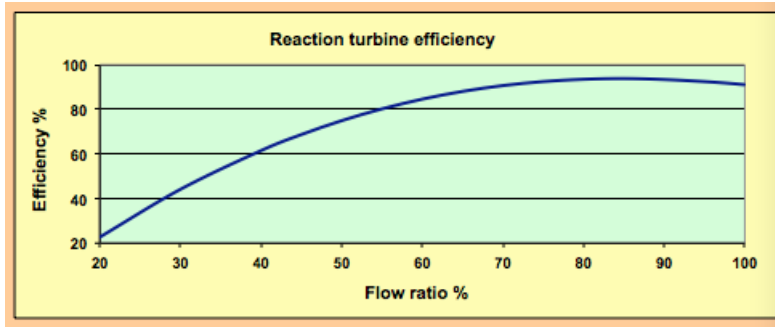


Figure 4.13: HydroHelp 1.6 reaction turbine selection for route H1

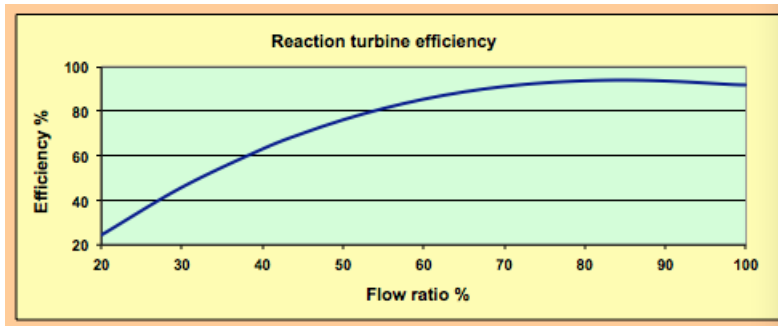


Figure 4.14: HydroHelp 1.6 reaction turbine selection for route L1

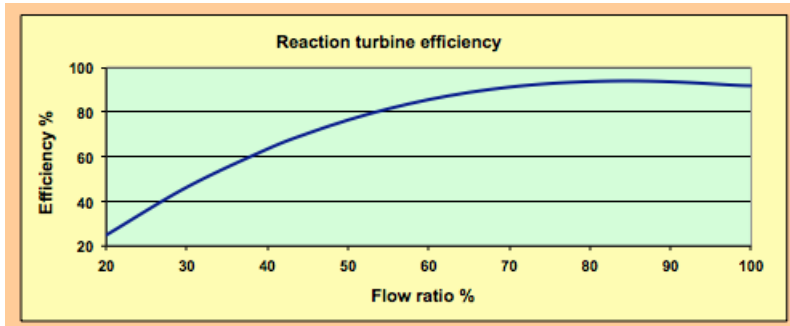


Figure 4.15: HydroHelp 1.6 reaction turbine selection for route L2



### 4.1.2 Economic comparison between conventional power plants and the pumped hydro storage scheme

Most of the power plants in Egypt are either steam turbine or gas turbine power plants, mainly combined cycle. In this economic analysis these power plants are compared with the Qattara Depression project. But, in case of route L2 the economic comparison is studied with the pumped hydro storage scheme shown in the Fig(4.16). The strategic comparison also between using Qattara Depression as a base load or pumped hydro storage is shown below. The fact that the pump pumping water upwards to the reservoir would be powered by a windmill to store energy and provide the extra head of 212.5 m to add up to 272.5 m would be very effective during the peak hours in Egypt.

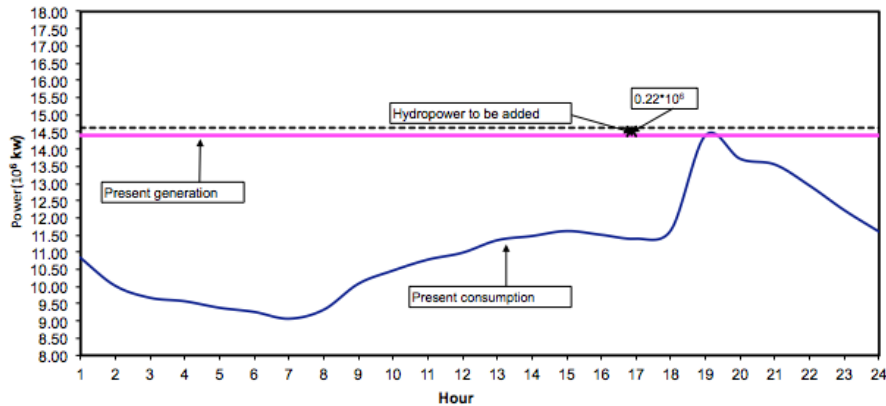


Figure 4.16: Power demand and supply with base load scheme [5]

Therefore, using route L2 in the pumped hydro storage scheme the cost of the windmills to pump the water to the upper reservoir where the energy would be stored. The average wind speed in Qattara Depression is 5-6 m/s and the needed power to pump the water to the reservoir is  $1.3 \times 10^3 MW$ . The average lifetime levelised cost of electricity generation of the wind turbines can be taken as 0.09 \$/KWh in Africa [19]. The installation cost ranges can be taken as 1500 \$/KW which amounts to \$1950 million. The following is the data when route L2 is taken as a pumped hydro storage scheme operating 6 hours per day during the peak hours. In that case the number of turbines chosen is 4 unlike all the previous designs where 8 turbines was the most

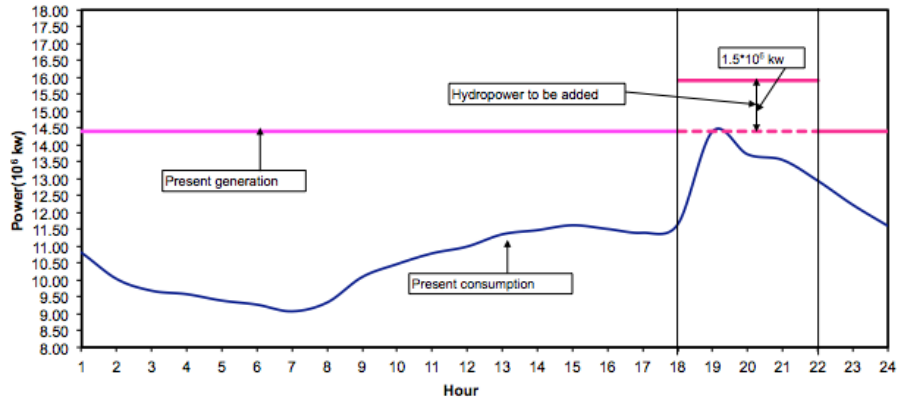


Figure 4.17: Power demand and supply with peak load scheme [5]

economical.

Volume excavated in route L2= $31.2 \times 10^6 m^3$

Excavation cost in route L2= $\$7.4 \times 10^2$  million

Power plant capacity=3017.42 MW

Water to wire cost of generating units (3% are added as transportation cost)=\$757 million

Type of reaction turbine to be used is a vertical axis Francis turbine with steel casing.

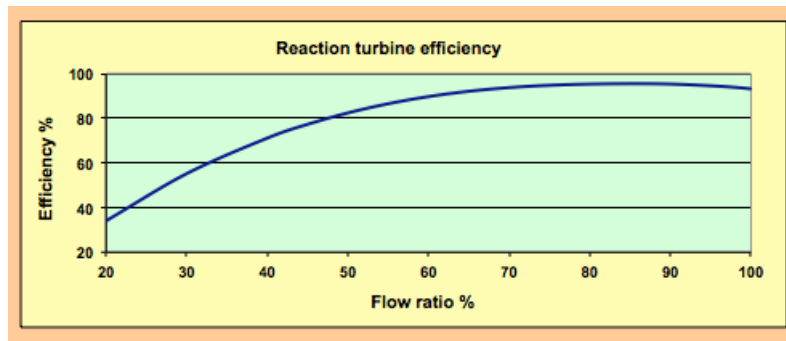


Figure 4.18: HydroHelp 1.6 reaction turbine selection for route L2

Cost of civil work on powerhouse, crane, draft tube gates/hoist and generating equipment=\$965.45 million

Turbine cost=\$639.14 million

Transformer cost=\$1.182 million

Station service transformer cost=\$0.193 million

Total cost=\$5052.97 million

Taking the fixed cost for a power plant substituting the energy that would be produced by route L2 as \$1810 million

The operation and maintenance cost= \$45 million

Fuel cost= \$1502 million

For a conventional power plant in Egypt connected to the central grid the specific annual power plant costs

$$C_{pp}=1810+1547*0.5=2583.5 \text{ million } \$/MW_e l/a$$

For Qattara Depression route D

$$C_{pp}=5052.97+126.3*0.25=5084.5 \text{ } \$/MW_e l/a$$

In this economic comparison the project break evens after 5 years again keeping in mind that the conventional power plant will last 30 years while as will be seen in the results the hydro power plant using this scheme would last up to 100 years.

For a conventional power plant in Egypt connected to the central grid

$$C_{el}=2583.5/0.5=5167 \text{ million } \$/MW_e l$$

For Qattara Depression route D

$$C_{el} = 5084.5/0.25 = 20338 \$/MW_e l$$

The strategic use of this scheme is that it would store energy for the central grid at zero cost, for usage during peak hours, as the water will be pumped using the wind turbines. While the price of energy storage using a battery would be 1000\$/KWh. The carbon foot print also will be reduced as  $1.9 * 10^{10}$  would be eliminated annually.

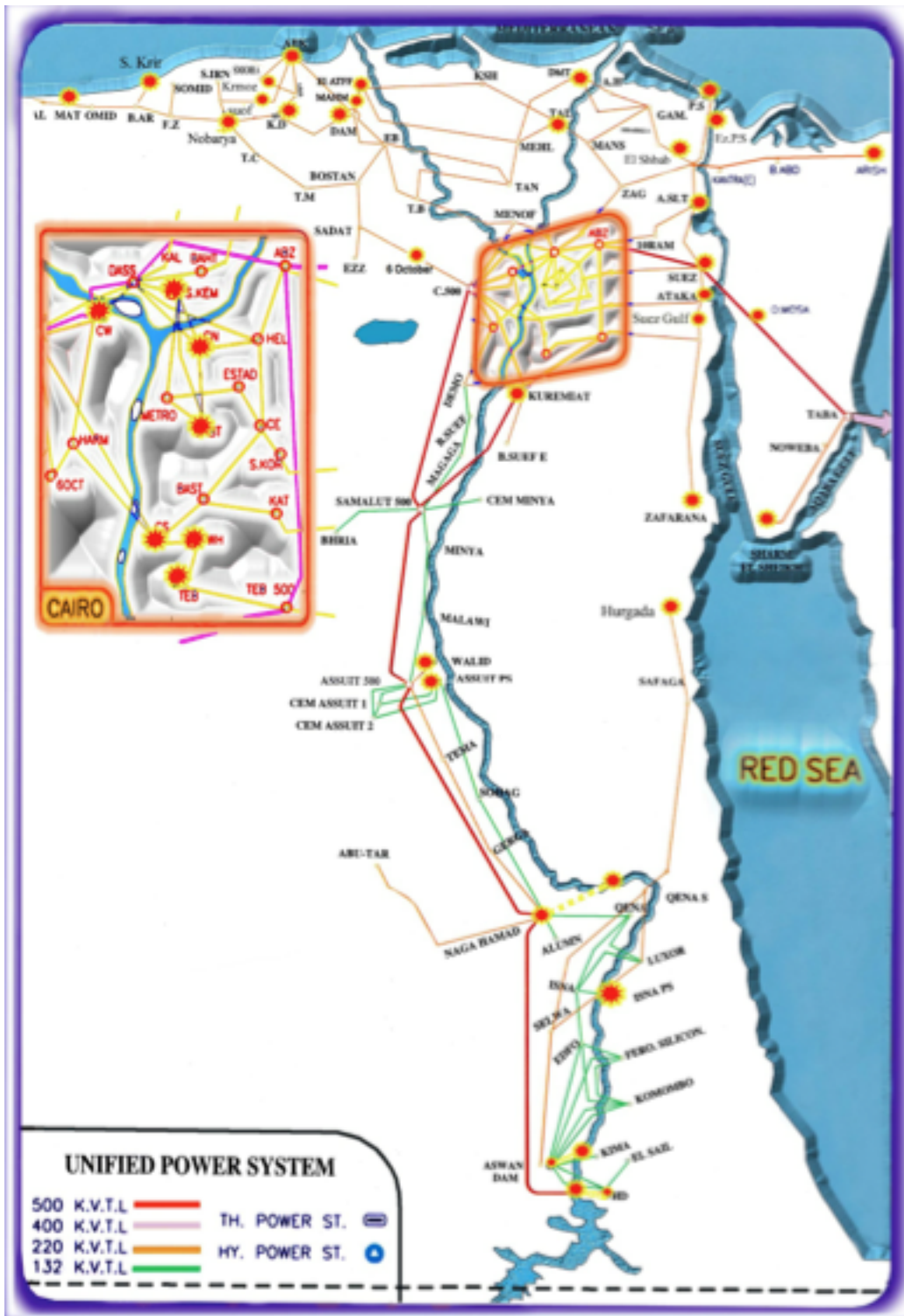


Figure 4.19: Egypt's Central Grid

# Chapter 5

## Discussion of Results

Route D is examined with flow rate  $656 \text{ m}^3/\text{s}$  with no seepage included only channel flow and from the results it shows that the inclusion of the channel flow is negligible, no matter the breadth taken.

For this flow, unlike the results from Ball that Bassler expected, the level continued to rise due to the increase in salinity, while no salinity included it stabilized. The energy developed from this scheme, provided the lake would be 50 m below sea level as Ball suggested, would be 270 MW. The results follow the same pattern as Ezz El Din's results and the extra factors studied showed the following. The channel affect of the water flow doesn't have any of an effect on the filling scenario. While using the seepage method previously explained leads to the Qattara Depression to last longer as the outward seepage has an affect on the mass balance equation that leads the level of the lake to increase at a lower rate. The outward seepage calculated that leads to that decrease in the level of the lake is an average of  $1.1 \cdot 10^9 \text{ m}^3/\text{month}$ . Finally the effect of the new detailed calculation of salinity is also shown and it shows a different pattern than the results that had been produced in past work.

Salinity was included, but calculated with Ezz El Din's method [5], which is simplistic, as the detailed method used in this thesis will show a different pattern. Figure 5.1 shows the affect of the channel flow on the evaporation calculation was negligible, and therefore had no affect on the total mass balance equation for the lake.

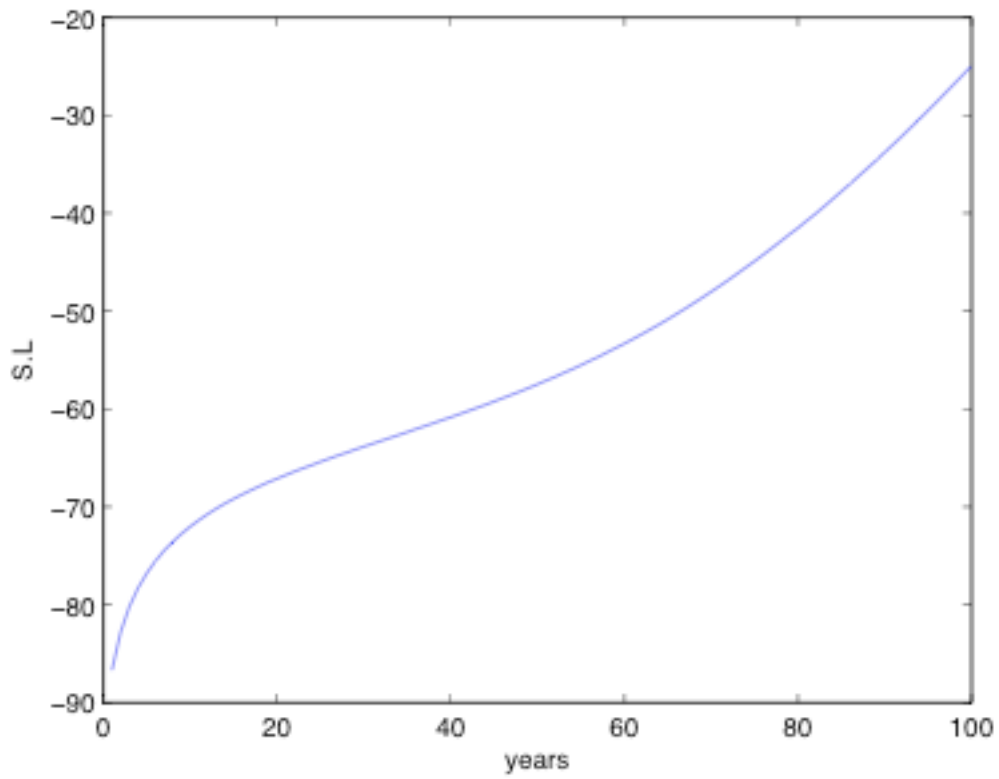


Figure 5.1: Increase in surface level (S.L) in years with a flow of  $656m^3/sec$  with no channel flow included was the same as when the channel flow was included

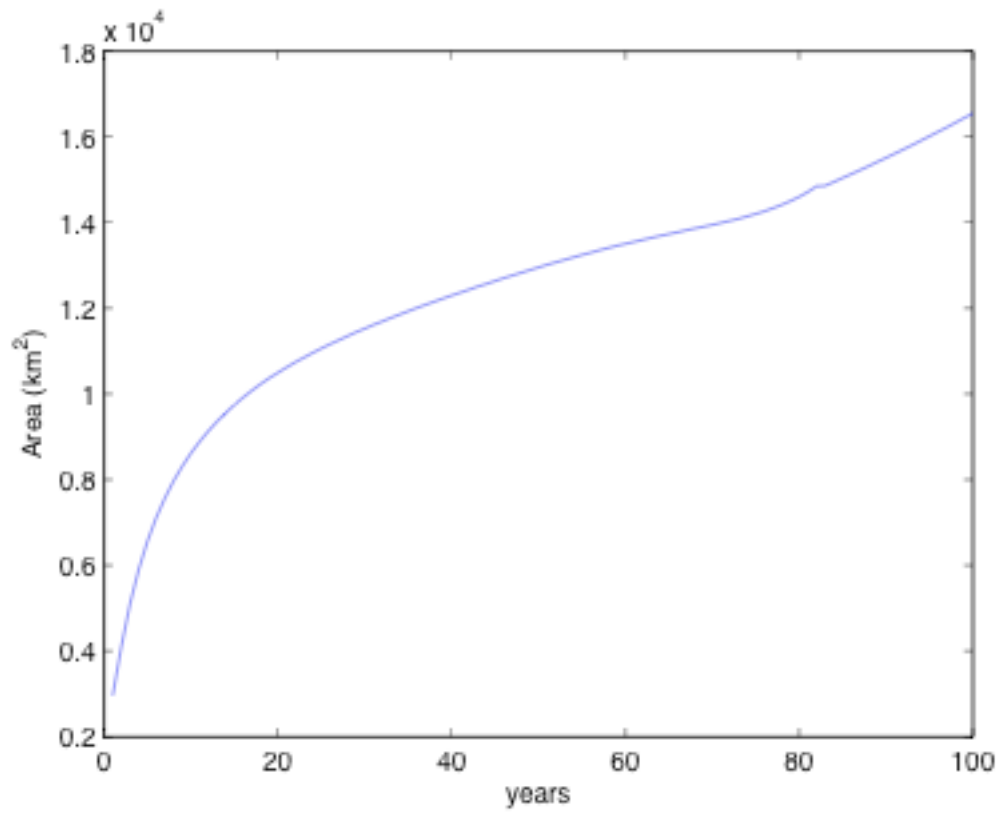


Figure 5.2: Increase in area in years with a flow of  $656m^3/s$  salinity included

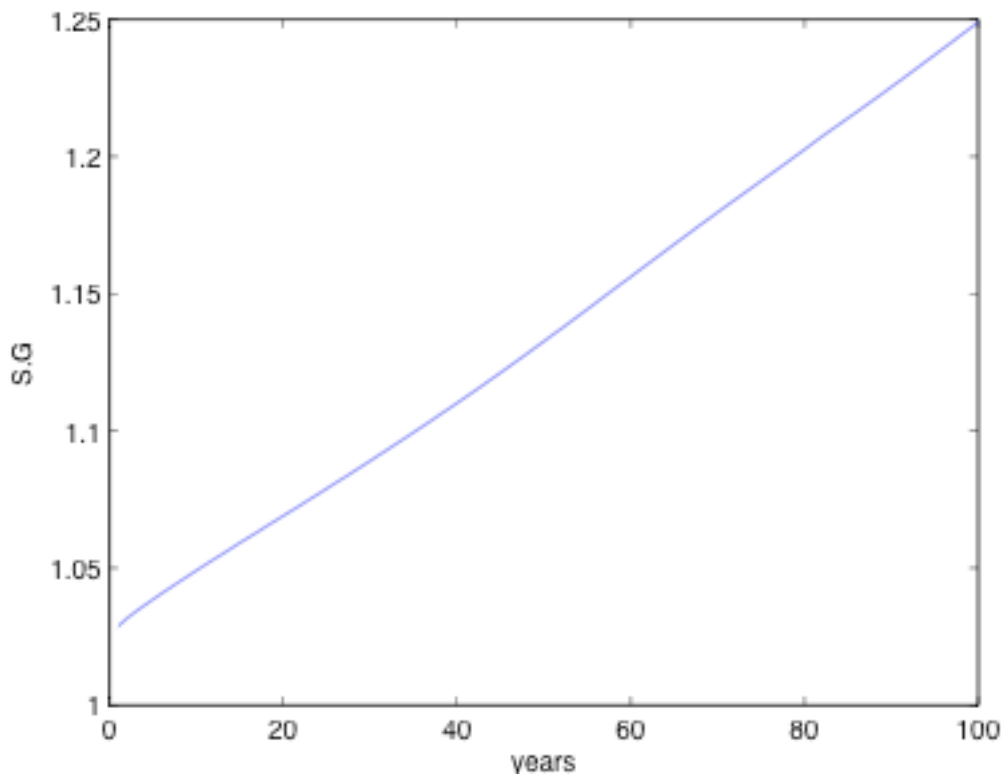


Figure 5.3: Increase in the specific gravity with time with a  $656m^3/sec$



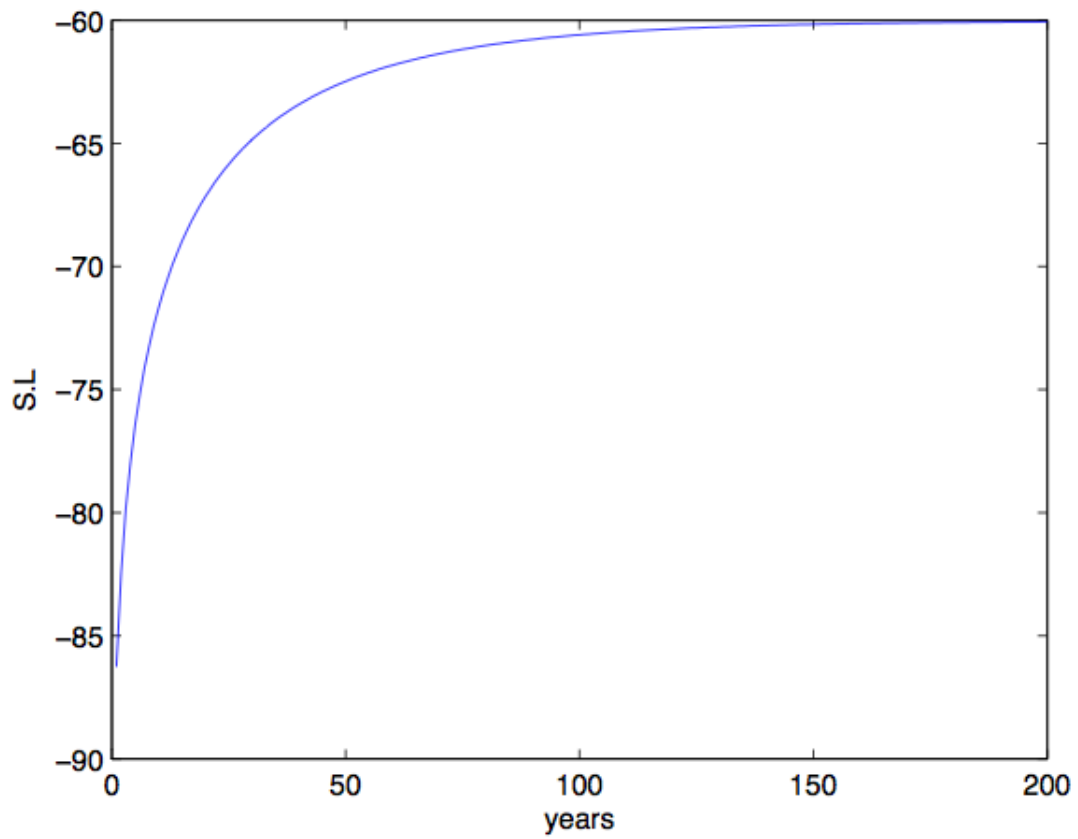


Figure 5.4: Surface level increase in years with a  $656m^3/sec$  flow and salinity not included

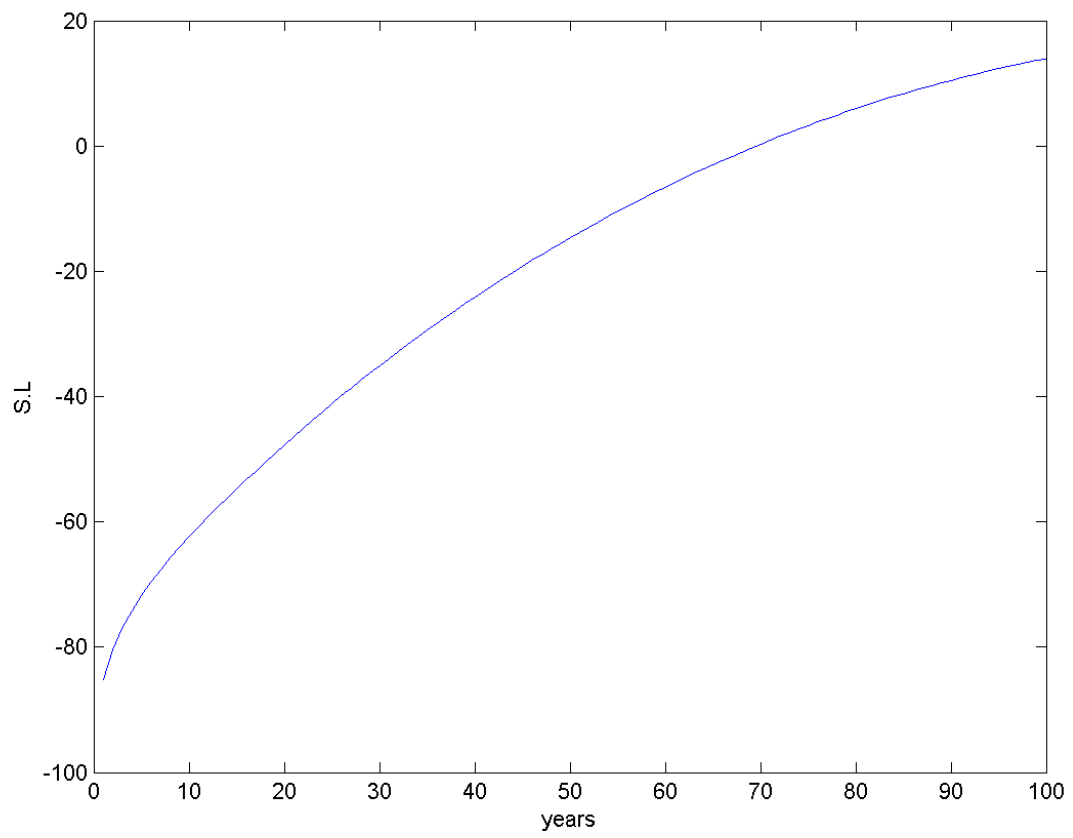


Figure 5.5: Surface level increase in years with seepage and salinity included and a  $656m^3/s$  Flow

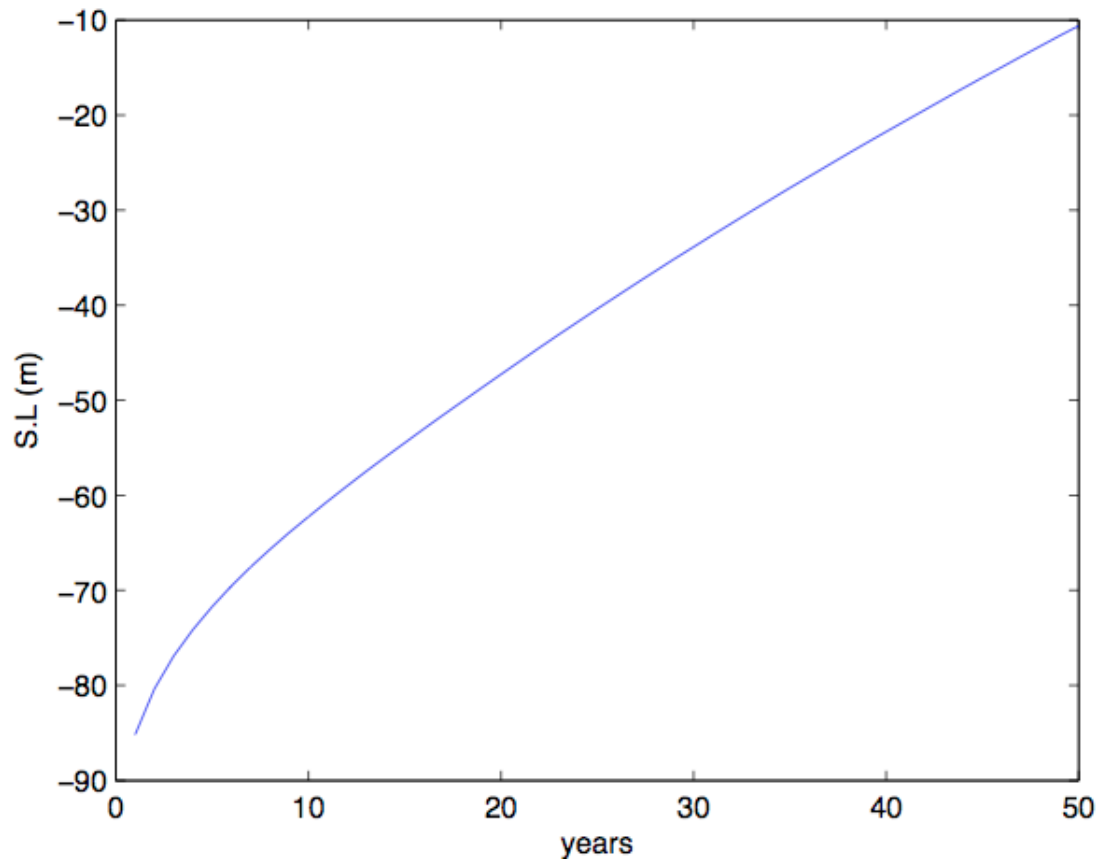


Figure 5.6: Surface level increase in years with no seepage but new salinity model included in the  $656m^3/s$  Flow

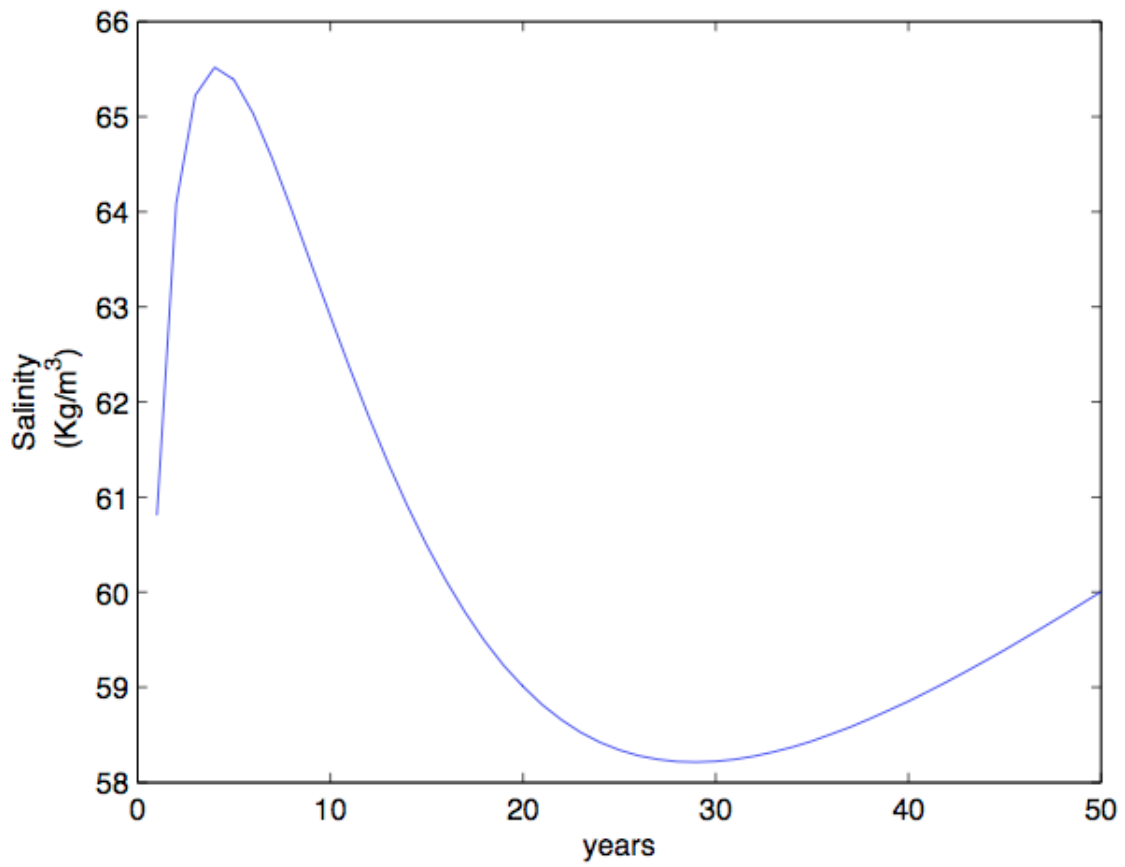


Figure 5.7: Salinity increase in years with no seepage included and a  $656m^3/s$  flow but the new salinity model included

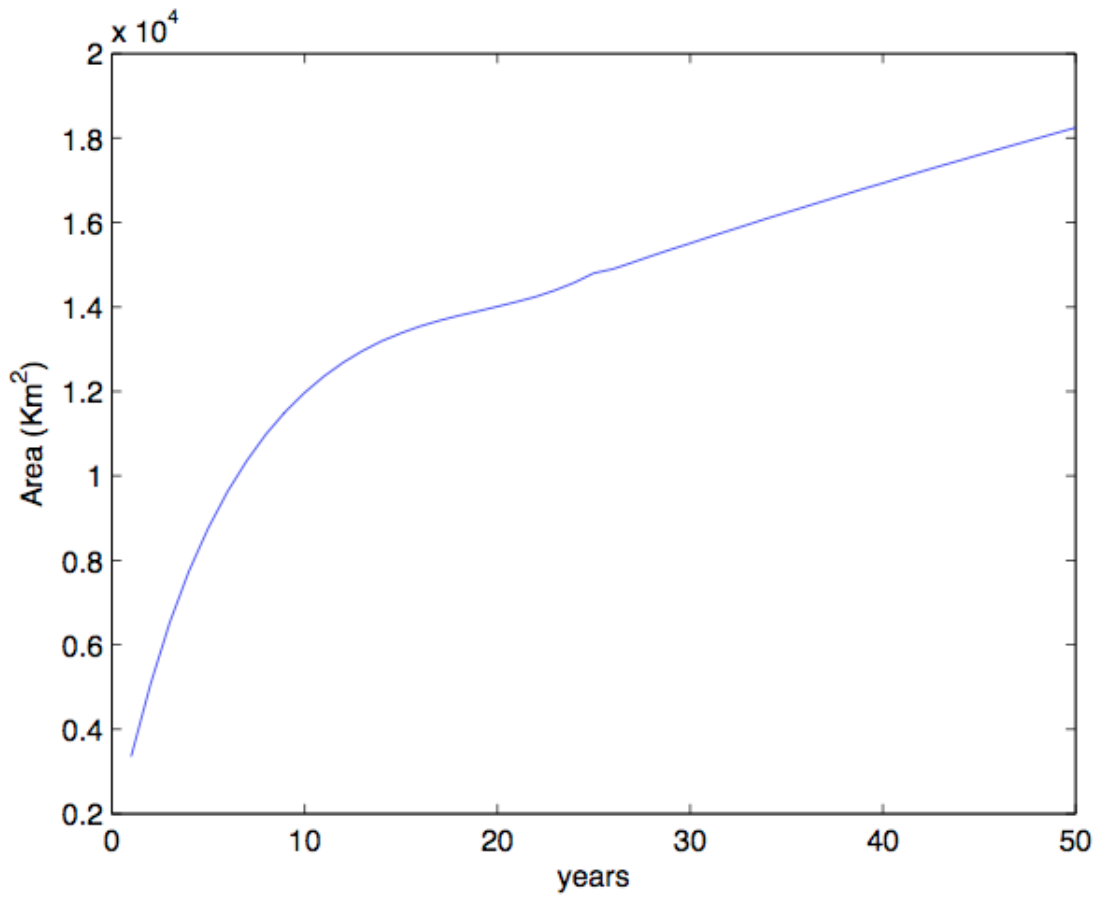


Figure 5.8: Area increase in years with no seepage included and a  $656m^3/s$  flow but the new salinity model included

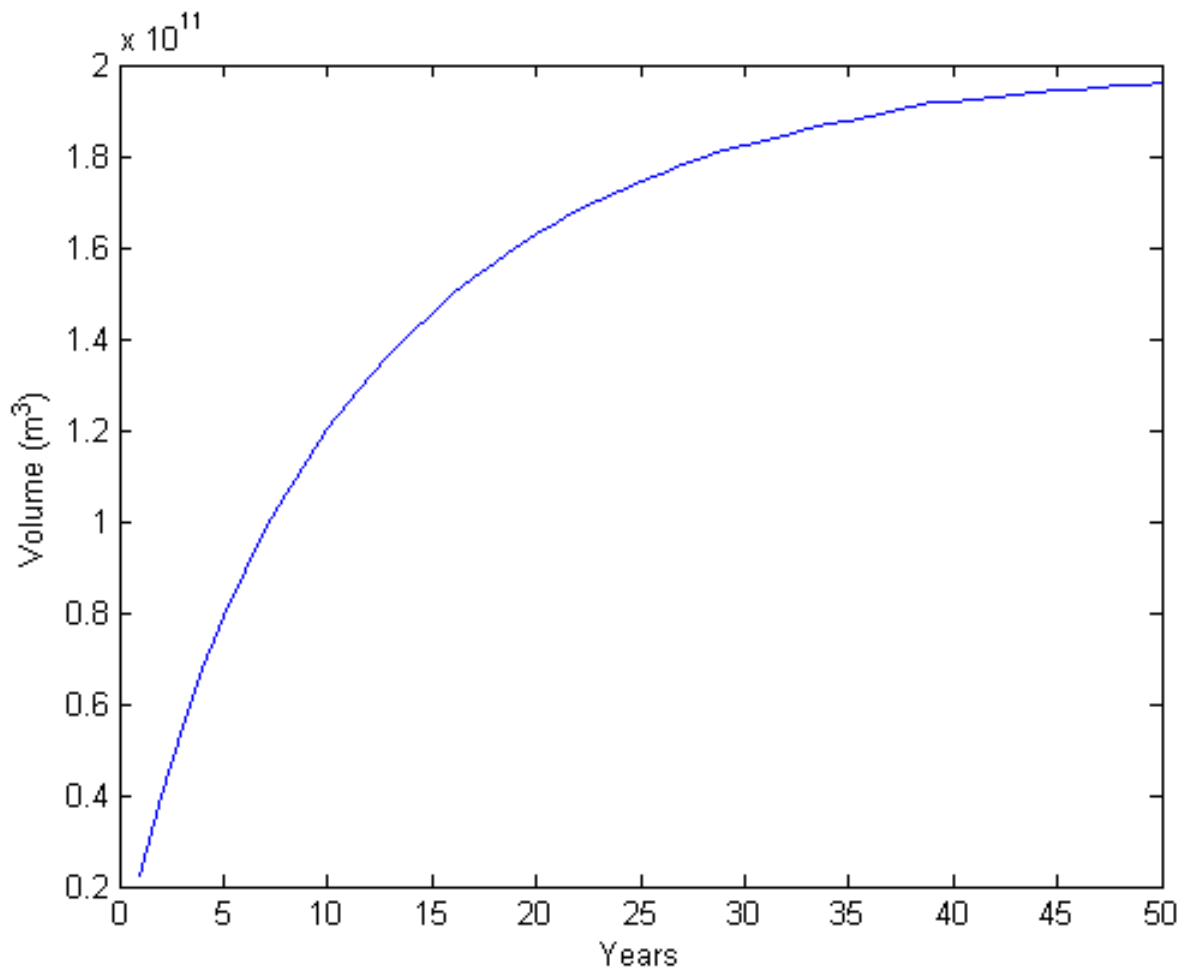


Figure 5.9: Volume increase in the years

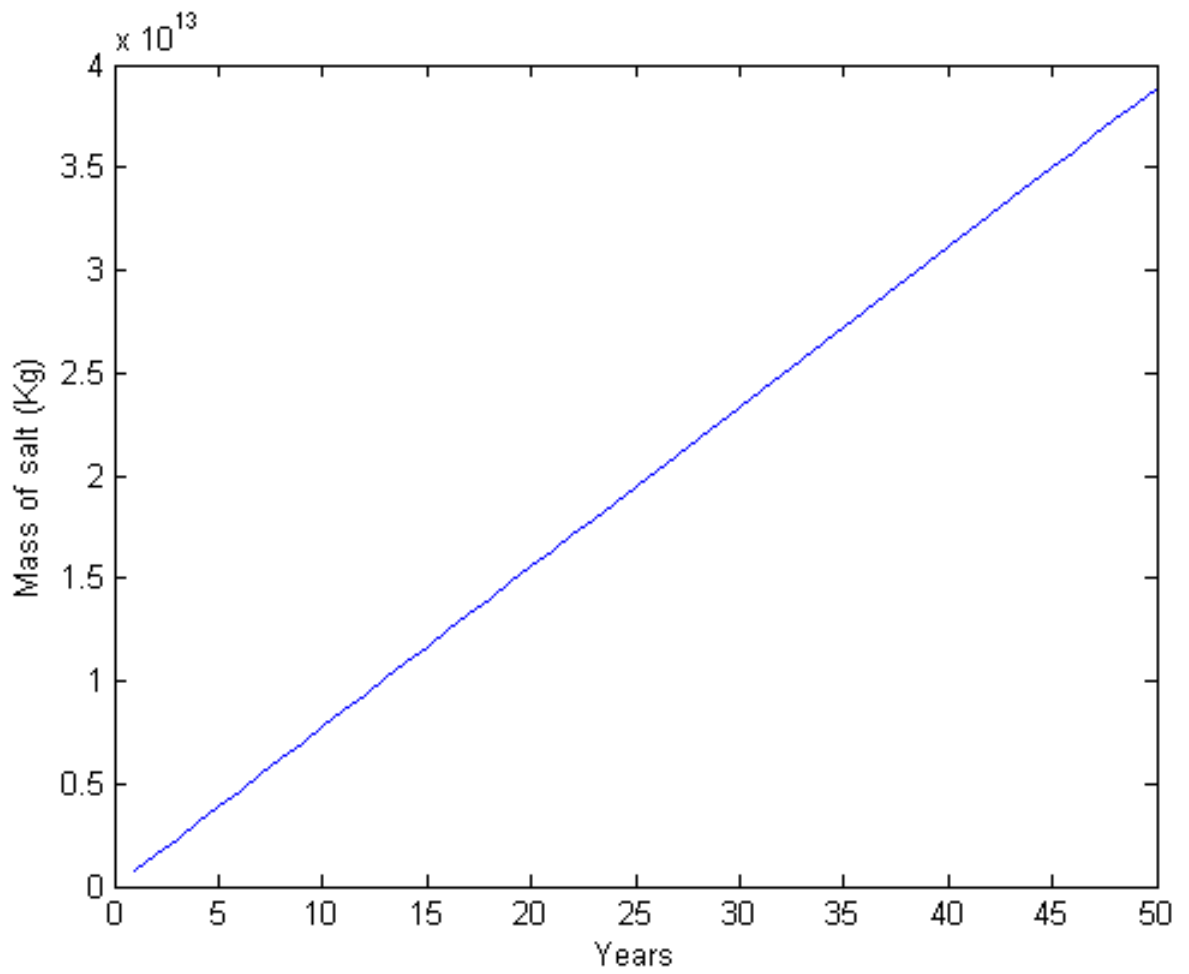


Figure 5.10: Mass of salt increase in the years

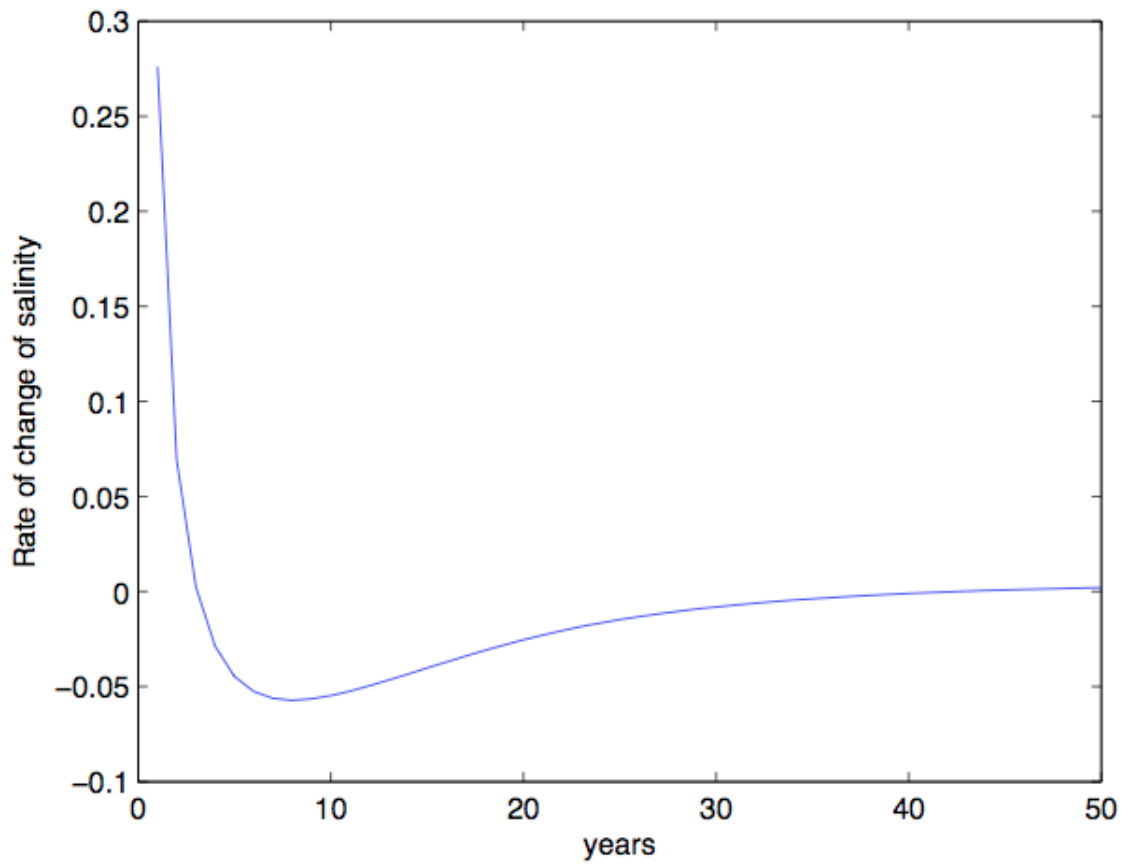


Figure 5.11: Rate of change in salinity decreases in years with no seepage included and a  $656m^3/s$  Flow but the new salinity model included



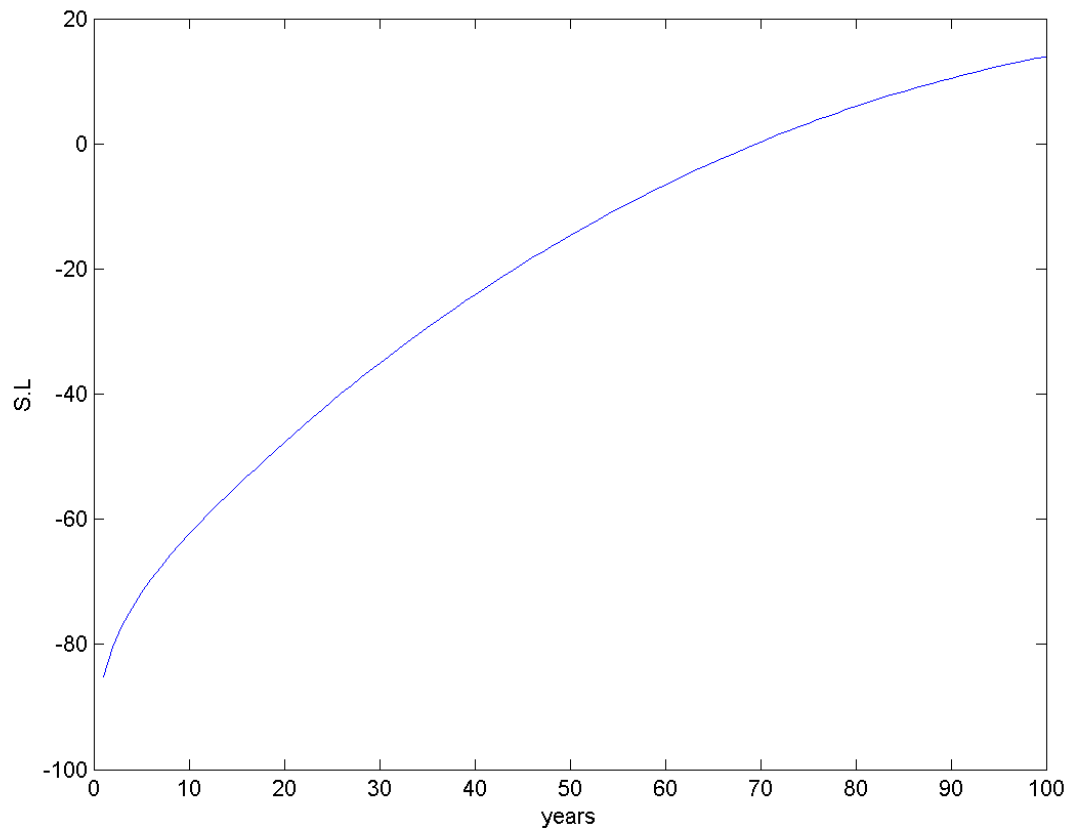


Figure 5.12: Surface level increase in years with seepage included and a  $656m^3/s$  flow but the new salinity model included

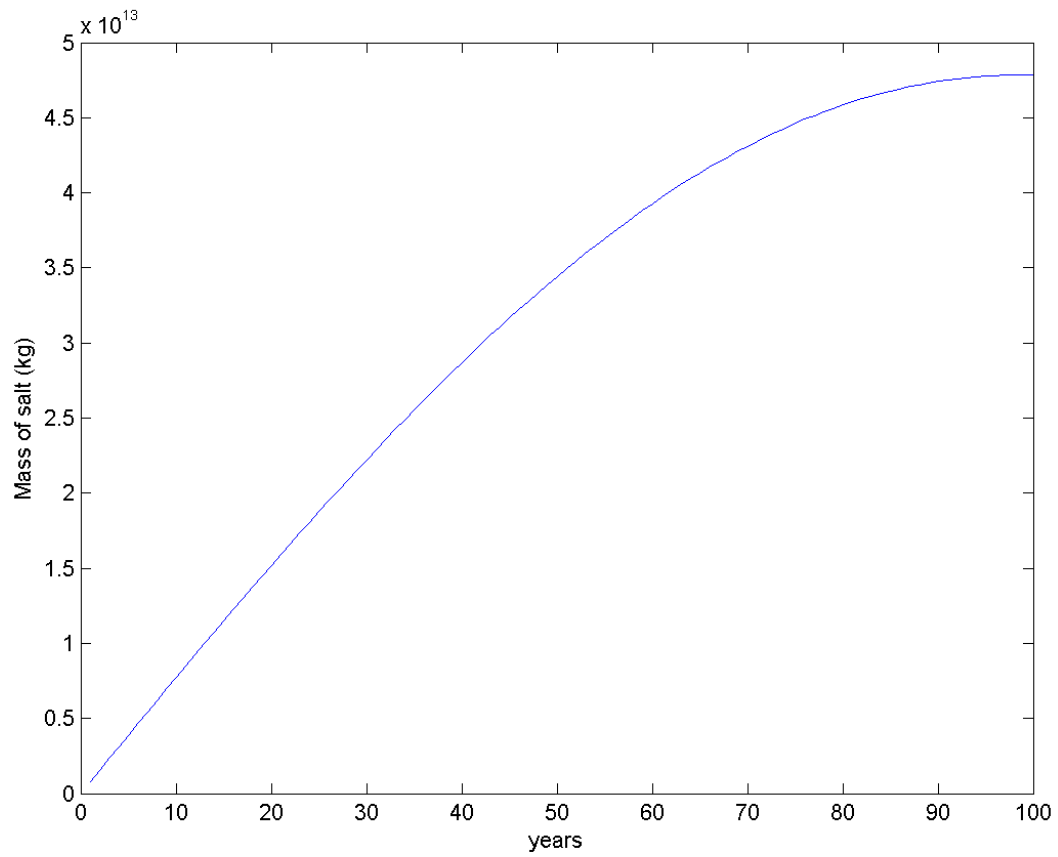


Figure 5.13: Mass of salt increases in years with seepage included and a  $656m^3/s$  flow and the new salinity model included

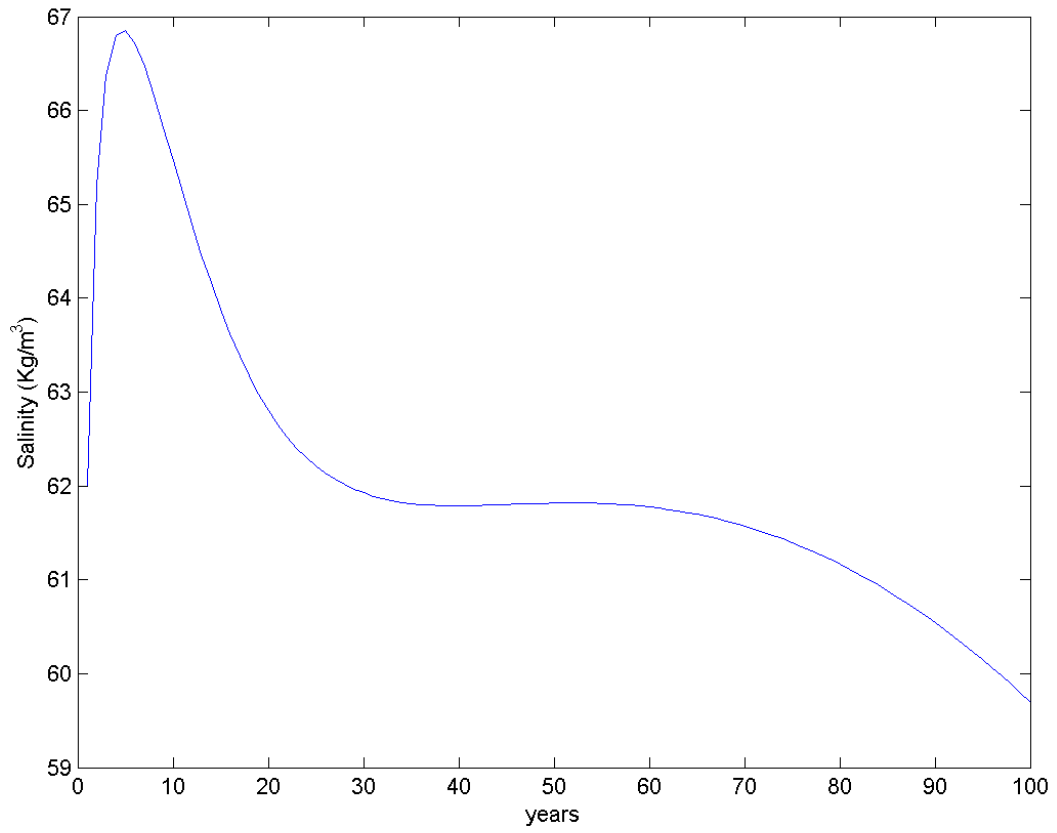


Figure 5.14: Salinity change in years with seepage included and a  $656m^3/s$  flow and the new salinity model included

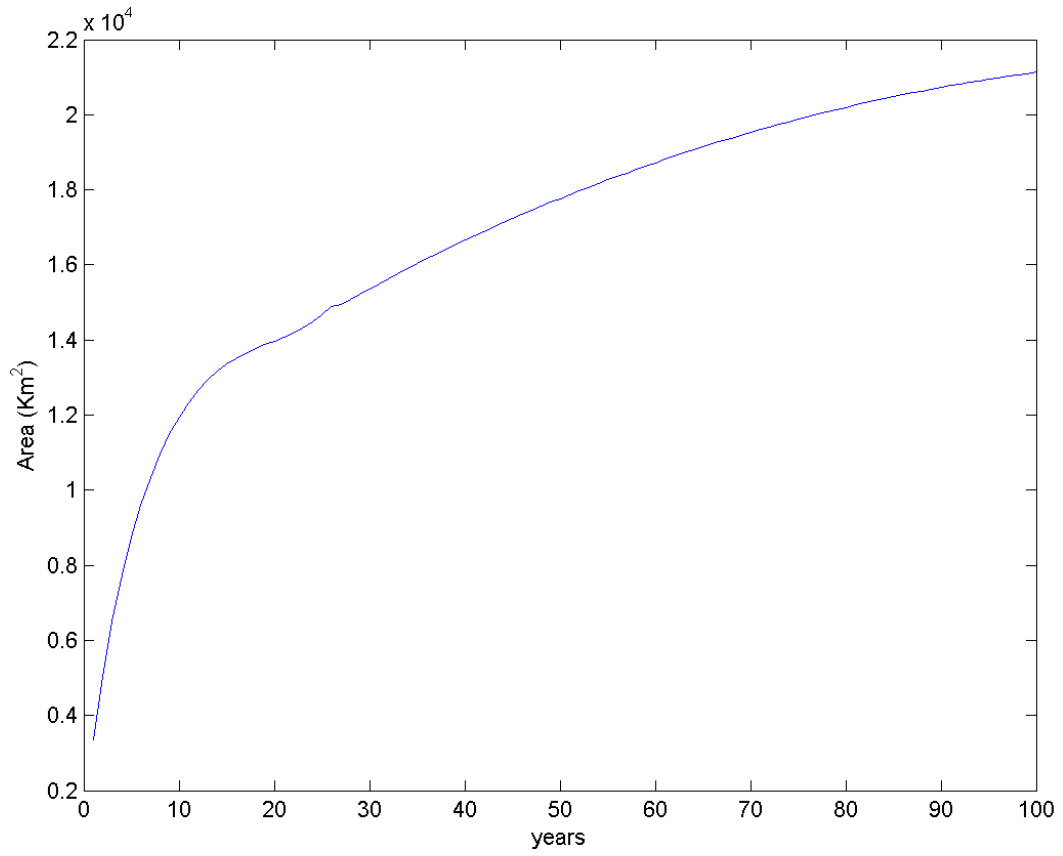


Figure 5.15: Area increase in years with seepage included and a  $656m^3/s$  flow and the new salinity model included

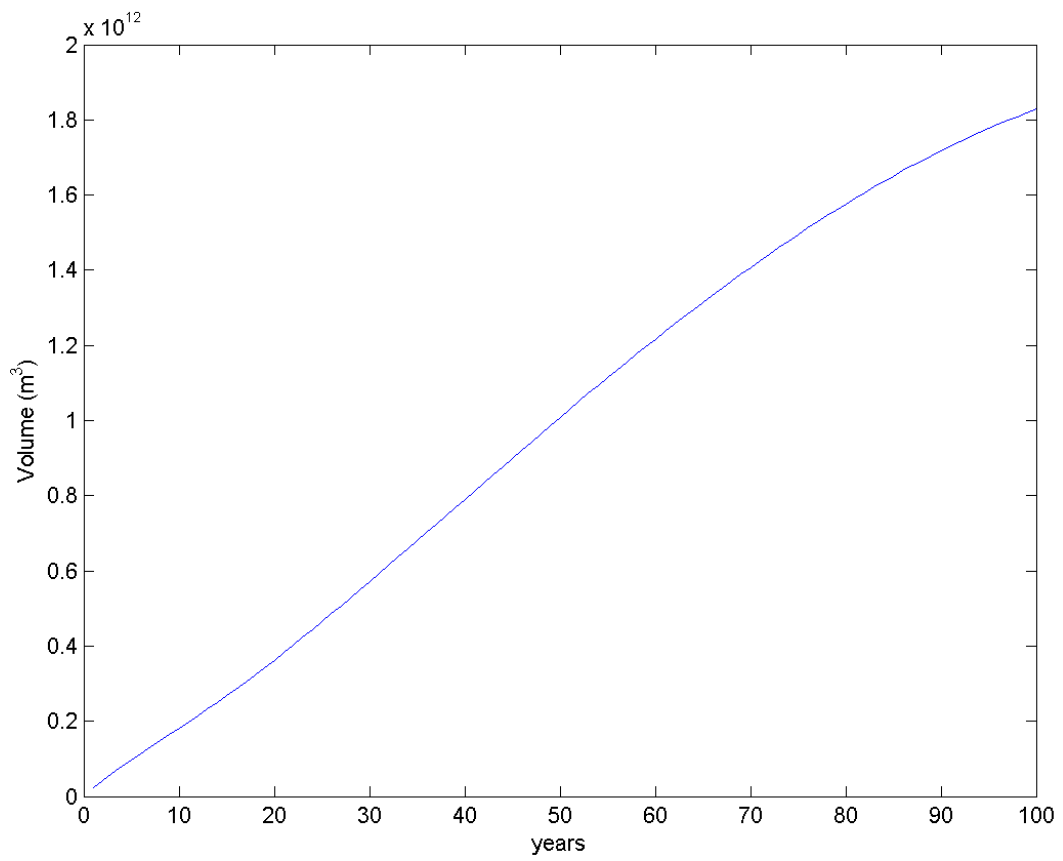


Figure 5.16: Volume increase in the years with seepage included

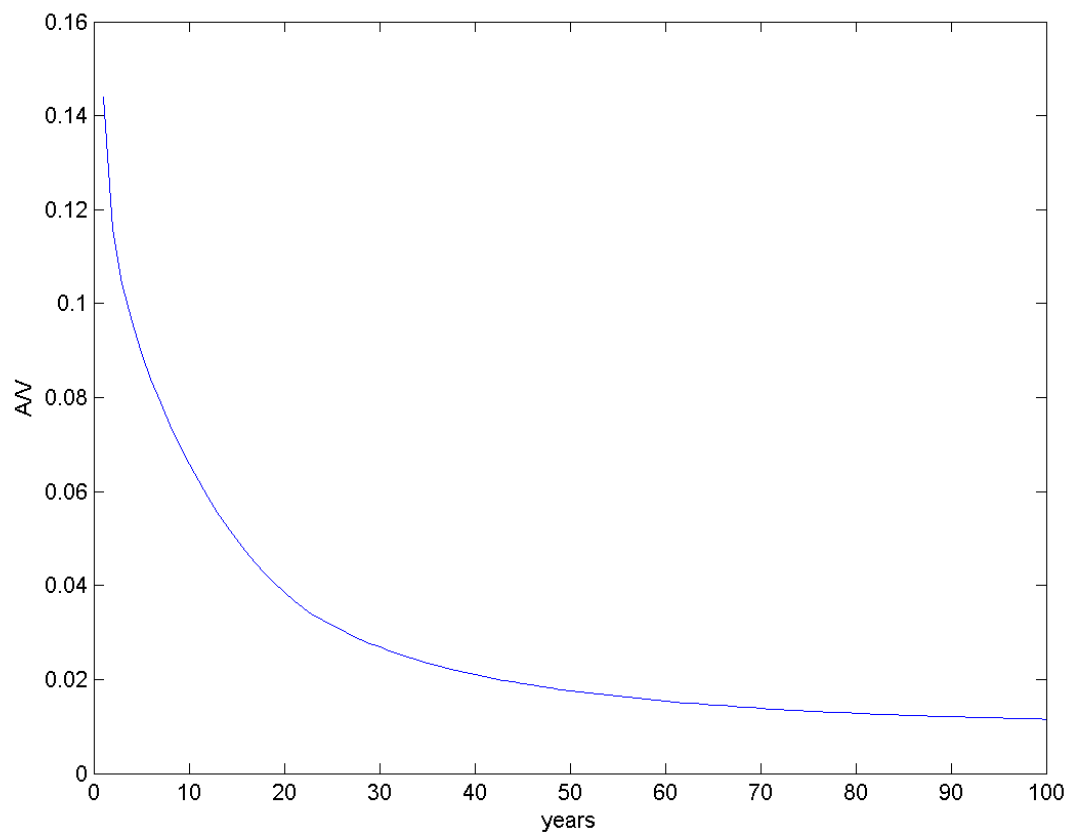


Figure 5.17: Area over Volume ratio decreases in the years

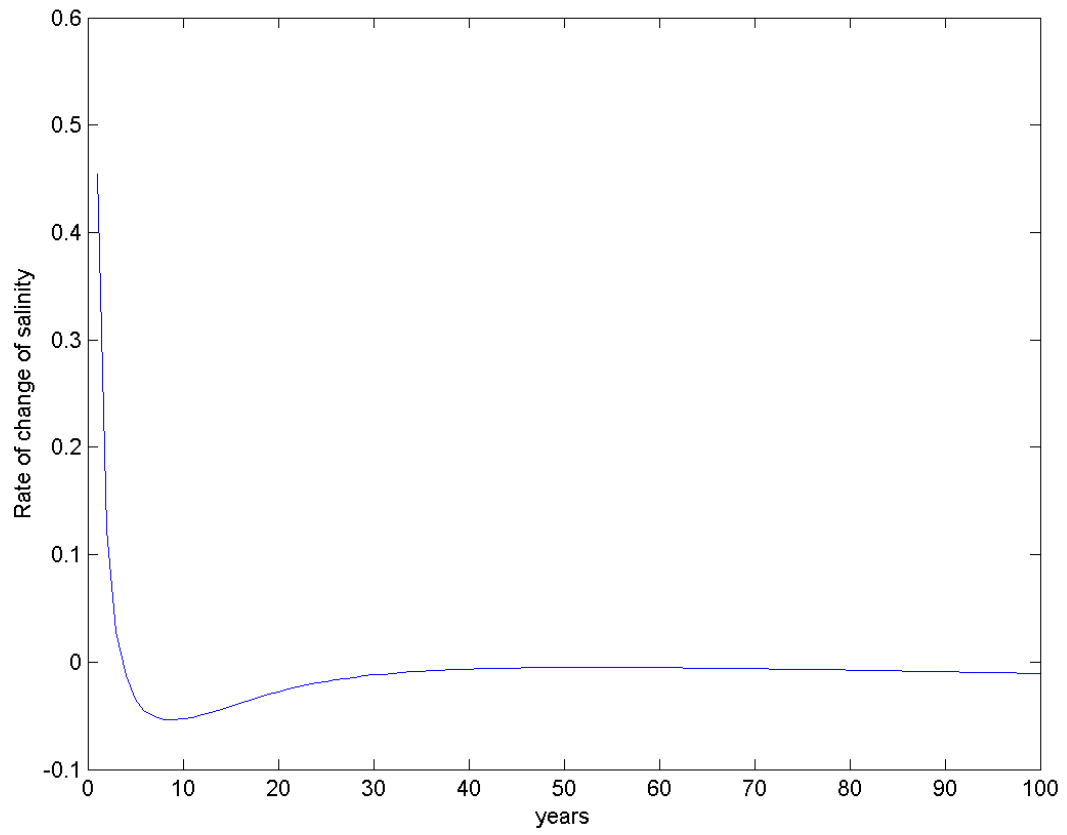


Figure 5.18: Rate of change of salinity decreases in the first years with seepage included and a  $656m^3/s$  flow but the new salinity model included

Comparing Figure 5.4 with Figure 5.1, where the salinity was included in the latter, shows the conclusion that the affect salinity has on the overall evaporation rate over the years and the mass balance equation, that leads to the evaporation decreasing significantly. This leads to the results shown in Figure 5.4 when salinity is not included the lake levels out, but when it is included in Figure 5.1 the surface level continues to increase. Figure 5.5 shows the surface level increase with salinity and seepage included in the model, which is done for the first time far as the author knows. This result shows that the surface level increases at a lower rate even when salinity is calculated with the detailed method used in this thesis. This is due to the affect of the outward seepage has an affect on the mass balance equation. Figure 5.6 is a different pattern from Figure 5.1 where the salinity when studied in detail is greater and has a greater affect on evaporation leading the surface level of the lake to increase faster, Figure 5.6 shows a different pattern to Figure 5.1, both had no seepage included in their model.

$$\frac{dc}{dt} = \frac{1}{V} [V_{sea} * C_{sea} + \sum V_{si} C_{si} - (V_{so} + V_{pumped}) C] - \frac{m_{salt}}{V^2} [V_{sea} + V_{rain} + \sum V_{si} - V_{so} - V_{evap} - V_{pump}] \quad (5.1)$$

Figure 5.7-5.9 depicts mathematically why salinity follows the pattern shown that as the area increases so does the volume (equation 5.1) the rate of evaporation increases and so does the rain. So in the first 10 years the increase in area is rapid which causes a much greater evaporation rate, which leads to salinity increasing steeply as shown in Figure 5.7. But later on, as the volume increases to a great extent as shown in equation 5.1, it takes over the rate of increase of salinity equation and the negative terms dominates, especially with the mass of salt continuing to increase in the lake as shown in Figure 5.10. In Figure 5.11, it further conveys the rate by which the rate of increase of salinity decreases in the first few years as the volume increases very fast. This leads to the salinity rate to decrease, especially when the volume dominates equation 5.1 until for a few years the change of salinity is actually negative. But, then when the volume levels in the later years the rate of change of salinity also levels.



The coming figures show the same results as our detailed salinity model, but with seepage also included which again leads to the level of the lake increase but at a lower rate, contrary to what other studies had stated that the effect of the outer seepage would be negligible. Figure 5.13 shows the an increase in the mass of salt and then leveling out for the future when the surface level and area are also leveling, alternatively from when the outward seepage was excluded as no mass of salt left so the mass continued to increase faster. Figure 5.14 shows that when outer seepage is included in the model, the salinity of the lake decreases with the volume of saline water continuously seeping from the lake, except for in the first 5 years where the increase in area is too great leading the salinity to increase, even with the volume of saline water seeping outwards. This period of increase was also present when seepage was excluded but it was greater, and the salinity never decreases more than the salinity of the sea. There is a period where the decrease in salinity slows down and levels due to the value of the area and the volume being still comparable while the volume is much greater as shown in Figure 5.17 the decrease in salinity returns. Figure 5.15 shows only the first few years witness a huge spike in the area of the lake, then it levels out due to the topography of the Qattara Depression. The area over volume ratio in Figure 5.17 is very important as it shows that the area increase, which is related to the rain and evaporation, decreases in relation to the total volume of the lake and for that reason the volume takes over equation 5.1. That causes the rate of change of salinity shown in Figure 5.18: as the total volume of the lake increases at a greater rate than the area, hence the total of the rain flow rate and evaporation subtracted from it as shown in Figure 5.21 decreases in relation to the total volume. That causes the rate of change of salinity to decrease but never more than the salinity of the sea. The affect of the rain on the rate of change of salinity is negligible and does not seem to have much of an effect. As when the total rain is increasing in the first few years, as shown in Figure 5.20, the salinity is increasing as shown in Figure 5.19. The increase in salinity is not enough compared to the total increase in the volume of the lake which is much more aggressive and dictates the changes in salinity as explained.

There is a large difference between these results and Ezz El Din's results [5] with the seepage model and new detailed salinity model as shown in Figure 5.5 and 5.6. where the salinity was increasing constantly and these new results have tremendous effects on the life cycle of the project and its economic analysis as previously discussed. The data present for the hydraulic conductivity of the soil in the region was not present, for that a sensitivity analysis is preformed to see what a variance in that number would cause for the overall results as shown in figures 5.22-5.24. The results show that the effect of increasing the hydraulic conductivity from 0.00025 m/sec to 0.0025 m/sec have a great effect on the overall results. The level at which the lake levels out is -90 m below sea level instead of continual increase. The same goes when decreasing the hydraulic conductivity to 0.000025 m/sec the level the lake increases faster. The mass of salt would increase to higher level with decrease in hydraulic conductivity and vice versa.

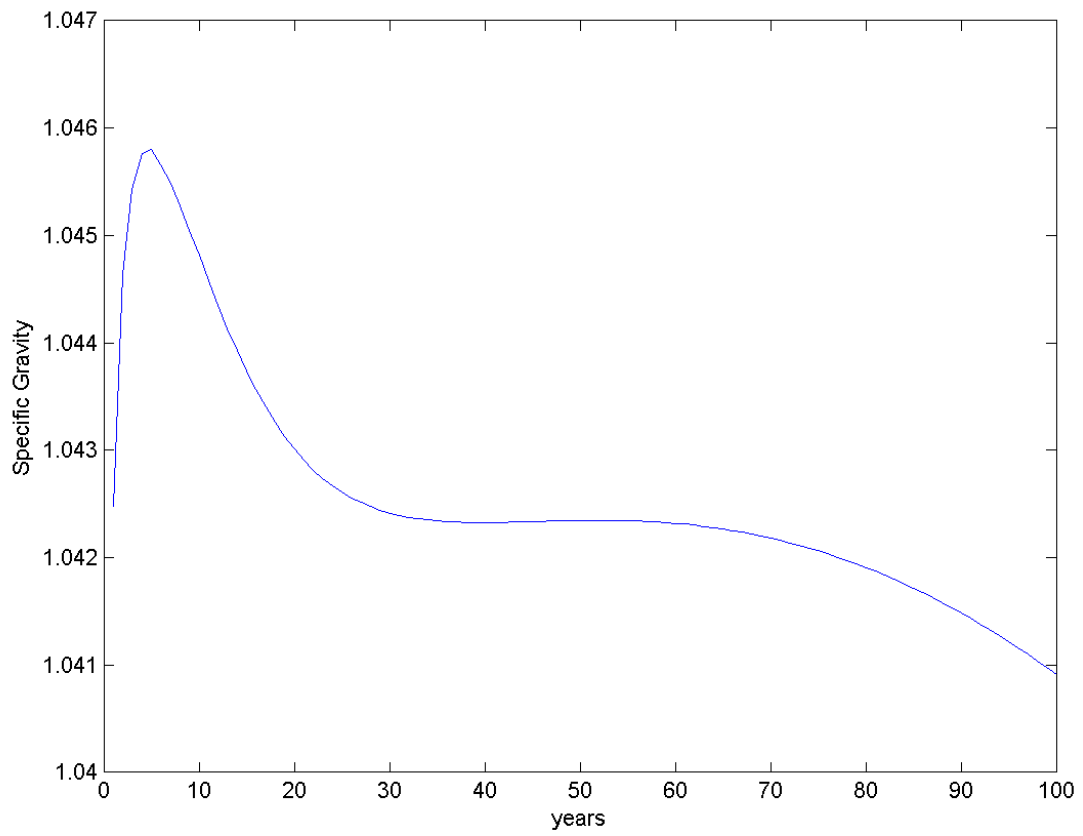


Figure 5.19: Specific gravity increase in the first years with seepage included and a  $656m^3/s$  flow and the new salinity model included

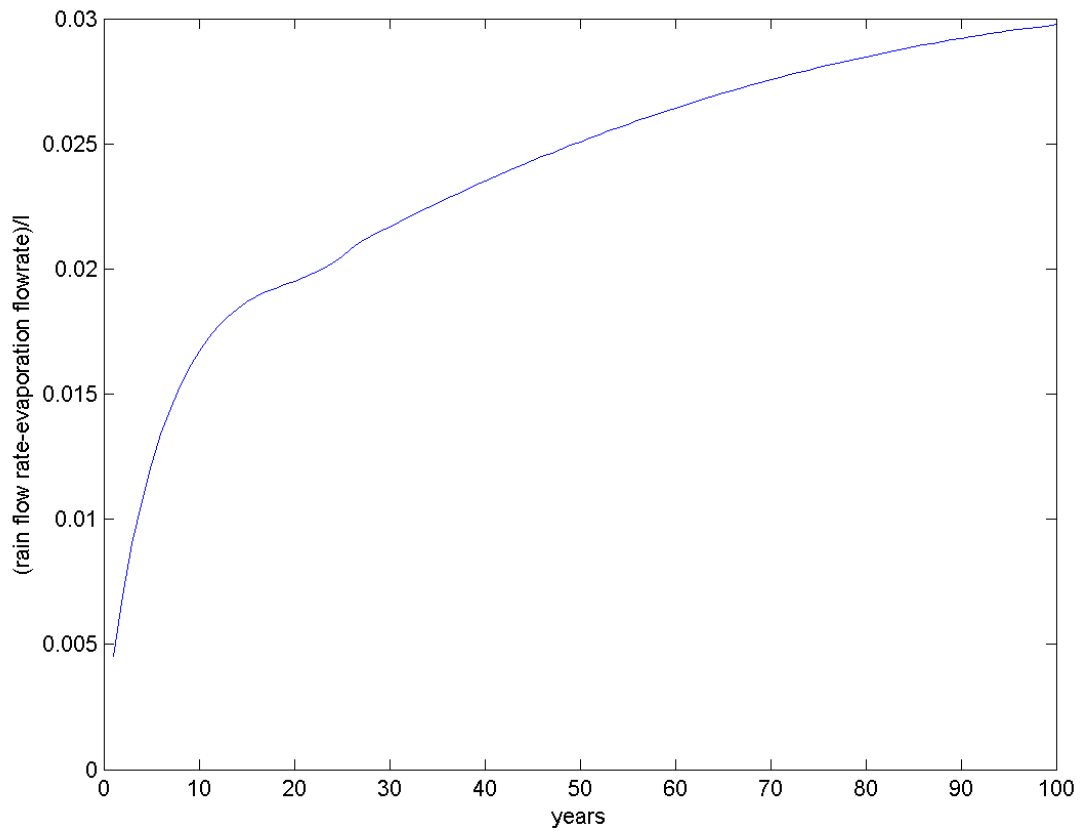


Figure 5.20: Difference between rain and evaporation increases generally with the years following the area increase

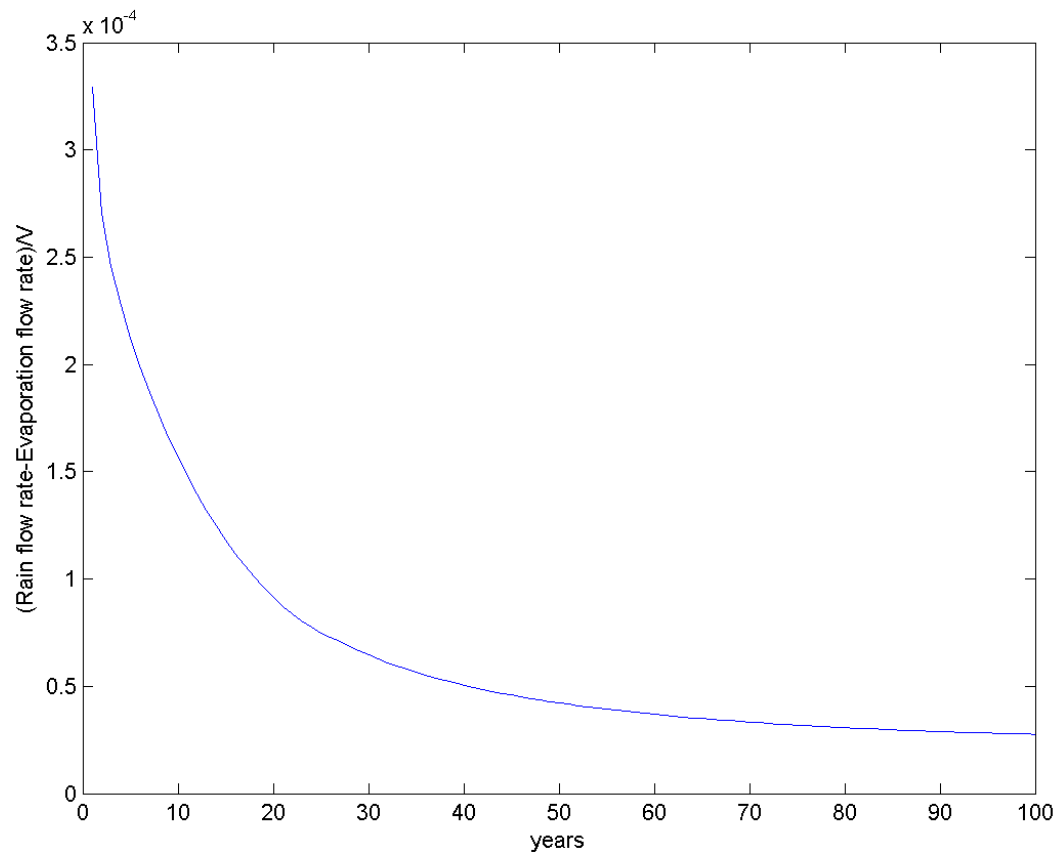


Figure 5.21: Difference between rain and evaporation decreases with the years when compared to the total volume of the lake

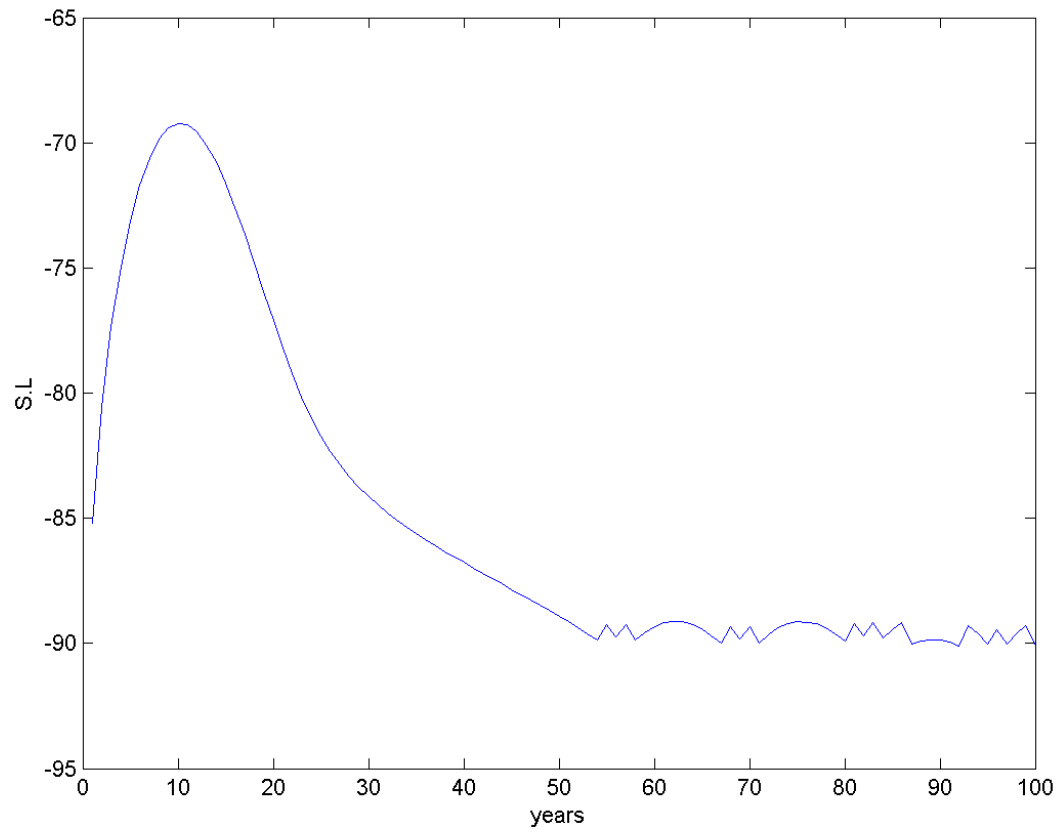


Figure 5.22: Surface level decreases to a lower level when hydraulic conductivity increases

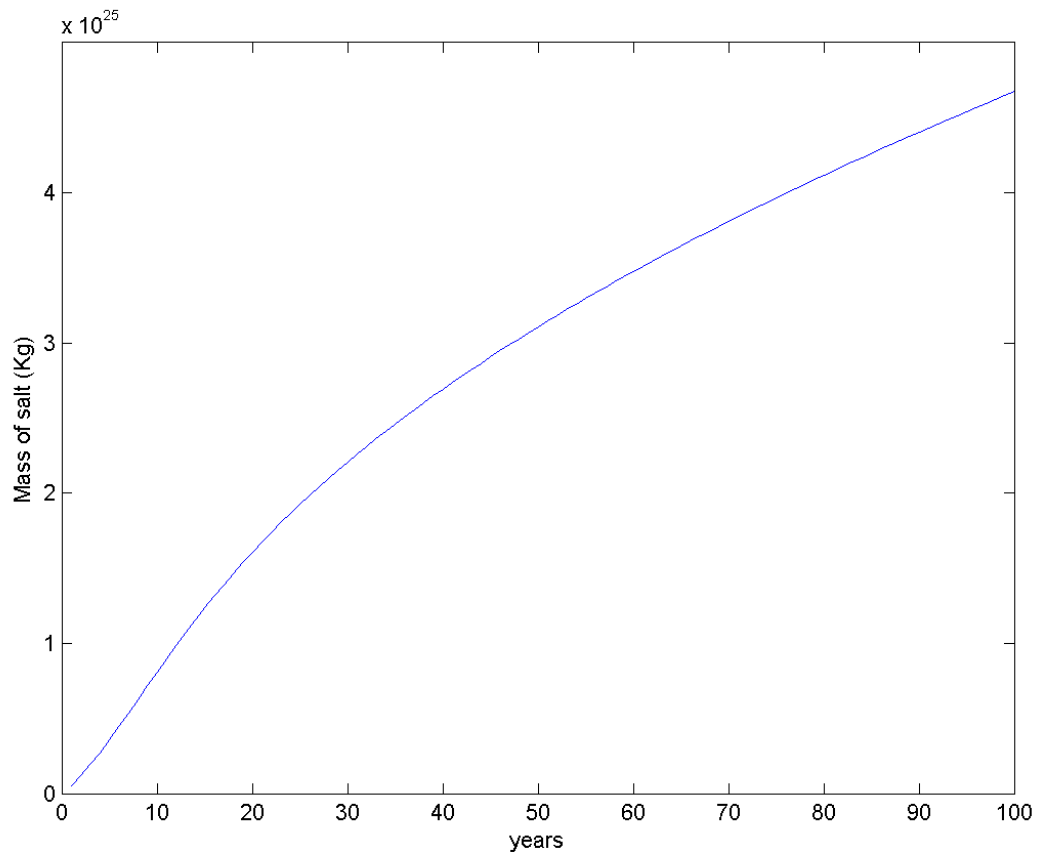


Figure 5.23: mass of salt increases to a higher level when hydraulic conductivity decreases

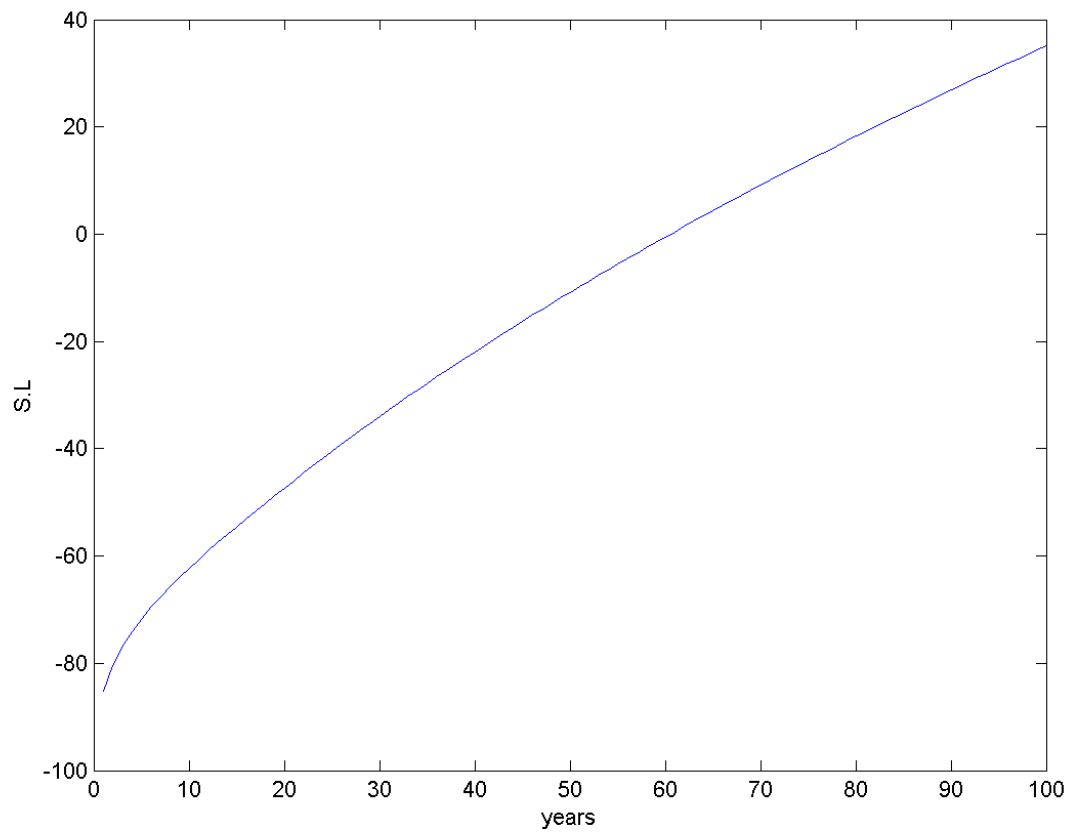


Figure 5.24: Surface level slightly increases faster when hydraulic conductivity of the soil decreases



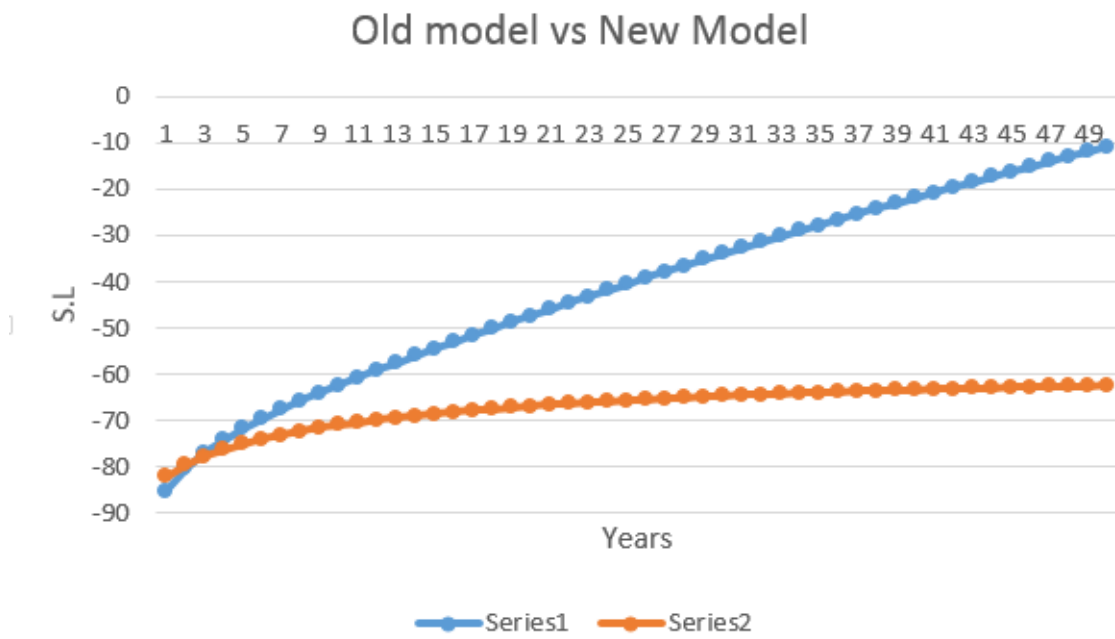


Figure 5.25: Surface level increases faster when salinity is included in model by comparison to old models

# Chapter 6

## Conclusion and Recommendations for Future Work

### 6.0.1 Conclusion

To the best of the author's knowledge, this is the first time the Qattara Depression project seepage outflow is included in its model and this study also presents an unprecedented economic analysis to the project to determine the most economic and feasible scheme. The previous investigations performed mentioned in the literature review presented a ground base for this work. Topographical and geographical data gathered in all these previous studies were used in the investigations. But, what was lacking was the effect of salinity on the plant life in the early studies and the economic feasibility of the project that have been answered through this work. A very important result shown through the model built is that after the results agreed with the previous results performed earlier when all the conditions were the same. But, the effect of the outward seepage that was always assumed to be very low and would effect the plant's life positively anyway was incorporated in the model and showed that the plant will last considerably longer even with the effect of salinity in the model, and the salinity was studied in more detail which showed a different pattern from Ezz El Din's results [5]. This makes the plant that was already economically feasible a compulsory project due to numerous advantages. Besides providing cheap

energy during peak hours and reducing the carbon foot print, both huge problems in Egypt, the huge area surrounding the Qattara Depression could be inhabited and different industries and work opportunities would be available. These industries could include salt factories as the specific gravity would increase as shown in the results, also tourism in the area covered with water in a country such as Egypt full of historical relics. It was concluded the the pumped hydro storage alternative would be the most economical solution available as it breaks even in the 5<sup>th</sup> year. That was calculated with the enhanced model including the seepage flow that extends the plant life as shown in the results and also included the seepage flow that decreases the plant life and that was accounted for in the calculations.

## **6.0.2 Recommendations for Future Work**

Further studies can be preformed to enhance the work, for example:

1. The effect the lake would have on the meteorological conditions of the area as the humidity would be affected by the evaporation rates
2. The excavation costs could be more precise if samples of the soil are taken from the area and stress analysis is preformed to have a more exact values of the cost
3. The nature of the soil in different areas in the depression can be also accurately preformed by taking samples that would enable us to have exact values for the hydraulic conductivity and storage coefficient values that effect the seepage flow. That would lead to knowing the exact affect of the project on the neighboring aquifers.

# Bibliography

- [1] G. Martino, "The qattara depression," *Water Power*, 1973.
- [2] R. Hafiez, "Mapping of the qattara depression,egypt, using srtm elevation data for possible hydropower and climatechange macro-projects," *International Journal of Water Resources and Environmental Engineering*, 2014.
- [3] M. Salem, "Water and hydropower for sustainable development of qattara depression as a national project in egypt," *Water Power*, 2012.
- [4] H. Wanger, "Introduction to pumped hydro storage," 2011.
- [5] M. E. E. Din, "Evaluation of potential hydropower of qattara depression," 2004.
- [6] A. Afify, "Hydro and solar-pond-chimney power scheme for qattara depression, egypt," 2013.
- [7] G. B. Magin, "Review of literature on evaporation suppression," 1960.
- [8] M. E. Jensen, "Estimating evaporation from water surfaces," 2008.
- [9] K. de Berg, "Raoult's law: A reinterpretation for concentrated strong 1:1 electrolyte solutions," 2011.
- [10] S. S. Ahmed, "Groundwater of egypt: an environmental overview," 2007.
- [11] Z. S.Rizk, "Impact of the proposed qattara reservoir on the moghra aquifer of northwestern Egypt," 1991.
- [12] O. A. H.F. Burcharth, "On the one-dimensional steady and unsteady porous flow equation," 1993.
- [13] M. Ragheb, "Integrated wind and solar qattara depression project with pumped storage as part of desertec," *G-Animal's Journal*, 2012.
- [14] M. F. N.T.M. Thieu, "Seepage modelling in a saturated/unsaturated soil system," 2001
- [15] A. I. Johnson, "Compilation of specific yields for various materials," 1999.
- [16] IRENA, "Renewable energy technologies:cost analysis series." 2012.
- [17] H. E.Shaalan, *Generation of Electric Power*, 2010.
- [18] M. R, "Energy interconnection europe - malta," 2008.
- [19] IRENA, *RENEWABLE POWER GENERTION COSTS IN 2014*, 2014.